

Soil-structure interaction of a permanent steel fibre reinforced underwater concrete floor system

Martijn Apon

Graduation Committee:

Dr. ir. M. Korff

Dr. ir. drs. C.R. Braam

Prof. Dr. K.G. Gavin

ir. Ruud Arkesteijn



-Soil-structure interaction of a permanent steel fibre reinforced underwater concrete floor system-

-Soil-structure interaction of a permanent steel fibre reinforced underwater concrete floor system-

Name: Martijn Apon
Faculty: Civil Engineering and Geosciences
Mater: Geotechnical Engineering
Student number: 4135687
Date: 8 April 2019
Section: Geo-Engineering
Subject: Soil-structure interaction of a permanent steel fibre reinforced underwater concrete floor system

Contact:
E-Mail: martijn-apon@hotmail.com (Personal)
m.apon@abt.eu (ABT)
Tel.: 06 57754999 (Personal)
015 767 6741 (ABT)

Technische Universiteit Delft
Faculty of Civil Engineering and Geosciences
Stevinweg 1
2628 CN Delft

ABT bv
Vestiging Delft
Delftechpark 12
Postbus 458 2600 AL Delft
T: +31(0)15 2703611

Graduation Committee:
Chair:
Dr. ir. M. Korff
TU Delft – Section Geo-Engineering
Room number: 00.140
M.Korff@tudelft.nl

Daily supervisor:
ir. Ruud Arkesteijn
Mobilis
rt.arkesteijn@mobilis.nl

Structural supervisor:
Dr. ir. drs. C.R. Braam
TU Delft – Section Concrete Structures
Room number: S2 2.06
C.R.Braam@tudelft.nl
015 2782779

Geo-Technical supervisor:
Prof. Dr. K.G. Gavin
TU Delft – Section Geo-Engineering
Room number: 00.480
k.g.gavin@tudelft.nl
015 2787128

-Soil-structure interaction of a permanent steel fibre reinforced underwater concrete floor system-

Preface

This is my master thesis to graduate from the faculty of Civil Engineering with specialisation Geo-Engineering at the Delft University of Technology.

During my master I focused on the field of subsurface structures. This field is an interaction between Geo-Engineering and concrete structures. The courses that I followed at the TU Delft were all chosen to deal with this interaction. Also the committee members were chosen to represent this interaction.

The subject underwater concrete floor was chosen by myself because it is a relatively new subject within civil engineering. Scientific research on this subject could be very helpful to better understand and improve subsoil building processes. This specific subject and other interesting projects led me to ABT. Within the last few years ABT had several projects where an integrated steel fibre reinforced concrete floor was used successfully.

Ruud Arkesteijn graduated 7 years ago on the dimensioning of underwater concrete floors and is involved in multiple projects and a CUR committee on the subject. René Braam is also involved in this CUR committee. The knowledge of Ruud Arkesteijn and René Braam, combined with the Geotechnical knowledge of Mandy Korff and Ken Gavin was a good basis for this master thesis. I would like to thank all the committee members for their willingness to accompany me during this research.

Martijn Apon
Delft, April 2019

Abstract

The focus of this research was the implementation of a permanent steel fibre reinforced underwater concrete floor (SFRUCF) as a permanent structural floor. A model was created that can describe the soil structure interaction of an SFRUCF including the highly non-linear behaviour of SFRC. The soil structure interaction of the UCF was modelled in Plaxis 2D with a plate element that includes the behaviour of SFRUC by means of an MN- κ diagram. This model was validated with measured data from the Albert Cuyp garage. It was shown that due to the uplift pressure heave occurred in the clay layer underneath the UCF, which increases the load on the UCF by 10%-30% and should be taken into account in the design. Also the heave from the deep Eemclay was considered. This heave had influence on the total deformations but hardly affected the internal forces in the UCF, justifying the fact that this heave is usually not included in the design of a UCF. A fictive E-modulus is often used to describe the cracked behaviour of steel fibre reinforced concrete. It was shown that using this fictive E-modulus in the building phase leads to an underestimation of the shear forces.

Additionally, a sensitivity analysis was done to show which parameters influence the calculation results, the design and the suitability of a permanent SFRUCF. The suitability of an SFRUCF is determined by the column loads in the final phase and the presence of a stiff raft. It was concluded that an SLS check should be included in the CUR 77 for water tightness, crack width and deformations if an SFRUCF is to be used permanently. The interaction between the raft can be modelled in Plaxis 2D with the plate element that has the behaviour of SFRC. For cases that do not include a stiff raft simpler models can be used such as the Plaxis model with springs or even a beam model with SFRC input.

Symbols

σ	Total Stress
σ'	Effective Stress
ϵ	Strain
C'	Cohesion
ϕ	Friction angle
α_t	shaft friction factor
$E_{50;ref}$	Secant stiffness in standard drained triaxial test
$E_{oed;ref}$	Oedometer stiffness
$E_{ur;ref}$	Unloading and reloading stiffness
$G_{0;ref}$	Small strain shear stiffness
$\gamma_{s;0.7}$	strain at which the secant shear modulus has reduced to about 70% of G_{0ref}
Δl_{el}	Elastic elongation
H	Pressure head
M	Bending moment
M_{max}	Maximum positive bending moment
M_{min}	Minimal negative bending moment
u	Deformation
Δu	Difference between maximal and minimal deformations
V	Shear force
V_{max}	Maximum shear force
N	Axial force
K	Curvature
E	Young's modulus
A	Cross-section
EA	Axial stiffness
EI	Bending stiffness
G	Shear modulus
w	Weight
ν	Poisons ration
C25/30	Concrete class
$f_{ctm,fl}/f_{ft1}$	average bending tensile strength
f_c	Compressive strength
f_{ft3}	Residual tensile strength
$f_{fctk,eq3} / f_{fctk,eq2}$	Average equivalent bending tensile strength
γ_{cc}	Safety factor concrete in compression
γ_{ft}	Safety factor concrete in tension
f_{tun}	Ratio of residual vs. peak tensile strength
L_{eq}	Equivalent length related to the mesh size
$L_{spacing}$	Centre to centre pile distance
γ	Unit weight
D	Diameter pile
T_{skin}	Axial skin resistance embedded beam
F_{max}	base resistance embedded beam
ISF	Interface stiffness factor

Abbreviations

ULS	Ultimate limit state
SLS	Serviceability limit state
UCF	Underwater concrete floor
SFRC	Steel fibre reinforced concrete
SFRUCF	Steel fibre reinforced underwater concrete floor
FEM	Finite element method

TABLE OF CONTENTS

1	Introduction	- 9 -
1.1	Brief introduction on underwater concrete floors	- 9 -
1.2	Recent developments in underwater concrete floor systems	- 9 -
1.3	Permanent SFRUCF	- 9 -
1.4	Current SFRUCF modelling techniques	- 10 -
1.5	Goal	- 10 -
1.6	Modelling possibilities	- 10 -
1.7	Check model results with measured field data	- 10 -
1.8	Sensitivity analysis	- 10 -
1.9	Research questions	- 10 -
2	Literature study	- 11 -
2.1	Current guidelines	- 11 -
2.2	Piled raft foundation	- 11 -
2.3	Steel fibre reinforced concrete	- 13 -
2.4	Behaviour of the shotcrete model	- 14 -
2.5	SCIA steel fibre reinforce module	- 15 -
2.6	Plate element in Plaxis 2D	- 15 -
2.7	Behaviour of the embedded beam row	- 16 -
2.8	Case study	- 17 -
3	Moment Axial force-curvature diagram steel fibre reinforced concrete	- 19 -
4	Albert Cuyppgarage case study	- 23 -
4.1	Introduction Albert Cuyppgarage	- 23 -
4.2	Function of the UCF	- 25 -
4.3	Monitoring data water head	- 25 -
4.4	Uplift monitoring data of the SFRUCF	- 26 -
4.5	SLS calculation	- 27 -
4.6	Plaxis input	- 27 -
4.7	Plaxis output	- 29 -
4.8	Heave	- 29 -
4.9	MN-k input	- 32 -
4.10	Compare Plaxis calculation to monitoring results	- 34 -
4.11	Conclusion Albert Cuyppgarage	- 35 -
5	Albert Cuypp garage micro piles	- 37 -
5.1	Failure test results	- 37 -
5.2	Suitability test results	- 37 -
5.3	Embedded beam row	- 39 -

-Soil-structure interaction of a permanent steel fibre reinforced underwater concrete floor system-

5.4	Pile spacing.....	- 40 -
5.5	Fitting the data in Plaxis	- 40 -
5.6	Complete Plaxis model.....	- 42 -
5.7	Conclusion embedded beam.....	- 43 -
6	Sensitivity analysis	- 45 -
6.1	Primary model.....	- 45 -
6.2	Output sensitivity analysis	- 46 -
6.3	Varied parameters.....	- 46 -
6.4	E-modulus of the SFRUCF.....	- 48 -
6.5	Thickness of the UCF.....	- 50 -
6.6	Heave in the clay layer under the UCF.....	- 50 -
6.7	Stiffness parameters Eemclay.....	- 52 -
6.8	Interface stiffness sheet pile wall.....	- 53 -
6.9	ISF	- 54 -
6.10	Type of GEWI anchor.....	- 55 -
6.11	Load variation	- 56 -
6.12	Stiffness parameters sand.....	- 57 -
7	Discussion.....	- 59 -
7.1	Modelling method.....	- 59 -
7.2	Validation of the Albert Cuyp garage case.....	- 59 -
7.3	Sensitivity analysis	- 59 -
8	Conclusion	- 61 -
9	Recommendations for further research	- 63 -
10	References.....	- 64 -
Appendix A	Python script for determining the MN- κ diagram	
Appendix B	Monitoring data pressure head under the UCF	
Appendix C	Monitoring data of the SFRUCF Albert Cuypgarage	
Appendix D	Plaxis Input stages Albert Cuypgarage	

1 Introduction

1.1 Brief introduction on underwater concrete floors

In large parts of the Netherlands the ground water level is just below surface level. When an excavation is done for a subsoil building a watertight layer is needed at the bottom of the excavation. If there is no watertight soil layer present at the required height a wet excavation with underwater concrete can be a solution. The soil is excavated underwater while the water level remains the same. After excavation a concrete floor is poured at the bottom of this building pit. After the concrete slab is hardened the water can be pumped out of the building pit. The underwater concrete floor usually has a temporary function.

1.2 Recent developments in underwater concrete floor systems

Most of the building pits that are realised with under water concrete floors have two floors. The first floor is the underwater concrete floor itself. This floor is used as a temporary floor to create a dry building pit. When the building pit is dry a normal reinforced concrete floor is created on top of the underwater concrete floor. This second floor is calculated as if there is no underwater concrete floor underneath. This is not an economical nor a sustainable solution. Due to the introduction of steel fibre reinforced concrete other floor systems became possible (Figure 1). The integrated floor system has been used in several projects. The Albert Cuyppgarage and an underpass in Zevenaar are examples of projects where the integrated floor system was used successfully. Additionally, the Dry dock "Royal Van Lent", which is under construction at the moment, uses the integrated floor system. Multiple projects that used steel fibre reinforced underwater concrete floors (SFRUCF) did not have as much leakage as was expected. The Groninger forum and the Mauritshuis are examples of projects where the leakage was less than expected (ir. Ruud Arkesteijn, 2013). The question arises whether a second floor on top of the steel fibre reinforced floor is always necessary.

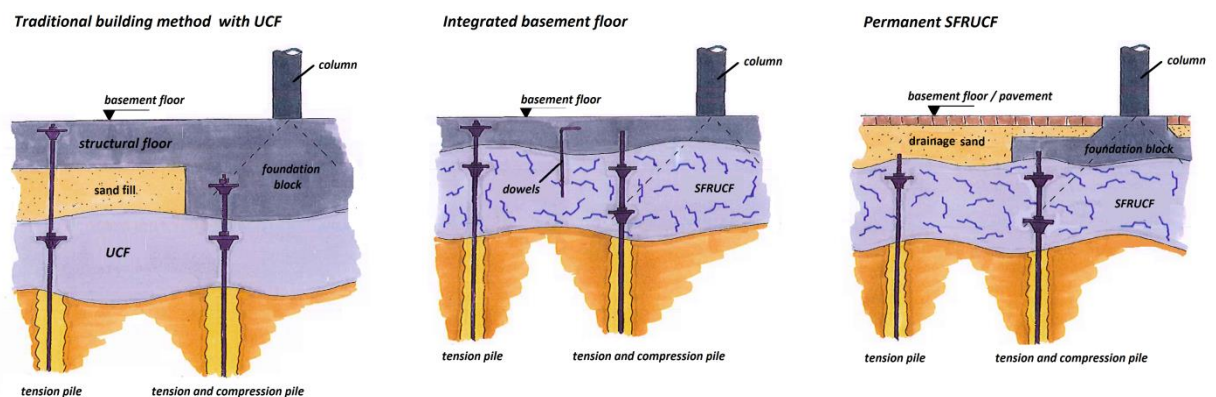


Figure 1 sketch of different underwater concrete floor systems. Modified figure from abt.eu (ir. Ruud Arkesteijn)

In 2014 a pre-advice committee performed a feasibility study for the permanent underwater concrete floor system. In 2016 they concluded that this floor system should be technically feasible, depending on specific project specifications (SBRCURnet, 2016). The difficulties are acceptance, mitigation of the risk of leakages and fatigue but the committee concluded that these difficulties can be solved.

1.3 Permanent SFRUCF

When a UCF is used only temporarily the main load on the UCF is the water pressure underneath the floor. However, when an SFRUCF is used permanently it might be loaded with high column loads as well. Due to steel fibres instead of traditional reinforcement the deformations are expected to be larger. Due to these large deformations it is expected that the soil in between the piles plays a bigger role in the load distribution of the SFRUCF. When the piles and the soil both play a role in the load distribution the foundation is a piled raft foundation.

1.4 Current SFRUCF modelling techniques

The most common modelling techniques consist of two separate calculations for the UCF and the soil behaviour. For the soil behaviour a Plaxis or a D-sheet piling calculation is done. The UCF is modelled as a load and a strut. The load is the weight of the concrete floor and the strut represents the total axial force that can be handled by the concrete floor. The second calculation is done with a structural program such as SCIA. With this calculation method there is almost no interaction between the structure and the soil.

1.5 Goal

This thesis focusses on developing a model that describes the interaction of a permanent SFRUCF system with the soil and also takes into account the non-linear behaviour of the SFRUCF. The aim of the model is to determine the most important parameters that influence the design of such a floor. With this knowledge the ideal circumstances for the permanent UCF can be defined and the influence of the soil underneath the SFRUCF can be determined.

1.6 Modelling possibilities

The current modelling techniques do not include the complex behaviour of steel fibre reinforced concrete nor do they account for the soil structure interaction between the raft and the UCF. Three different modelling techniques were investigated on suitability for modelling a permanent SFRUCF system.

- Plaxis volume model for steel fibre reinforced concrete (Concrete model)
- SCIA steel fibre reinforced concrete module
- Plaxis plate model with MN-κ input

1.7 Check model results with measured field data

Conclusions based on FEM (finite element method) calculations only are not conclusive without verification with field data. Therefore, the model outputs were compared to measured data from a building pit in Amsterdam: the Albert Cuypgarage. The Albert Cuypgarage is a two story deep parking garage underneath one of the canals in Amsterdam. It was built with an integrated UCF floor. During the dewatering phase of this building pit the upward deformations of the SFRUCF were measured. During this dewatering phase the structural floor on top of the SFRUCF was not poured yet, so the field data reflect the behaviour of the SFRUCF only. Additionally, the micro piles were subjected to a load test before the SFRUCF was poured. The combination of the pile load tests and the deformations of the SFRUCF was used to validate the model.

1.8 Sensitivity analysis

The important design parameters of a building pit with SFRUCF were visualized by means of a sensitivity analysis. This analysis had two main goals. The first goal was to determine the sensitivity of the FEM model itself. What are the differences between the measured data and the calculated values and which parameters could be responsible for these differences. The second goal was showing the best conditions of the use of a permanent SFRUCF and what determines these conditions.

1.9 Research questions

This thesis answers the following research questions. The main question is:

What determines the suitability of a permanent steel fibre reinforced underwater concrete floor and how can the soil structure interaction of this non-linear steel fibre reinforced underwater concrete be modelled?

Sub questions:

1. What is a good modelling method to describe the soil structure interaction of an SFRUCF?
2. A fictive E-modulus of 10.000 MPa is often used as an assumption for the cracked stiffness. What is the effect of this assumption?
3. Which parameters have the most influence on the design of an SFRUCF system?
4. How does the static load distribution work in such a floor system? And can it be seen as a piled raft foundation?
5. What are the best conditions to apply a permanent SFRUCF instead of the traditional or integrated principal?
6. What should change in the current guidelines to implement a permanent SFRUCF?

2 Literature study

2.1 Current guidelines

For current building pits a UCF is designed using the CUR 77 (CUR, 2014). This CUR is a guideline for the design of an unreinforced UCF that is used only temporarily. Because of its temporary function the floor is allowed to have some leakage. In contrast to the structural floor on top of the UCF, the crack width and the deformations of the UCF are not checked. Therefore, only ULS calculations are required for the temporary UCF. According to the CUR 77 the UCF can be designed with a linear elastic beam model.

The latest development of the integrated basement floor uses a UCF reinforced with steel fibres as a permanent part of structural floor. The SFRUCF and the structural floor are connected with dowels (Figure 1). For the design of the SFRUCF a combination of CUR 77 and CUR 111 is used. CUR 111 is a guideline for the design of steel fibre reinforced stockroom floors (CUR, 2007). The SFRUCF is also designed for the ULS only. The integrated floor is then calculated in both ULS and SLS. In projects of ABT the same beam model that was prescribed by CUR 77 was used to design an SFRUCF. The calculation remained linear elastic and a fictive E-modulus of 10.000 MPa was used.

2.2 Piled raft foundation

It was expected that a permanent SFRUCF will behave as a piled raft foundation. Three types of piled raft foundations are defined (Figure 2) (H.G.Poulos, 2001):

- Type 1: combined pile raft foundation
The bearing capacity of the piles is calculated with the normal safety factors and the load is mainly taken by the piles.
- Type 2: Piles as settlement reducers
For this type of foundation the bearing capacity of the piles is not checked in the ULS. This type is mainly interesting when the settlements are dominating the design instead of the bearing capacity.
- Type 3: Piles as targeted settlement reducers
This type is used when differential settlements are governing the design. By placing piles at the locations where the largest settlements are expected the differential settlements can be controlled.

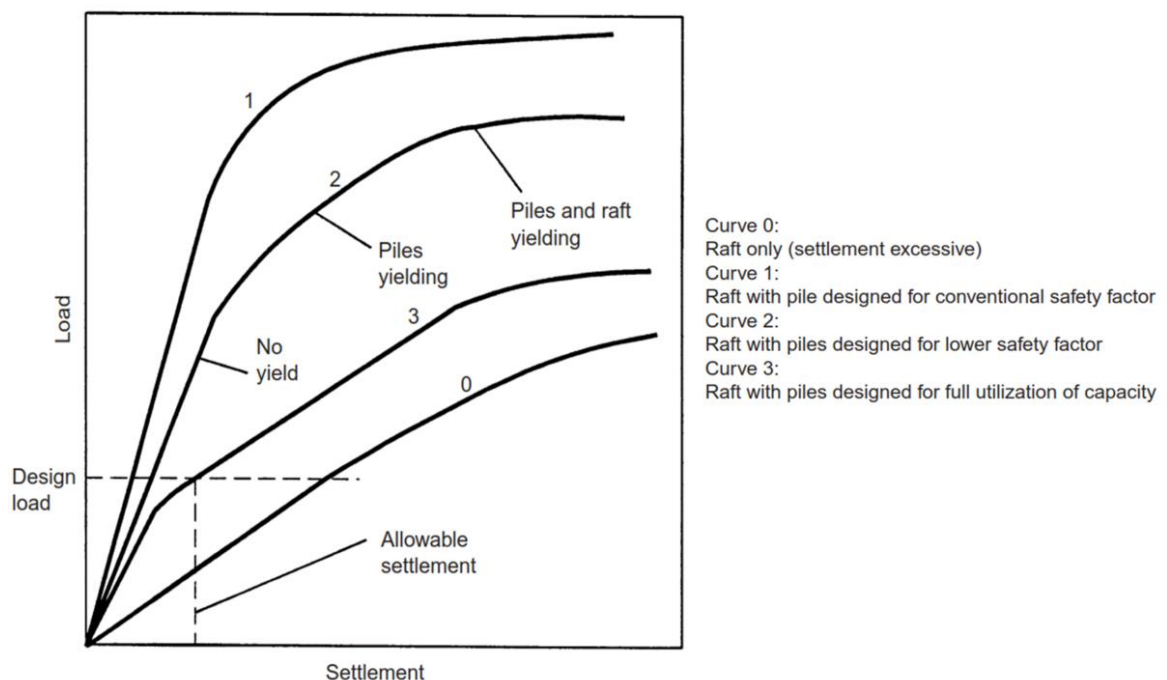


Figure 2 Three types of piled raft foundations (H.G.Poulos, 2001)

-Soil-structure interaction of a permanent steel fibre reinforced underwater concrete floor system-

It was expected that the permanent SFRUC is suitable for the piled raft foundation design type 2. Taking into account the bearing capacity of the soil underneath high column loads might reduce the pile loads, as well as the deformations and bending moments within the UCF.

The soil should be reasonably stiff and not inclined to creep under loading (SBRCURnet, 2017). In the Netherlands there are multiple locations that are suitable for a piled raft foundation due to a sand/Silt layer at surface level or at shallow depth. Also highly overconsolidated clay layers can be used for a piled raft design.

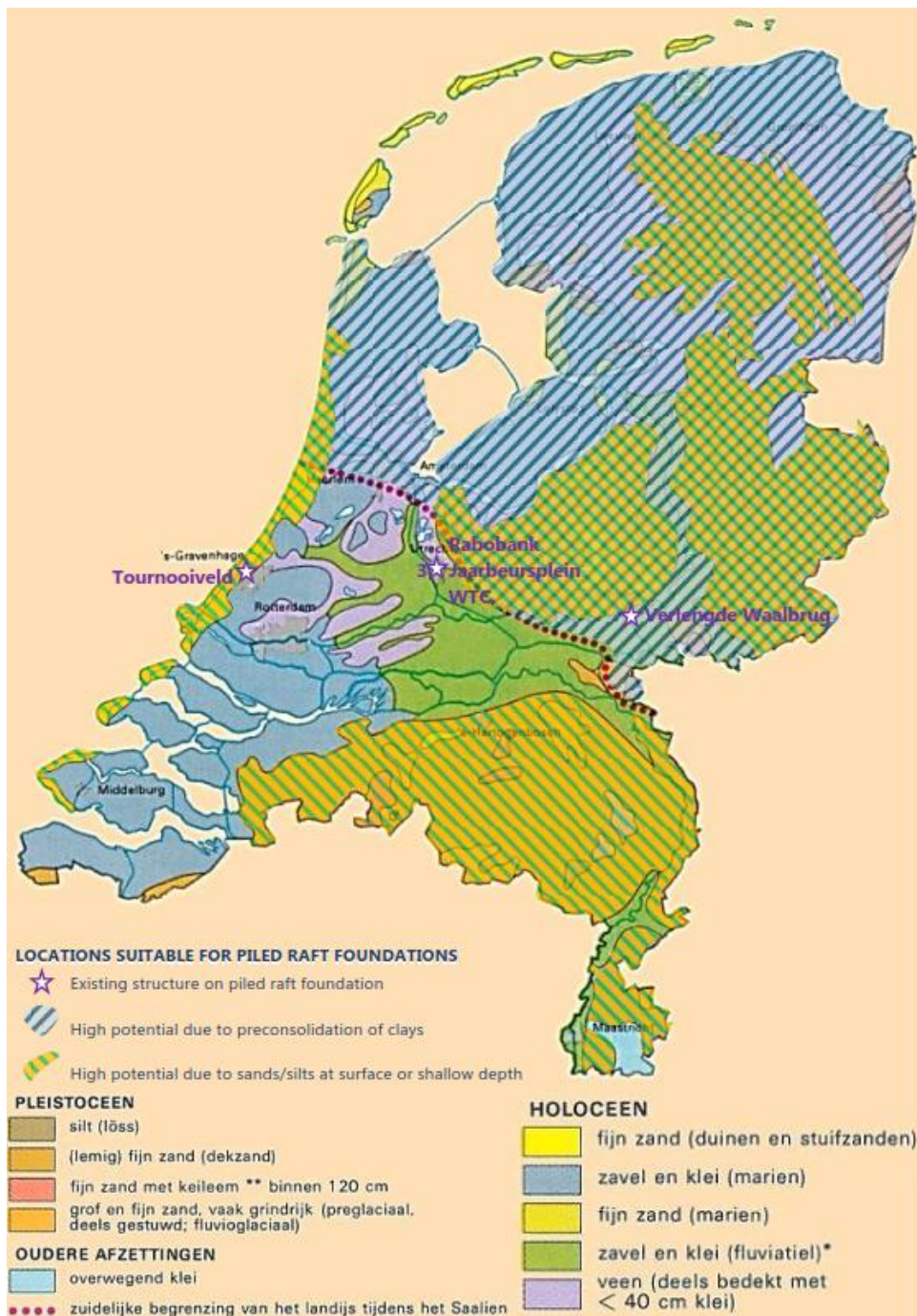


Figure 3 Locations within the Netherlands that are suitable for a piled raft foundation (SBRCURnet, 2017)

-Soil-structure interaction of a permanent steel fibre reinforced underwater concrete floor system-

The CUR committee had the following recommendations for modelling a piled raft foundation.

- The hardening soil model should be used to model the raft.
- The hardening soil small strain model should be used for modelling the soil directly under the pile tips.
- Allow gapping should be switched on to allow for a gap to occur when the UCF is lifted due to the water pressure.

2.3 Steel fibre reinforced concrete

Using traditional reinforcement in underwater concrete is not preferred because placing the reinforcement bars under water makes the execution very difficult. This is why traditional underwater concrete floors were unreinforced. Some of these UCFs had continuous cracks due to the hydration of the concrete. To resolve this issue, steel fibres can be added to the concrete to increase the tensile strength and the ductility of the concrete (A.G. Kooiman, 2000). The fibres reduce the crack formations during the first days of the hydration.

The main advantage of adding steel fibres is the post cracking tensile strength. Depending on the amount of fibres tension softening or tensions hardening can be obtained (Figure 4). For tension hardening at least one volume percent of steel fibres is needed. For bending hardening this volume percentage is around 0.5% (ir. Ruud Arkesteijn, 2013). The common steel fibre percentage in a UCF is around 0.5% which means that tension softening occurs in combination with bending hardening. This bending hardening can be seen in Chapter 3 where an MN- κ diagram was derived.

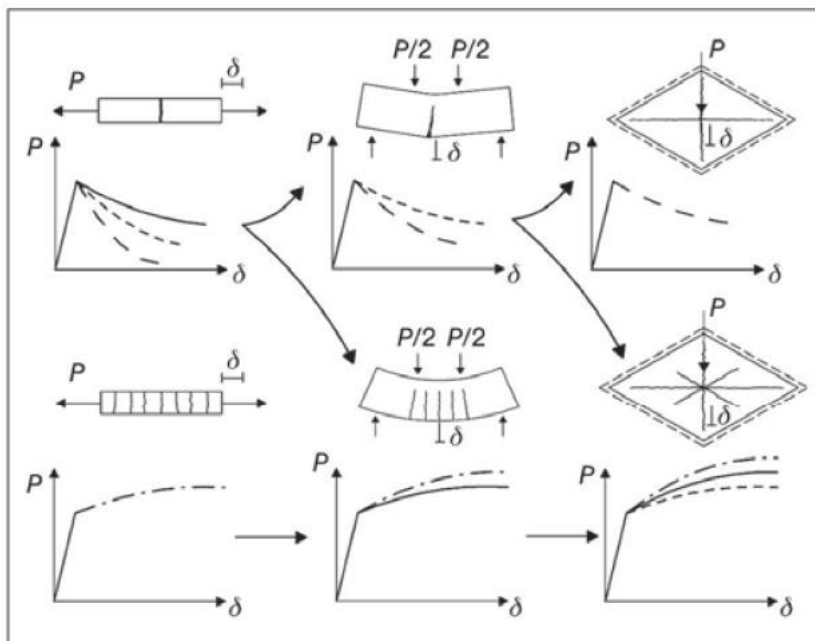


Figure 4 Different responses of structures made of fibre reinforced concrete having softening or hardening behaviour under uniaxial tension or bending loads (CEB-fib model code 2010, 2013).

For normal strength steel fibre reinforced concrete the behaviour of steel fibre reinforced concrete in compression is the same as normal concrete. For high strength concrete the behaviour might be different but that is not the scope of this research. The behaviour in tension is influenced by the post cracking tensile strength. The stress strain diagram shows that the post cracking behaviour is determined by the average equivalent bending tensile strength $f_{fctk,eq3}$ and $f_{fctk,eq2}$ (Figure 5). This average equivalent bending tensile strength should be determined with a three point bending test. The amount of steel fibres follows from the desired average equivalent bending tensile strength. For the behaviour of the SFRC the CUR 111 was used, which is a guideline for the practical use of SFRC.

-Soil-structure interaction of a permanent steel fibre reinforced underwater concrete floor system-

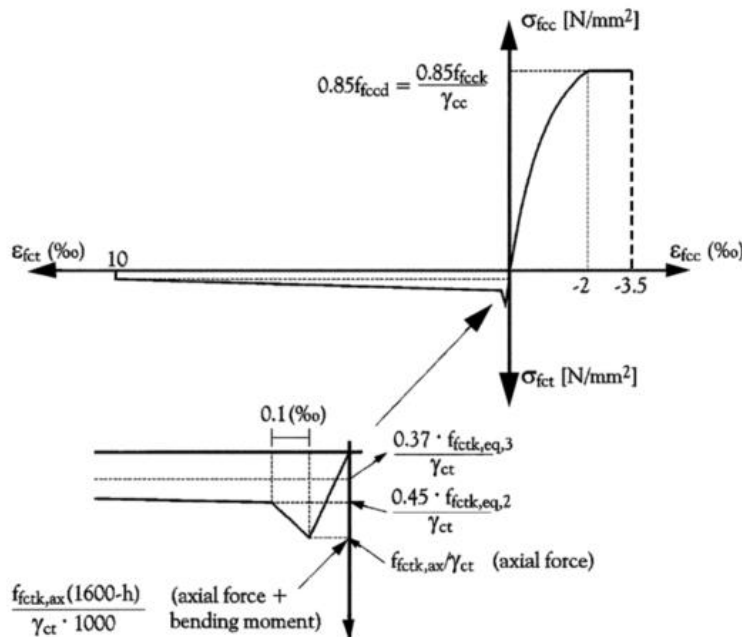


Figure 5 Behaviour of steel fibre reinforced concrete (A.G. Kooiman, 2000)

The static behaviour of steel fibre reinforced concrete is known and described in a detailed way by the existing literature (A.G. Kooiman, 2000). However, both the dynamic behaviour and the fatigue behaviour of SFRC are still uncertain. The existing literature on these subjects contains a lot of contradictions and it is not possible to draw conclusions that can be used in this research. The dynamic behaviour and the fatigue behaviour are not in the scope of this research.

2.4 Behaviour of the shotcrete model

At the time of this thesis the shotcrete model was not officially implemented in Plaxis. From 2018 the shotcrete model was introduced as the concrete model in Plaxis. The shotcrete model can be used for modelling unreinforced concrete. For unreinforced concrete there is no softening behaviour in the tension zone. However, the shotcrete model provides a parameter that includes the softening behaviour. The parameter f_{tun} describes the ratio of residual vs. peak tensile strength. The stress strain relation of steel fibre reinforced concrete in tension shows comparable behaviour to the shotcrete model due to the softening behaviour (Figure 6).

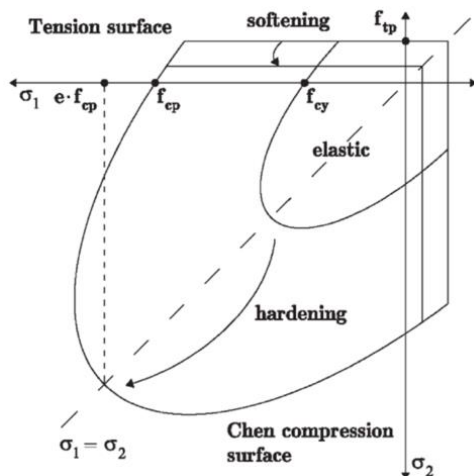


Figure 6 Compression and tension yield surfaces of the shotcrete model (R. Schütz, 2011).

-Soil-structure interaction of a permanent steel fibre reinforced underwater concrete floor system-

It should be noted that the shotcrete model is a volume model. The concrete is modelled as the actual volume of the concrete instead of a thin slab. When the concrete cracks due to tension the steel fibres take over the load. This softening behaviour is modelled with the fracture energy (R. Schütz, 2011). The fracture energy is depicted as the grey area under the σ - ϵ graph in Figure 7.

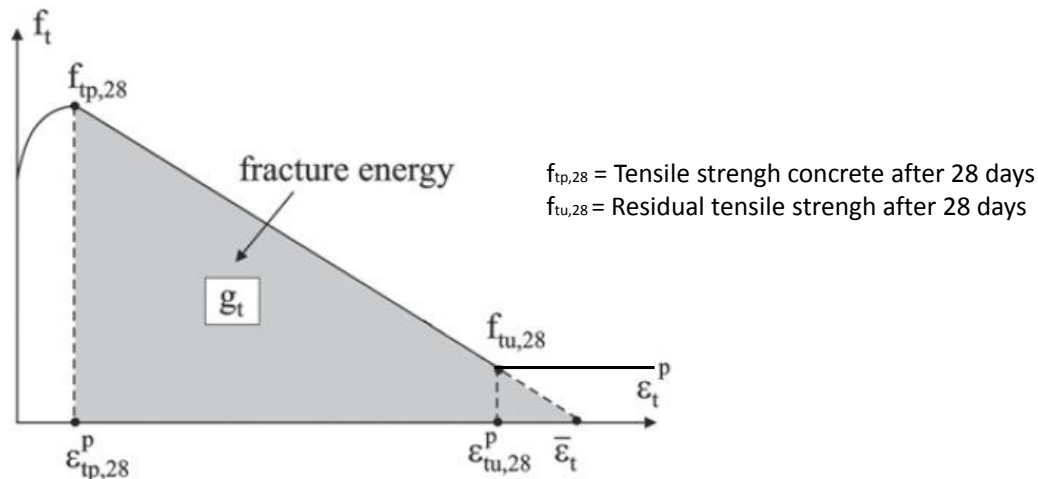


Figure 7 Determination of the fracture energy for the shotcrete model (R. Schütz, 2011)

When the softening behaviour occurs cracks can be observed in the volume element. The behaviour of this model depends on the crack formation. Due to the formation of small cracks a very fine mesh is needed which is not suitable for modelling a complete building pit. The model has lots of complex input parameters that are difficult to determine such as the fracture energy and the L_{eq} (Equivalent length related to the mesh size). Additionally, the internal forces (bending moments and shear force) are difficult to retrieve.

It was never investigated if the shotcrete model could be used to model SFRC. For this research an analysis was done to check the suitability of this model. The shotcrete model gave an overestimation of the expected bending moment capacity of 20%. The main reason why this model was not used is the following warning in the Plaxis manual. Softening behaviour with a small fracture energy could influence the convergence of the Plaxis calculation. The crack initiation massively increases the global error even though the step size is gradually reduced by the global iteration procedure (Plaxis, 2018).

Even though the input parameters gave the impression that this shotcrete model would be perfect to model SFRC, the suitability is questionable. The focus of this thesis was on the interaction between the soil and a permanent SFRUC. It was therefore decided that this complex model was unnecessary for modelling this behaviour. Other tools such as the plate element are more suitable for modelling a complete building pit.

2.5 SCIA steel fibre reinforce module

In 2018 a new SCIA module was created especially for steel fibre reinforced concrete. This module was created in cooperation with Bekaert, one of the manufacturers of the steel fibres. This module uses a slab which was given the behaviour of SFRC. The slab does not have a thickness and the input is comparable with an MN- κ input. The SCIA model cannot describe the behaviour of the soil so this calculations should always be done in an iterative way with a geo-technical calculation. Further in this report the plate element in Plaxis is discussed. A Plaxis plate element can have an MN- κ input and can model the interaction with the soil. Therefore the Plaxis plate element is preferred over the SCIA module. The SCIA module is not used in this thesis but can be a useful tool for situations where the soil interaction is less important.

2.6 Plate element in Plaxis 2D

The plate element is a structural element in Plaxis. The main advantage is the easy access to the output of these plates. Plaxis output can plot the bending moments, shear forces and normal forces.

-Soil-structure interaction of a permanent steel fibre reinforced underwater concrete floor system-

The input can be both linear elastic and non-linear elastoplastic M- κ (bending moment-curvature) (Table 1). According to the Plaxis manual the bending moments are not influenced by the normal force in the structure. Only the M- κ input determines the bending moments. This means that the normal force should be included in the M- κ diagram.

Table 1 Input parameters of the plate element

	Linear elastic	Elastoplastic	Unit
Axial stiffness	EA	EA	kN/m
Bending stiffness	EI	M- κ diagram	kNm ² /m
Weight	W	W	kN/m/m
Poissons ration	ν	ν	-

2.7 Behaviour of the embedded beam row

For this research the behaviour of the micro piles was modelled with two different methods in Plaxis 2D. The piles were modelled with fixed end anchors and with the embedded beam row (Table 2). A spring stiffness can be given to the fixed end anchor. It should be noted that when such an anchor is used the anchor force is not transferred to the soil, so the model is not in equilibrium.

An embedded beam row models a row of piles. The embedded beam row is not in the 2D mesh but superimposed on the mesh while the underlying mesh is continued (Plaxis, 2018). Due to this superimposed position the soil can flow through the piles. The embedded beam row is wished in place and the installation effect is not taken into account. For displacement piles it is important to properly evaluate the pile skin friction.

The embedded beam row has the bearing capacity as input parameters (Table 2). The lateral and axial skin resistance are input parameters and these must be calculated by the engineer. The maximum skin resistance can be inputted in 3 different ways. Firstly, with a linear input the skin resistance at the top and bottom is needed and is interpolated linearly. Secondly, with a multilinear input the user can define a tabulated input for the skin resistance. Lastly, a layer dependent input can be used, where Plaxis determines the skin resistance with the friction angle and the cohesion of the surrounding soil (φ_{soil} , c_{soil}).

Table 2 Input parameters for fixed end anchor and embedded beam row

	Fixed end anchor	Embedded beam row	Unit
Axial stiffness	EA	-	kN
Centre to centre distance	$L_{spacing}$	$L_{spacing}$	m
E-modulus	-	E	kN/m ²
Unit weight	-	γ	kN/m ³
Diameter	-	D	m
Area	-	A	m ²
Axial skin resistance	-	T_{skin}	kN/m
Base resistance	-	F_{max}	kN
Interface stiffness factor	-	ISF	-

The lateral stiffness of the pile was calculated by Plaxis. The lateral stiffness is determined by the shear modulus of the soil, the spacing of the piles and the interface stiffness factor (Figure 1). The interface stiffness factor is normally calculated by Plaxis and depends on the pile spacing and the pile diameter, but this does not take into account the installation effect of the micro piles. For this research the ISF was changed manually to take into account the installation effect.

-Soil-structure interaction of a permanent steel fibre reinforced underwater concrete floor system-

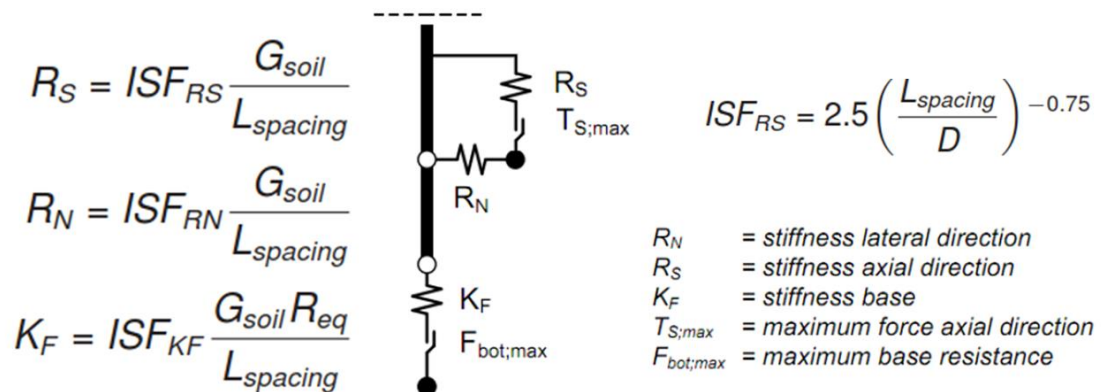


Figure 8 Stiffness of the embedded beam (Plaxis, 2018)

The suitability for micro piles of the 2D embedded beam row model was investigated and compared to that of the 3D model. The load displacement diagram of the pile behaviour in both Plaxis 2D and 3D fitted to failure load tests on micro piles. It was therefore concluded that both Plaxis 2D and Plaxis 3D are suitable to model micro piles. However, the 3D volume element gives the opportunity to model the installation effect as well, which gives a more realistic stress and displacement distribution in the soil (Molendijk, 2017). In the study of Molendijk (2017) the micro piles had a length of 23 m and the grout body was only 5 m. It should be noted that the displacements were dominated by linear elongation of the free anchor length. In this study, however, the free anchor length was almost zero, which makes it more difficult to fit the load displacement behaviour of Plaxis to the measured data.

Another study compared the behaviour of a 2D embedded beam row to a 3D embedded beam. The ISF values were used to fit the pile behaviour in Plaxis 2D to the pile behaviour in Plaxis 3D (J.Sluis, 2012). The ISF derived in this study is now used as the custom ISF in Plaxis (Figure 34). It should be noted that this study was done for bored piles, for which the embedded beam row is mainly suitable. The micro piles probably have a different behaviour because they are grouted under high pressure.

2.8 Case study

In this thesis the Albert Cuyp garage was used as case study. Max Bögel was the contractor, and ABT and CRUX were responsible for the geotechnical design of the building pit. The deformations of the UCF and the sheet pile walls were monitored and pile load tests were performed (Max Bögl, 2016). The design reports with the sheet pile wall calculation (CRUX, 2015), behaviour of the complete building pit (CRUX, 2015), the foundation advise (CRUX, 2015) and the design of the UCF (ABT, 2016) were used as a basis for the case study. The geometry, soil layers, sheet pile wall types, GEWI types and locations and geometry of the building pit were taken from these design reports. In the design report of ABT (2016) the UCF was calculated with a fictive E-modulus. The implications of such an assumption are investigated in this research.

-Soil-structure interaction of a permanent steel fibre reinforced underwater concrete floor system-

3 Moment Axial force-curvature diagram steel fibre reinforced concrete

The behaviour of steel fibre reinforced concrete can be described in the form of an Moment axial force-curvature graph MN- κ . This MN- κ can be used for comparison with the shotcrete model or as input in the Plaxis Plate model. The method used to derive the analytic M- κ diagram is an extended version of the method proposed by CUR 111 (Figure 9 and Figure 10). The following assumptions were made in order to derive an M- κ diagram. Firstly, a bilinear σ - ϵ relationship was assumed for concrete, in order to simplify the analytic calculations. Secondly, a single value was assumed for the post cracking tensile strength, while in reality the post cracking tensile strength decreases from f_{ft2} towards f_{ft3} . This simplification was made because the shotcrete model only has f_{ft1} and f_{ft3} as input parameter.

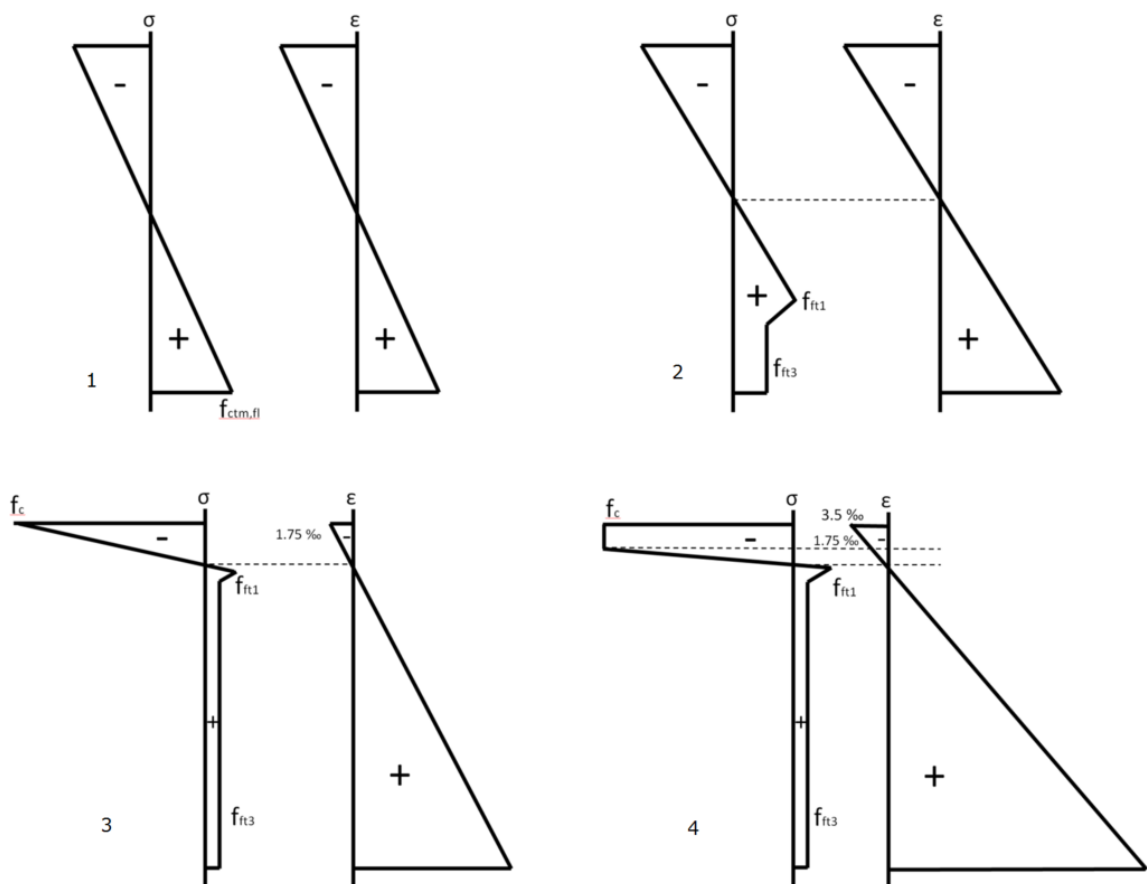


Figure 9 Stress and strain diagrams over the height of a steel fibre reinforced concrete beam in bending in different phases. 1) Concrete tensile strength is reached. 2) Post cracking tensile strength mobilized by steel fibres. 3) Concrete compression strength is reached with a strain of 1.75‰. 4) The ultimate compressive strain (3.5‰) in concrete is reached.

The M- κ diagram is based on the horizontal equilibrium and the moment equilibrium (Figure 10). The M- κ diagram is made with a Python script which is added in appendix A. The main input parameters for this script are width, height, Concrete tensile strength and the residual tensile strength after cracking (Table 3). The same procedure was used to derive the MN- κ diagram.

-Soil-structure interaction of a permanent steel fibre reinforced underwater concrete floor system-

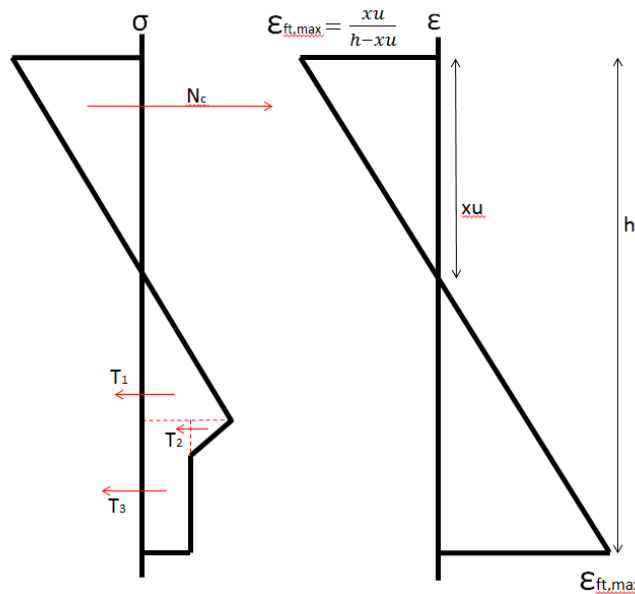


Figure 10 Stress strain cross-section used for horizontal force and moment equilibrium in order to derive the M-κ diagram.

Table 3 Input parameters MN-κ diagram

Parameter		Unit
b	Width	m
h	Height	m
E	Young's modulus	kN/m ²
f _c	Concrete compressive strength	kN/m ²
f _t	Concrete tensile strength	kN/m ²
f _{tp}	Residual tensile strength	kN/m ²
N	Normal force in the UCF	kN
Y _{cc}	Safety factor concrete in compression	-
Y _{ft}	Safety factor concrete in tension	-

The ultimate phase of this diagram is determined by the maximum compressive strain in the concrete. But another mechanism might play a role in the failure of steel fibre reinforced concrete. The pulling out of the fibres will also result in failure. The pull out of the steel fibres depends on the strain and on the thickness of the plate (Figure 11) (Bos, 2011).

The steel fibre reinforced UCF from the Albert Cuyp garage is used to create an SLS MN-κ diagram as an example (Figure 12). The input parameters for this graph are based on the design reports from ABT (see chapter 4).

-Soil-structure interaction of a permanent steel fibre reinforced underwater concrete floor system-

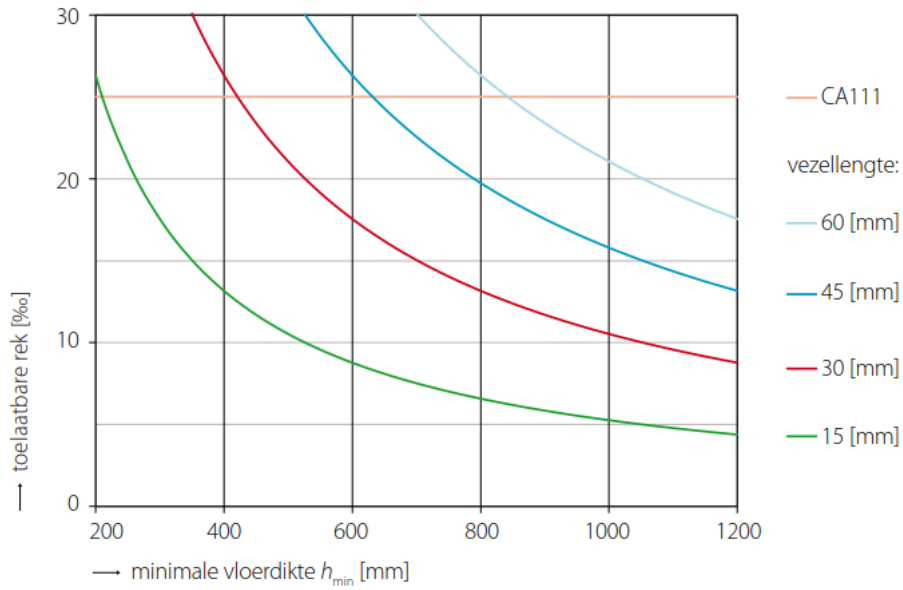


Figure 11 maximum allowable strain to prevent pull out (Bos, 2011).

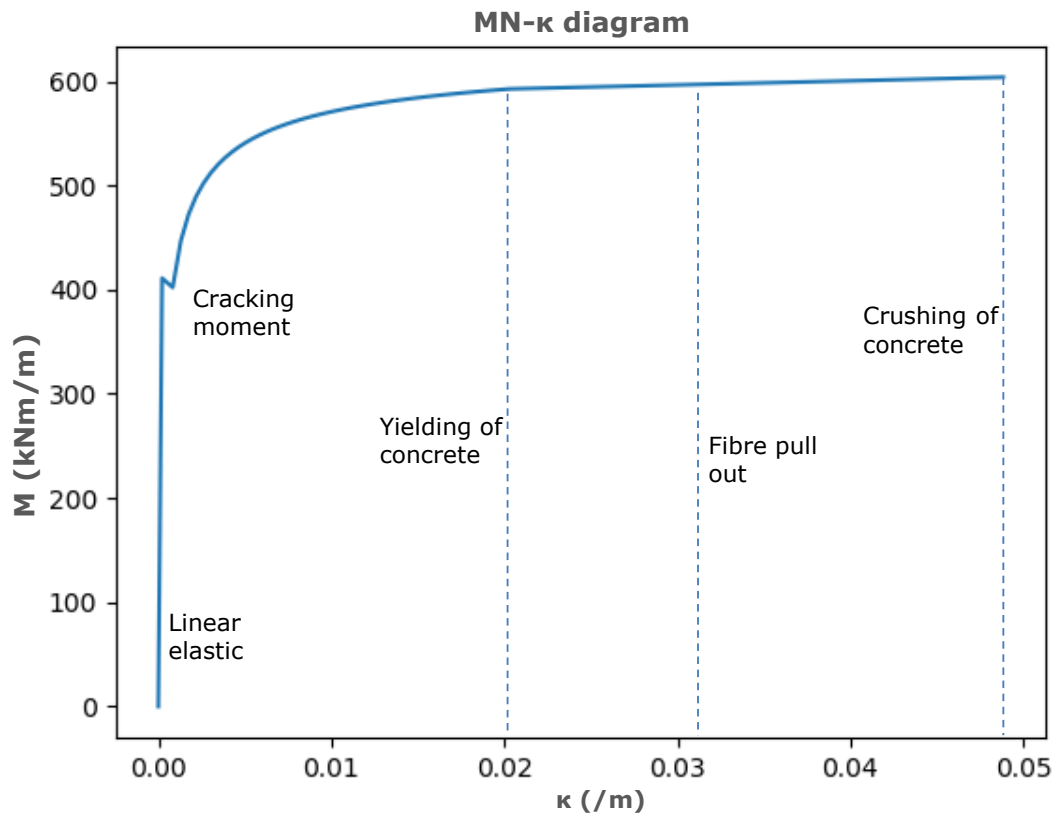


Figure 12 MN- κ example

-Soil-structure interaction of a permanent steel fibre reinforced underwater concrete floor system-

-Soil-structure interaction of a permanent steel fibre reinforced underwater concrete floor system-

4 Albert Cuyppgarage case study

To determine the soil structure interaction of a steel fibre reinforced underwater concrete floor (SFRUCF) system a sensitivity analysis is necessary. To make sure the modelling technique used is correct, a known input case was validated. For the validation the Albert Cuyppgarage was used. The Albert Cuyppgarage was a building pit of 10 m deep (dimensions: ±30m x ±260m). The uplift of the concrete floor and the water head underneath the underwater concrete floor (UCF) were monitored during the construction phase. The building pit length of 260 m makes it suitable for 2D calculation.

4.1 Introduction Albert Cuyppgarage

The Albert Cuyppgarage is a two layer parking garage underneath a canal in Amsterdam (Figure 13a). This garage was one of the first structures that was built with an integrated underwater concrete floor system (Figure 13b). The steel fibre reinforced underwater concrete floor was connected to the structural floor with dowels. Because the monitoring took place during the dewatering phase, which means without the structural floor, the data can be used to validate the modelling techniques of the UCF alone.

CRUX Engineering B.V. was responsible for the geotechnical design, which was summarised in the following three reports:

- RA14153c2 Resultaten UO damwandberekening (CRUX, 2015),
- RA14153e1 Totaal gedrag bouwkuip – incl. paalfundering (CRUX, 2015)
- RA14153f2 UO Funderingsadvies (CRUX, 2015)

The integrated underwater concrete floor system was designed by ABT and the results were summarised in the following report:

- 13722G UO Geïntegreerde keldervloer (ABT, 2016)

For all the calculations in this study the input parameters from the reports were used, unless the monitoring data contradicted this input.



Figure 13 a) Cross-section of the Albert Cuyppgarage (ABT, 2016) b) sketch of the Integrated floor system (ABT, 2016)

The input parameters for the UCF are based on the design reports from ABT (Table 4). The concrete class is (C25/30), the average equivalent bending tensile strength is 3.0 N/mm² and the normal force in the concrete is 400 kN.

Table 4 Input parameters MN-κ diagram Albert Cuyppgarage

Parameter		Unit
b	1	m
h	0.9	m
E	3.1*10 ⁷	kN/m ²
f _c	25000	kN/m ²
f _t	2600	kN/m ²
f _{tp}	1100	kN/m ²
N	400	kN
Fibre length	60	mm

-Soil-structure interaction of a permanent steel fibre reinforced underwater concrete floor system-

The soil profile was determined by CRUX for the D-sheet pile calculations (Table 5). This profile was also used in the following calculations. The soil parameters needed for a Plaxis calculation are more advanced than a D-sheet pile calculation and cannot be determined using the information from the CRUX reports. Instead, soil parameters were used from other ABT projects in the area of Amsterdam (Table 6). The soil layers from the ABT projects can be recognized as the same layers that were used by CRUX. Also the constitutive model that corresponds to the properties of each layer was shown (Table 5).

Table 5 Layers with corresponding Plaxis model

Layer [-]	Top of layer [m NAP]	$\gamma_{sat}/\gamma_{dry}$	Constitutive model
Toplayer sand	0.5	17.0/20.0	HS small
Clay organic	-1.0	15.0/15.0	HS
Peat (Hollandveen)	-4.0	10.5/10.5	HS
Clay weak	-4.5	15.0/15.0	HS
Sand loose	-7.0	18.0/20.0	HS small
Clay, silty	-10.0	16.0/16.0	HS
Peat (Basisveen)	-12.0	12.0/12.0	HS
First sand layer	-12,5	20.0/21.0	HS small
Sand with clay layers	-15.0	19.0/19.0	HS
Second sand layer	-17.0	20.0/21.0	HS small

Table 6 Soil parameters in Plaxis (Parameters from projects in the surroundings)

Layer [-]	C' [kPa]	Phi [deg]	$E_{50:ref}/E_{oed:ref}/E_{ur:ref}$ [MPa]	M [-]	$G_{0:ref}$ [MPa]	$\gamma_{s:0.7}$ [-]
Toplayer sand	1	27.5	35/35/105	0.5	114	0.12E-03
Clay organic	1	15.0	2.0/1.0/8.0	1	29	-
Peat (Hollandveen)	1	17.5	0.8/0.4/3.2	1	-	-
Clay weak	1	22.5	2.1/1.05/8.4	1	33	-
Sand loose	1	31.1	60/60/180	0.62	77	0.15E-03
Clay, silty	2	22.5	3.2/1.6/12.8	0.9	55	-
Peat (Basisveen)	0	17.0	0.8/0.4/3.2	1	-	-
First sand layer	0	34.3	100/100/300	0.54	125	0.12E-03
Sand with clay layers	1	27.0	7.5/7.5/22.5	0.8	77	-
Second sand layer	0	34.3	100/100/300	0.54	125	0.12E-03

At the Hobbemakade a sheet pile wall AZ18-700-240 was used and at the Ruysdaelkade a AZ-26-700-240 was used. Because two different sheet pile walls were used and the initial canal was not in the middle of the building pit, the building pit was non-symmetrical.

The UCF was calculated in the design report with a linear elastic beam model in SCIA. A fictive E-modulus of 10.000 MPa was used and an uplift of 14 mm was predicted in the in the SLS situation (Figure 14).

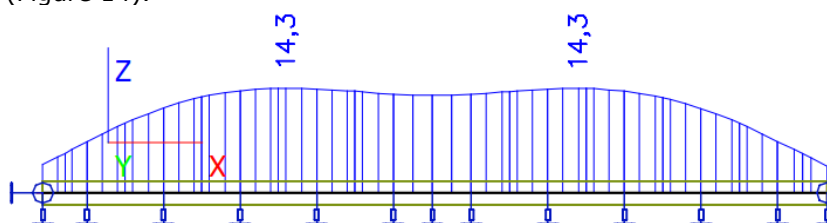


Figure 14 SLS Uplift (in mm) of the UCF over the width according to the design report (ABT, 2016)

-Soil-structure interaction of a permanent steel fibre reinforced underwater concrete floor system-

4.2 Function of the UCF

It is important to know the function of the underwater concrete floor in this particular case. Generally, the main functions of an underwater concrete floor are:

- Water retaining layer
- Horizontal force equilibrium (strut)
- Vertical force equilibrium (uplift / heave)

The function of an underwater concrete floor depends on the soil conditions and the water head under the underwater concrete floor (Figure 15). In this specific case, an impermeable clay and peat layer is present underneath the UCF. Water pressure release pipes are installed through the UCF from the gravel layer under the UCF until a height of NAP -2.75 m. This means that the water head directly under the UCF could not be higher than NAP -2.75 m. Because of these pressure release pipes the design of the UCF in the building stage could be based on an upward force corresponding to the uplift-pressure instead of the naturally present water head. The main functions of the UCF were to prevent uplift of the impermeable layers underneath the floor and to provide horizontal force equilibrium (strut).

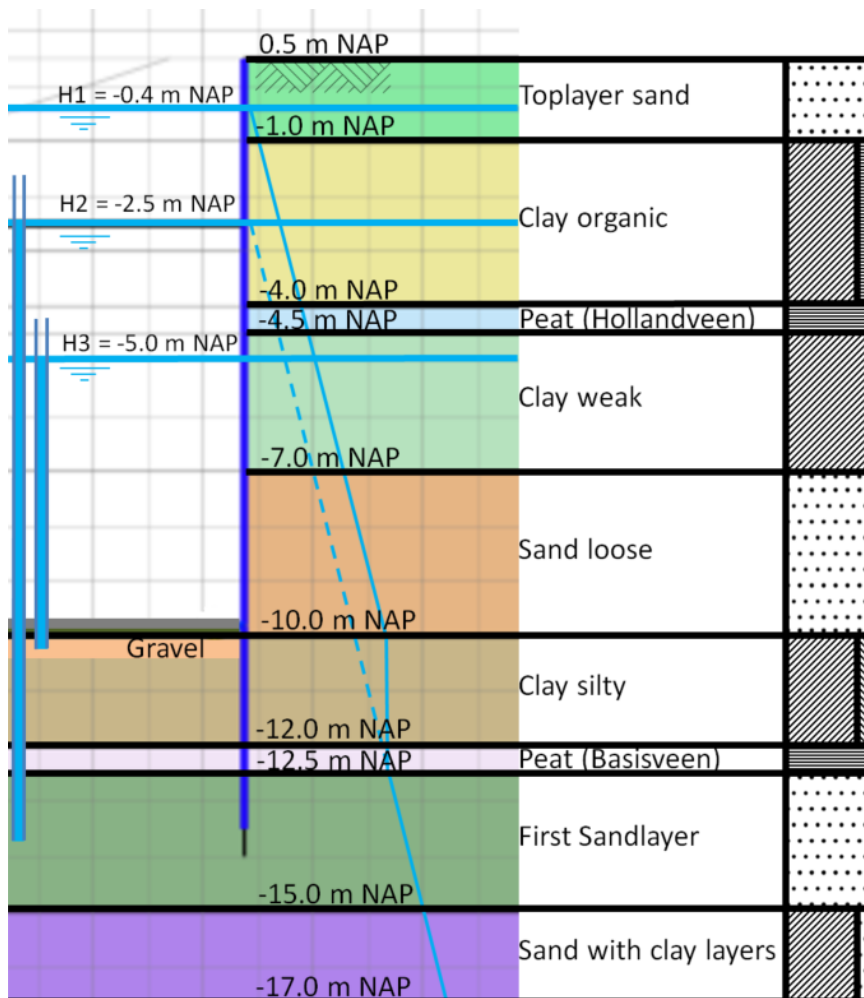


Figure 15 Soil profile and water head

4.3 Monitoring data water head

The water pressure in the gravel layer directly underneath the UCF was measured. The maximum value is NAP -2.75 m but in reality the head dropped towards NAP -5.0 m when the building pit was dewatered. The NAP -5.0 m is the approximated average value of the monitoring data (Appendix B). This can be explained as follows: more leakage occurred through the UCF than through the impermeable clay and peat layers.

-Soil-structure interaction of a permanent steel fibre reinforced underwater concrete floor system-

The displacement of the UCF over the length (Figure 18) cross-section (B-B') is more difficult to explain. With a length of 260 m it was expected that the uplift in the middle parts would be constant, which was not observed. The real cause for this result is unknown but it might be that the heave from the "Eemklei" (Overconsolidated clay layer) has more effect on the middle of the building pit than at other locations.

This monitoring result raises the question whether a 2D calculation is appropriate for this building pit. In this thesis it was assumed that elongating the building pit would not lead to more deformation of the UCF which allows for 2D calculation. It was also assumed that 2D calculations could be very useful for the basic understanding of the soil structure interaction.

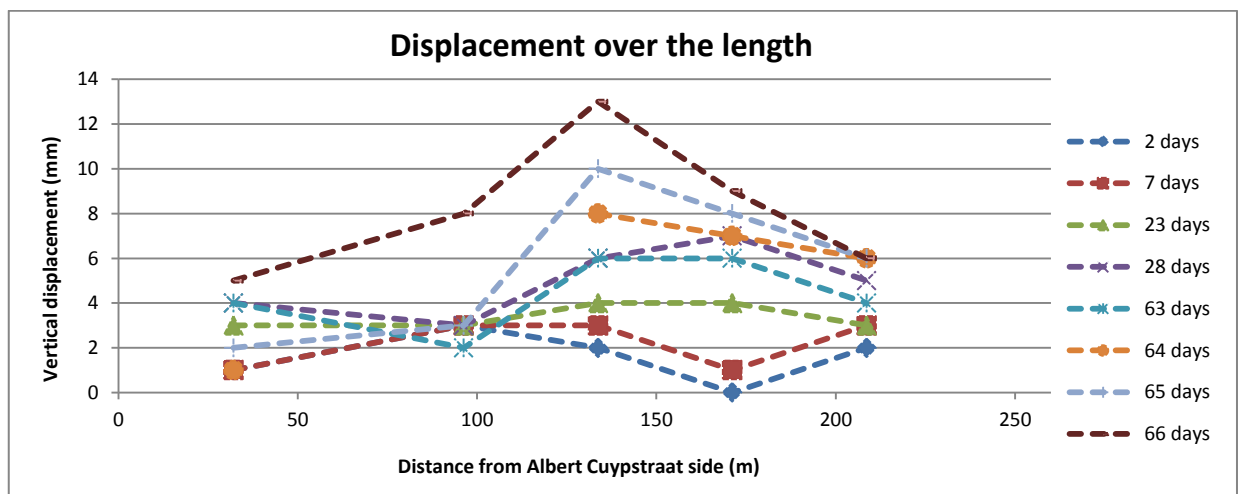


Figure 18 Vertical displacement of the UCF over the length (B-B') of the building pit during dewatering (Max Bögl, 2016)

4.5 SLS calculation

To compare the results of the monitoring data to the model calculation an SLS calculation was performed. However, an SLS calculation alone cannot be compared to the monitoring results. In an SLS calculation a variation factor of $\sqrt{2}$ was applied to the spring stiffnesses of the piles and the spring stiffnesses of the walls. To compare the monitoring results to the calculated values the spring stiffnesses without variation factors were used. Without applying variation factors the maximum deflection in the SCIA calculation is 10.8 mm (Figure 19).

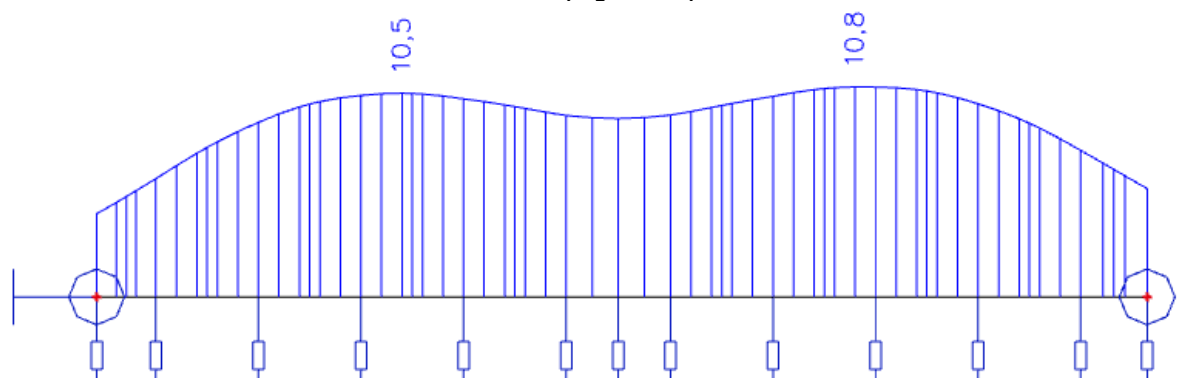


Figure 19 SCIA deformations SLS without variation factors.

4.6 Plaxis input

The soil structure interaction of a permanent UCF was modelled in Plaxis. Subsequently, the Plaxis calculation was compared to the SCIA calculation and the monitoring results. The aim is to achieve a calculation method, taking into account soil structure interaction, that is closer to reality than the current modelling technique with SCIA.

-Soil-structure interaction of a permanent steel fibre reinforced underwater concrete floor system-

The Hardening Soil model was used for cohesive soils because of the importance of a realistic loading, unloading and reloading behaviour. The HSsmall model is used for the non-cohesive soils in order to model the small strain stiffness and the possibility of hysteresis. These models are also advised by the CUR piled raft foundations (SBRCURnet, 2017).

The Plaxis calculation consisted of multiple phases. The different phases are elaborated on in appendix D. The final stage is a dry building pit with a UCF slab (Figure 20). Firstly, the UCF plate was modelled with the self-weight as input parameter. When the plate was activated directly stresses occurred in the plate due to moments in the structure. In reality, however the concrete is poured without initial bending moments that work on the plate. In order to solve this problem the input weight was set to 0 and in the dewatering phase an additional line load was added to take into account the self-weight of the UCF.

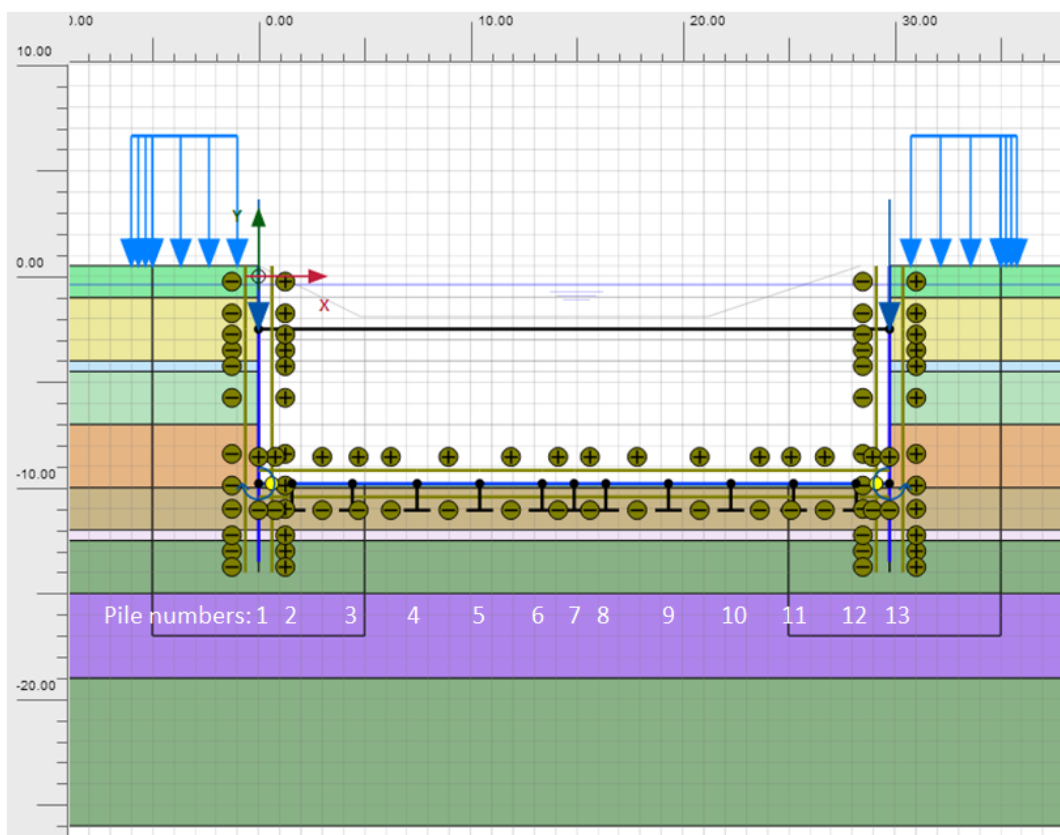


Figure 20 Phase 9: a dry building pit

When installing the UCF plate in Plaxis large vertical deformations occurred during this phase. After the excavation phase, heave occurred in the soil layers at the bottom of the building pit. The plate is then placed on top of this soil and has the same vertical deformation as the soil, but in reality this heave will already take place during the excavation. The soil deformation in the y direction is then excavated. Because of these initial deformations of the plate it is important to look at the phase displacements instead of the total displacements.

For the first calculation the plate was modelled linear elastically with an E-modulus of 10.000 MPa as was used in the original design. Also, the piles were modelled as linear elastic springs. The spring stiffnesses of the GEWI-anchors were determined by CRUX (Table 7). It is important to note that, for the first calculation, the original pile plan is combined with the original pile stiffness. The GEWI-anchors had to be tested in the field to validate the calculated strength. During these tests the anchors failed and more anchors had to be installed. Within the spring stiffness also the group effect is taken into account so placing additional anchors will not have a big effect on the overall stiffness

-Soil-structure interaction of a permanent steel fibre reinforced underwater concrete floor system-

of the piles (per m² of floor). Therefore the calculation was done with the springs and the old pile plan for a first order estimation.

Table 7 Spring stiffness of the GEWI-Anchors

Pile Numbers from left to right (Figure 20)	Pile types	Spring stiffness [kN/m/m]
1	Left sheet pile wall (Only in the SCIA model)	20.000
2	GEWI-63.5 mm	7.100
3,4,5,9,10,11	GEWI-50.0 mm	13.530
6,8	GEWI-63.5 mm	17.700
7	GEWI-63.5 mm	7.520
12	GEWI-63.5 mm	11.800
13	Right sheet pile wall (Only in the SCIA model)	20.000

4.7 Plaxis output

Firstly the Plaxis output was compared to the SCIA calculation. Secondly the results will be compared to the monitoring results. It should be noted that the UCF already has an initial deformation when it is activated in the Plaxis calculation. For the deformations of the UCF the phase deformation should be used instead of the total deformation. The total stress (pore pressure and effective stress) on the UCF was higher in the model than was calculated in advance. The reason for this is explained in chapter 4.8. If the pressure on the floor is the same in both the SCIA and Plaxis calculation the results are almost the same (Figure 21). The main difference between the deformation in Plaxis and SCIA was the deformation at the sheet pile walls. In Plaxis the sheet pile walls are actually modelled as walls, whereas in SCIA the sheet pile walls are modelled as linear elastic springs. Only when the sheet pile wall springs in SCIA were adjusted to 15.000 kN/m/m the difference between the deformations in SCIA and Plaxis is negligible (Figure 21). This comparison showed that the Plaxis plate model can be the same as the SCIA model if the spring stiffness of the sheet pile walls is determined correctly. Concluding, the Plaxis model is the same as the SCIA model, but has the advantages that the spring stiffness of the sheet pile walls does not have to be calculated and the soil reaction can be taken into account (see chapter 4.8). This makes the Plaxis plate model a more complete and more complex model than the SCIA plate model.

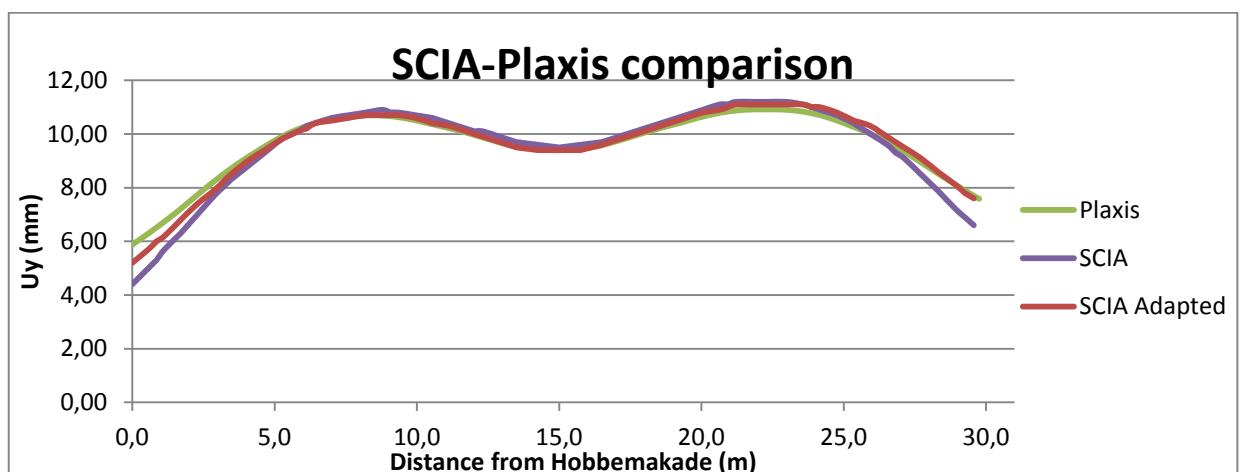


Figure 21 Plaxis and SCIA result (SCIA calculation with original sheet pile stiffness).

4.8 Heave

During the building phases heave occurs, since the effective soil stress reduces as an effect of the excavation. When the building pit is excavated to NAP -10.8 m heave will occur in the soil layer beneath the excavation level. In Plaxis the UCF is placed on top of this soil that has undergone heave. In reality the this heave will already take place before the excavation is finished. This heave should not cause stresses in the UCF. Also because of this heave the plate has additional

-Soil-structure interaction of a permanent steel fibre reinforced underwater concrete floor system-

deformations. In order to check the actual deformations the phase deformations should be taken instead of the total deformations.

The total stress against the UCF in the building phase was expected to mainly consist of the water pressure. But from the monitoring data in the gravel layer under the UCF it was concluded that the water head was located at NAP -5 m. Therefore the main pressure against the UCF is determined by the uplift pressure at level NAP -12 m. If no heave occurs it is expected that the effective stress should be zero at the height of the uplift level. Without taking heave into account the expected total pressure against the UCF would be 70 kPa. However, the total stress in the Plaxis calculation was 77 kPa directly under the UCF.

The expected uplift pressure is calculated for three situations (Table 8):

- Situation 1: The water head in the clay layer is -2.75 m NAP. The uplift pressure is determined by water pressure only (Design conditions).
- Situation 2: The water head in the clay layer is lower than -4.0 m NAP. The uplift is determined by the uplift pressure against the peat and clay layer. Uplift level is -12.5 m NAP (Monitoring conditions).
- Situation 3: Plaxis calculation taking into account the heave.

Table 8 Uplift calculations for different situations.

Situation	Uplift calculation	σ_v (kPa)
1	$\sigma_v = \gamma_w * H$ $\sigma_v = 10(kN/m^3) * (9.8 - 2.75)(m)$	70
2	$\sigma_v = \gamma_w * H - \gamma_{clay} * d - \gamma_{peat} * d$ $\sigma_v = 10(kN/m^3) * (12.5 - 2.5)(m) - 16(kN/m^3) * 2.2(m) - 12(kN/m^3) * 0.5(m)$	59
3	Total stress calculated by Plaxis	77

The total pressure against the UCF was 10% higher than was calculated in advance (situation 1). The total pressure against the UCF is 30% higher than what would be expected based on the monitoring data when not taking into account heave.

The effective stress (Figure 22), pore pressure (Figure 23) and the total stress (Figure 24) were plotted against the depth underneath the UCF before and after the dewatering stage. These plots show that the effective stress is not zero at the height of the uplift level. The layers between the UCF and level NAP -12.5 m are pushed upwards. This weight decrease causes a drop in the effective stress and this causes heave. A plot of the deformation of the soil in the y direction shows that the heave occurred mainly in the peat and clay layers (Figure 25).

The water head was measured under the UCF. During the execution of the project the water head was not expected to be so low (NAP -5 m). Nevertheless, a lower water head was not considered a problem because it meant that the pressure against the floor would not exceed the maximum value. The heave, however, was not taken into account. The Plaxis model showed that a lower water head in the gravel layer would mean more heave and thus a higher pressure on the UCF. Therefore, the low water head was actually not as favourable as expected.

-Soil-structure interaction of a permanent steel fibre reinforced underwater concrete floor system-

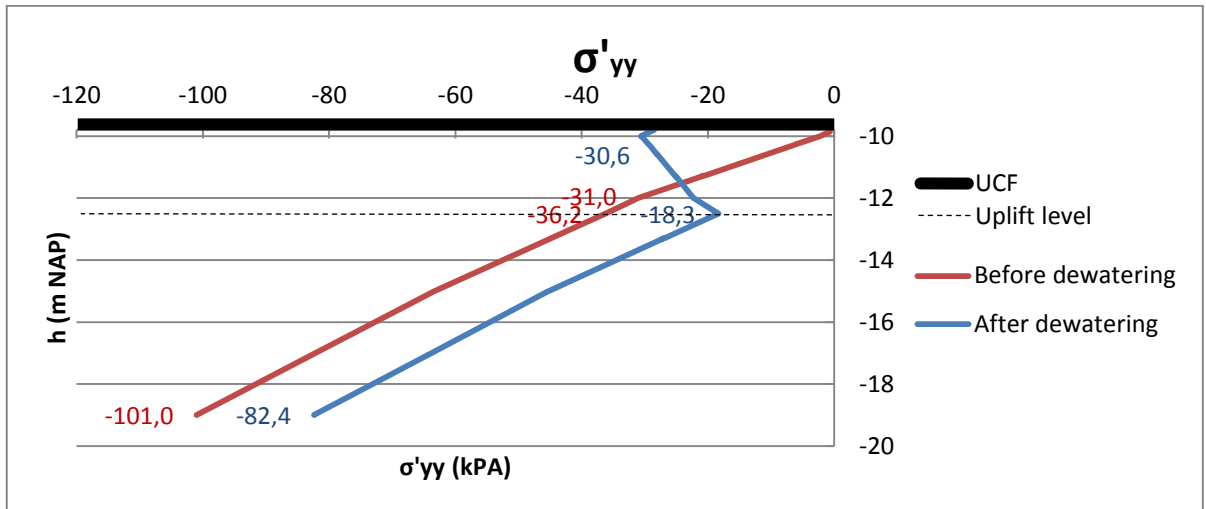


Figure 22 Effective stress in y direction under the UCF

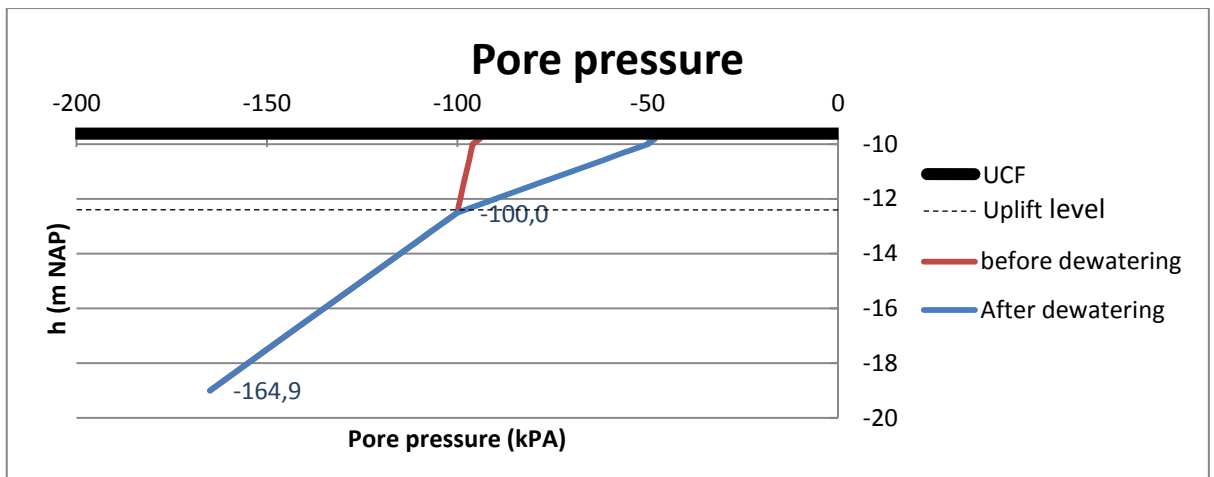


Figure 23 Pore pressure under the UCF

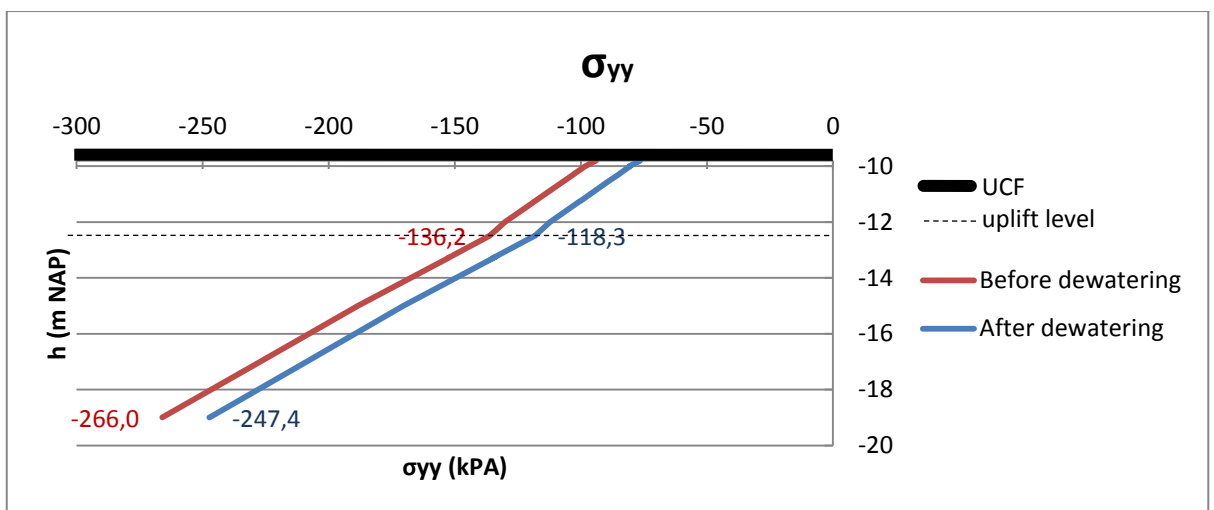


Figure 24 Total stress in y direction under the UCF

-Soil-structure interaction of a permanent steel fibre reinforced underwater concrete floor system-

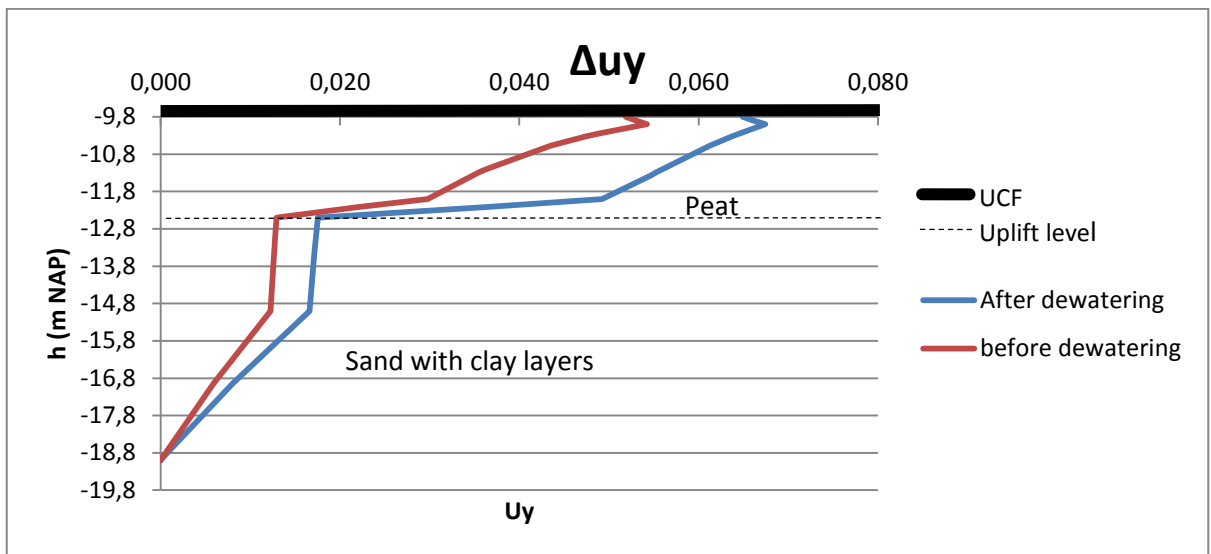


Figure 25 Soil deformation in y direction (U_y) over the height in order to determine the heave layers

4.9 MN-κ input

In section 4.7 it was concluded that the Plaxis plate model is a more complex and more complete version of the SCIA calculation. In order to make the model even more complete an MN-κ diagram can be assigned to the plate.

Not every MN-κ diagram is possible as input. Only positive and decreasing $dM/dκ$ values are possible as input table. Although it depends on the input parameters of the steel fibre reinforced concrete most MN-κ graphs have a negative $dM/dκ$ directly after the first crack occurs. In order to overcome this problem these negative values are deleted from the table. It is assumed that this small adaption will not affect the output significantly. The difference between these MN-κ diagrams was plotted in a graph (Figure 26). The normal force in the MN-κ diagram is 400 kN.

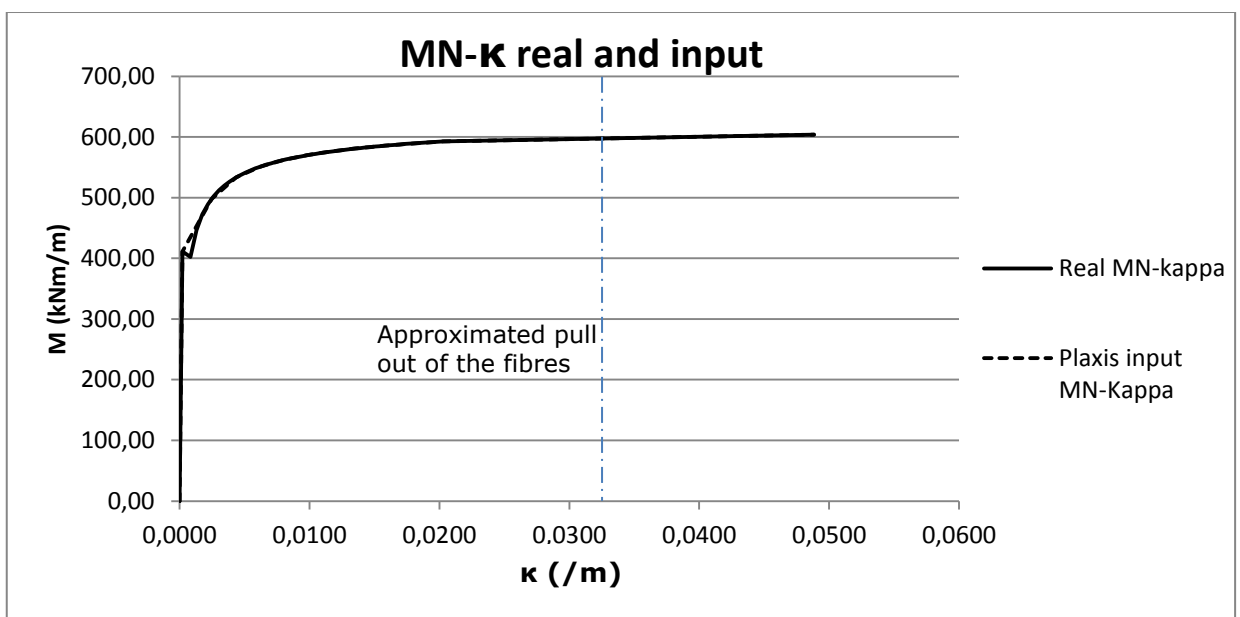


Figure 26 MN-κ Real and input graph

The linear input and the MN-κ input were compared to each other. The Young's modulus of the MN-κ plate is nearly 30.000 MPa. The bending moments in the structure have not reached the cracking

-Soil-structure interaction of a permanent steel fibre reinforced underwater concrete floor system-

moment for this load case. The deformations of the plate models and the monitored data (Figure 27) shows that adapting the Young's modulus only will not lead to the monitored deformation.

In the plate models the three middle piles are modelled stiffer than the other piles, which can be seen in the deformation line and the moment line (Figure 28). However, this cannot be seen in the deformation line of the monitored data. It is therefore expected that the group effect of the piles is of more influence than the individual stiffness of the piles.

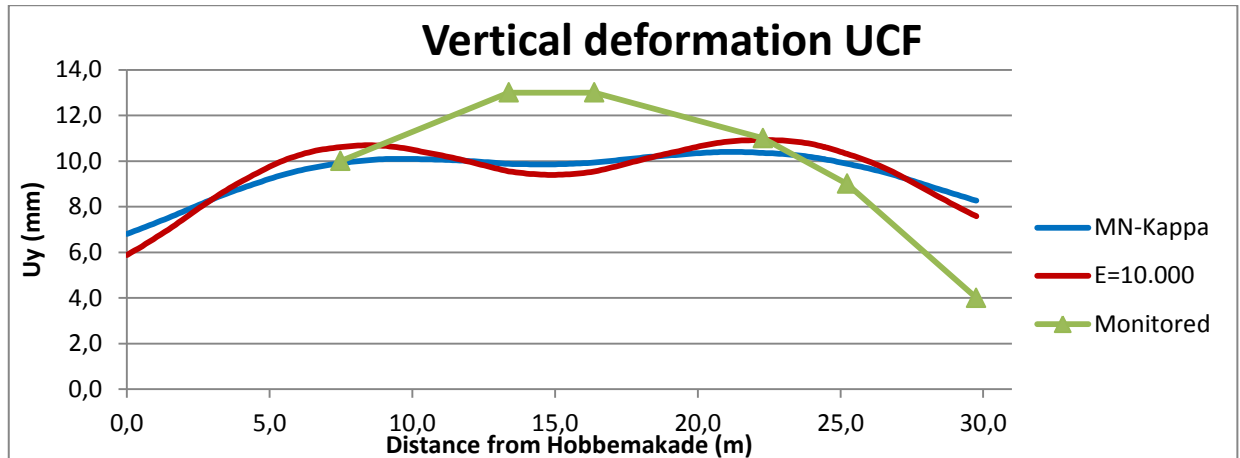


Figure 27 Deformations of the UCF

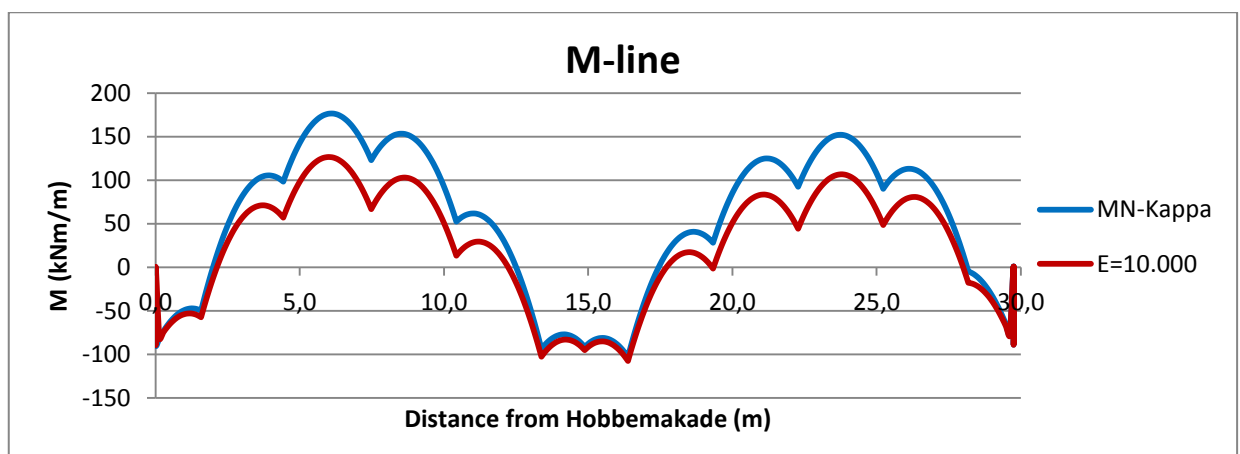


Figure 28 Moment line of the UCF

The moments remained under the cracking moment which means that the behaviour was still linear elastic for this load case. Therefore, the behaviour of the MN-κ input is not really tested in this model. In order to see the behaviour of the plate the load was increased until total failure. This was done in Plaxis by increasing the water head in the gravel layer. The final situation had such a high water head in this gravel layer that the situation is not realistic anymore. It is, however, an excellent way to study the behaviour of the plate in extreme conditions.

As expected, the behaviour of the plate is non-linear. The moments and the deformations were plotted against the pressure on the UCF (Figure 29). When at a certain point the cracking moment is reached a plastic hinge is generated. Because the stiffness decreases dramatically in such a hinge the moments will redistribute over the structure. Eventually Plaxis failed to model this behaviour because the deformations became too large and not because the maximum moments were exceeded. The pressure against the UCF is 100 m water, which is not realistic at all. This proves that the plate is absolutely not likely to fail on bending moments in the structure.

-Soil-structure interaction of a permanent steel fibre reinforced underwater concrete floor system-

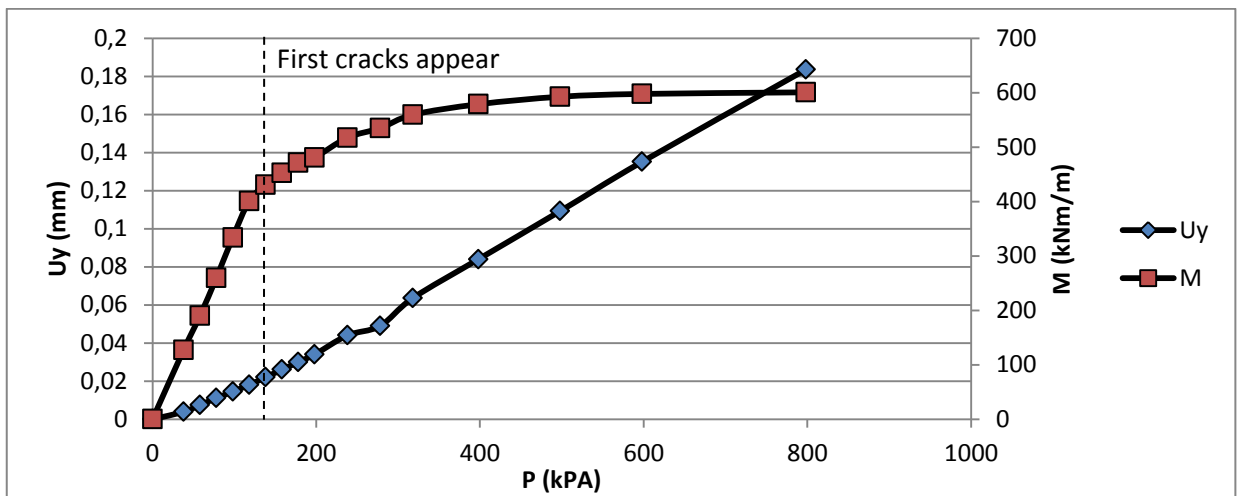


Figure 29 Behaviour of plates with MN-k input

The fibre pull out strain (Chapter 0) was also checked in this model. The fibre pull out strain is not reached yet so also pulling out of the fibres is not likely due to redistribution of the bending moments. This redistribution can be seen in the moment line just before failure (Figure 30). The maximum and minimum moments are equally spread over the structure.

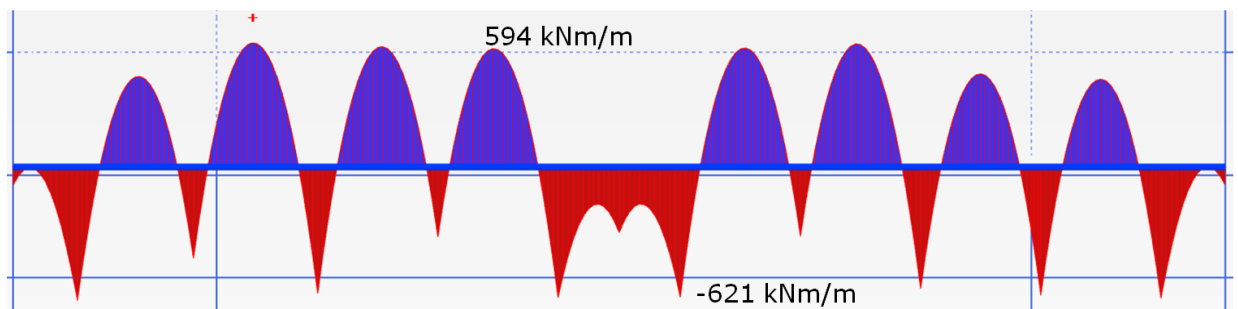


Figure 30 M-line MN-k input before the deformations become too large for Plaxis (900(kPa))

4.10 Compare Plaxis calculation to monitoring results

The order of magnitude of the Plaxis calculation is correct when compared to the monitored results. The plate model can be confirmed when it is compared to the SCIA model. However there are still some uncertainties that cause different results than was monitored. The biggest uncertainty in the Plaxis model are the piles modelled as springs. Due to these kind of piles the Plaxis model is not in force equilibrium and no interaction with the soil is modelled. In chapter 0 the springs are replaced by embedded beam rows to optimize the results.

Another difference between the measured and calculated data are the deformations at the sheet pile walls. In reality the sheet pile walls seem to react stiffer than was calculated. In chapter 6 the interaction stiffness of the sheet pile wall was varied to show the influence of this interaction stiffness. Also the heave parameters and the Young's modulus of the UCF were varied to show the influence of the uncertainties in these parameters.

4.11 Conclusion Albert Cuyppgarage

Based on the Plaxis calculation the following conclusions can be drawn:

- Heave can be expected during the dewatering phase due to the uplifting and unloading of the impermeable layers.
- A low water head in the gravel layer under the UCF is not favourable and will even lead to a higher pressure on the UCF due to heave.

Concerning the plate model the following conclusions can be drawn:

- The Plaxis plate model was verified using the SCIA calculation and yielded the same results.
- The Plaxis plate model is more advanced than the SCIA model because it takes into account the reaction of the soil.
- The spring stiffness of the sheet pile walls is determined more accurately in the Plaxis model than in the SCIA model.
- The order of magnitude of both the Plaxis and the SCIA calculation is similar to the monitoring data.
- With the MN- κ input it was shown that it is possible to redistribute the moments within the plate. Therefore failure due to a bending moment is highly unlikely.

Based on the Monitoring data and the Plaxis calculation the following conclusions can be drawn:

- The uncertainties that remain in the Plaxis model are the heave parameters, the stiffness of the piles, the pile plan and the Young's modulus of the UCF.

Due to these uncertainties the difference between the Plaxis calculation and the monitoring data are still significant (9%). It is expected that a sensitivity analysis will give more insight in the important parameters of the model. The sensitivity analysis will provide more insight into which parameters should be determined in more detail. It is expected that mainly the stiffness of the piles will play a significant role in modelling the deformation of the UCF.

-Soil-structure interaction of a permanent steel fibre reinforced underwater concrete floor system-

-Soil-structure interaction of a permanent steel fibre reinforced underwater concrete floor system-

5 Albert Cuyp garage micro piles

The micro piles modelled as springs are the largest factor of uncertainty in the Plaxis model (Chapter 0). Therefore, in the present chapter an alternative modelling method for the piles is discussed: the 2D embedded beam.

Prior to the design of the Albert Cuypgarage failure tests were performed on micro piles in the first and second sand layer to determine the α_t (shaft friction factor) of these layers. The pile design was made in accordance with these α_t values and after the piles were installed a suitability test was performed on 3% of the piles. This resulted in failure of multiple piles. Both the results of the failure tests prior to the excavation and the suitability tests after the excavation were used to model the behaviour of the piles.

5.1 Failure test results

The failure tests were performed as follows. Six micro piles – three for each sand layer – were installed from surface level with a grout body of 5m in the sand layers (Figure 31a). The first sand layer is only 2.5m deep so the α_t value is equal to the combined α_t value of this sand layer and the underlying alleröd (Sand with clay layers). The α_t values that were derived from the failure tests are 1.2% for the first sand layer and 2.25% for the second sand layer. The results of the failure tests were used to determine the ratio of bearing capacity between the sand layers.

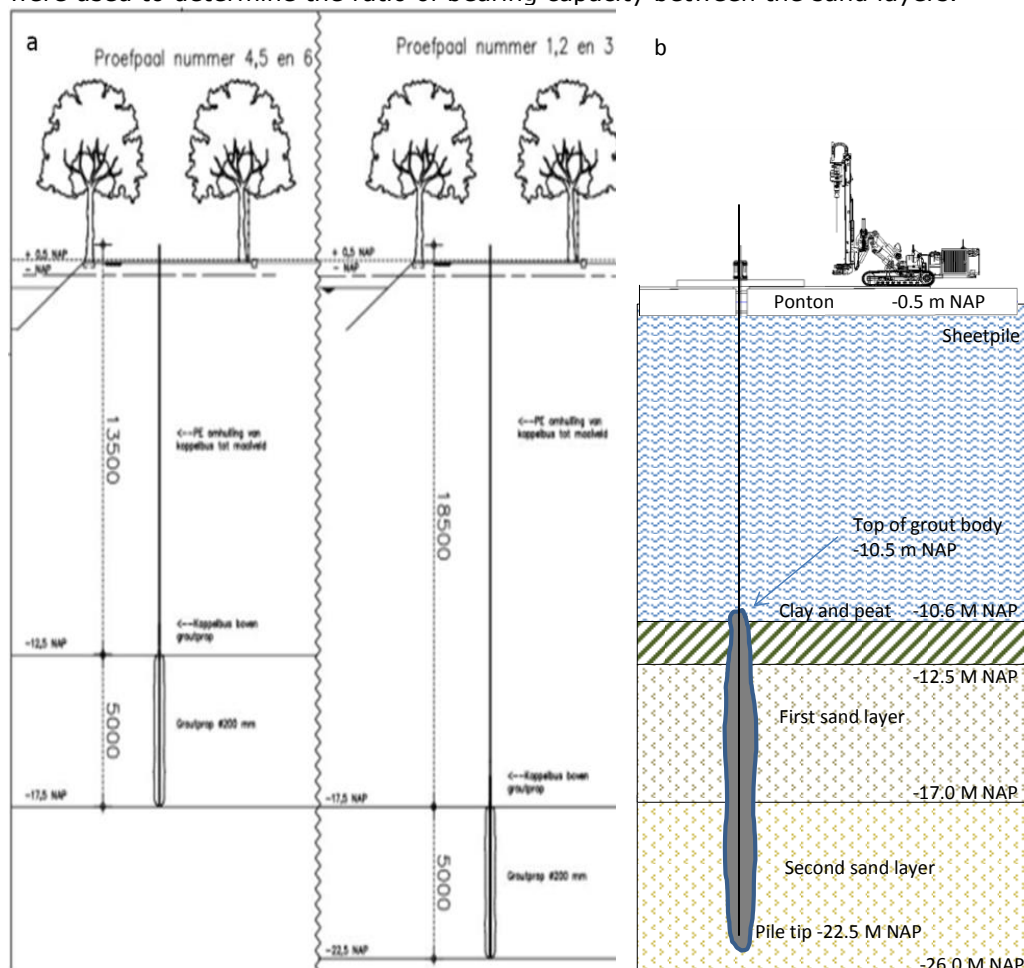


Figure 31 a) Failure tests (Volker Staal en Funderingen, 2015) b) Suitability tests, Modified picture from: (Volker Staal en Funderingen, 2016)

5.2 Suitability test results

When the excavation was finished the piles were installed and tested from a pontoon (Figure 31b). The test load is determined by: $F_p = F_d * n$ where F_n is the tensile load, F_d is the tensile design value

-Soil-structure interaction of a permanent steel fibre reinforced underwater concrete floor system-

and n is the group effect. The bearing capacity of the micro piles was insufficient during the suitability tests so additional piles were installed. The piles were tested with a load range of 70% F_p to 100% F_p in steps of 5% F_p . The displacement of the micro piles were measured at the top of the pontoon from the shore of the building pit so the deformation of the pontoon will not influence the measurements.

The suitability test results describe the behaviour of the micro piles in a more realistic way than the failure tests results, so these measurements should be leading in modelling the micro piles.

The measured deformation is the sum of the deformation of grout body in the soil and the elastic deformation of the grout body and the free anchor steel. To correct for this when fitting the deformations into the Plaxis calculation, the elastic deformations should be subtracted from the total deformations. The elastic deformation of a steel anchor with a free length of 13 m will be dominant to the total deformation behaviour. Therefore the fit will always be close to the field data if the elastic deformation is not subtracted from the total deformation. The properties of the GEWI anchors determining their elastic behaviour are listed in Table 9. The deformation of the free length can be easily calculated with the formula:

$$\Delta l_{et} = \frac{F * l_{Free}}{EA}$$

Table 9 Properties of GEWI anchors

GEWI Type	Effective cross-section A (CUR 236, 2011) (mm ²)	E (SBRCURnet, 2017) (kN/m ²)	L _{free} (m)
50	1963	195*10 ⁶	13
63.5	3167	195*10 ⁶	13
75	4418	195*10 ⁶	13

The elastic deformation the grout body is more difficult to determine because the normal force is not constant over the grout body. It is unknown which parts of the grout body are loaded for the different load steps and what the load distribution is over the different soil layers. Therefore the deformations at the top of the grout body were plotted for both the field data and the Plaxis calculation.

Thirty suitability tests were done spread over the whole building pit. For the Plaxis calculation a cross-section in the middle of the building pit was chosen. The behaviour of the piles near this middle cross-section had the most influence on the deformation of the cross-section. The building pit was divided into three areas (A,B,C). Area B is the 1/3 middle part of the building pit and these piles are expected to have the most influence on the middle cross-section. All the measurements within cross-section B are used to fit the Plaxis calculation. The suitability tests were done on both GEWI 50 and GEWI 63.5. Because the stiffnesses of these pile types are different the results were plotted separately (Figure 32).

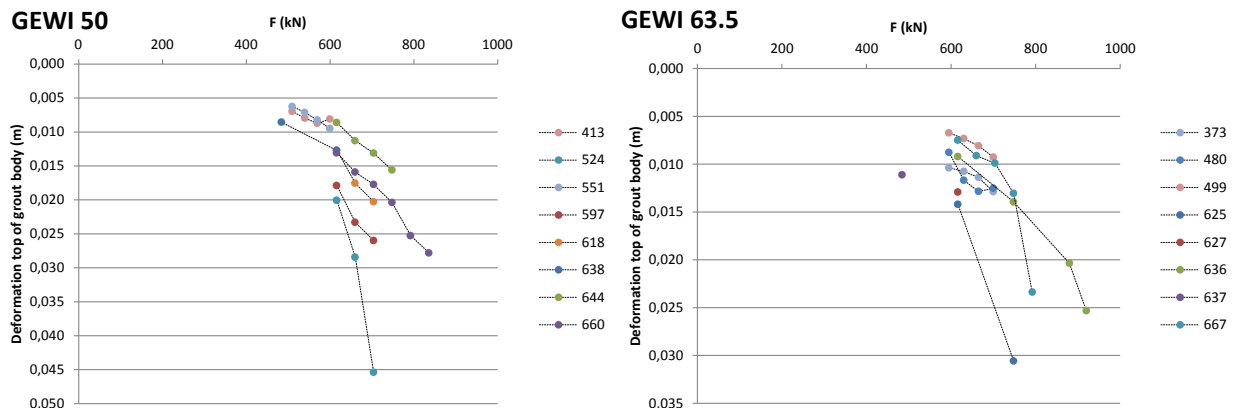


Figure 32 a) Load displacement graph GEWI 50 b) Load displacement graph GEWI 63.5

-Soil-structure interaction of a permanent steel fibre reinforced underwater concrete floor system-

5.3 Embedded beam row

The embedded beam row can be used to model a row of piles. The input of the embedded beam row is the maximum skin friction over the height of the pile. This maximum skin friction was calculated with the average failure load of the failure tests. The skin friction is divided over the two sand layers with the same ratio as the failure tests. It is assumed that the skin friction in the failure tests was constant and that the Normal force was linear over the height. For the suitability tests the average value of the failure load was used (689.0 kN and 707.5 kN for GEWI 50 and GEWI 63.5, respectively).

Table 10 Failure loads suitability test and failure test

Sand layer [-]	Maximum Load Failure test [kN]	Grout body in sand layer [m]	Skin friction [kN/m]	Grout body in sand layer [m]	Maximum load Suitability test [kN]	Skin friction [kN/m]
1	377	5.0	75.4	4.5	123.4	27.4
2	1414	5.0	282.8	5.5	565.6	102.8
Total	1791	10.0		10.0	689.0	

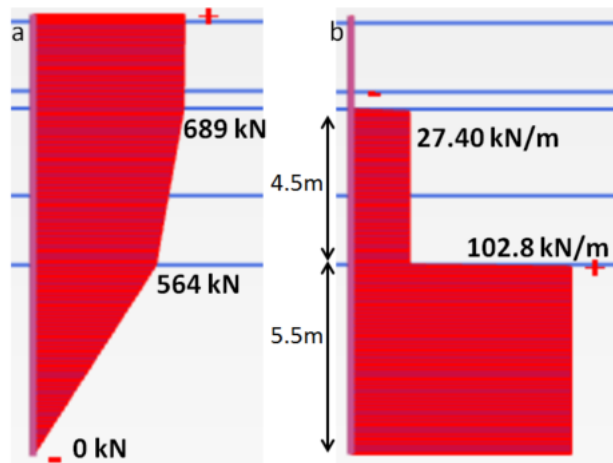


Figure 33a) Maximum Normal force in the micro pile b) Maximum skin friction in the different sand layers

The lateral stiffness of the pile was calculated by Plaxis. This stiffness is equal to the shear modulus of the soil divided by the spacing of the piles times the interface stiffness factor (Figure 34). The interface stiffness factor is normally calculated by Plaxis and depends on the pile spacing and the pile diameter, but this does not take into account the installation effect of the micro piles. The ISF was changed manually to take into account the installation effect and to fit the behaviour to the field data.

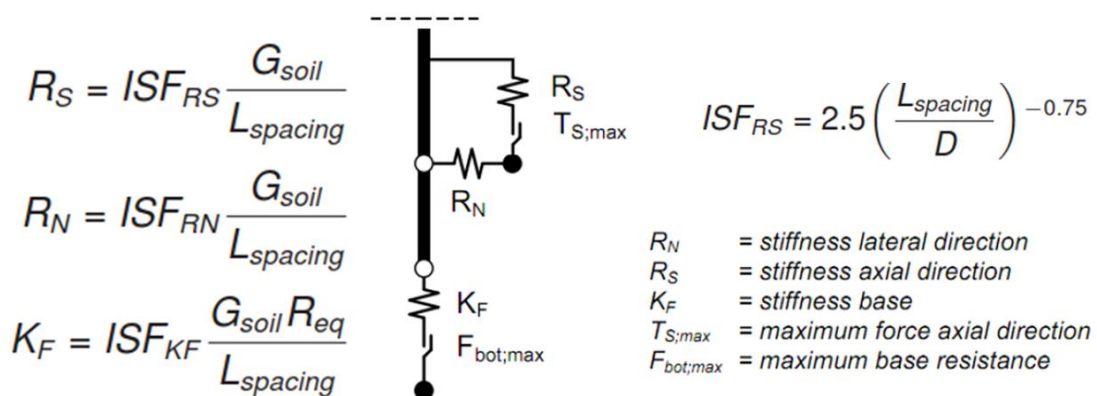


Figure 34 Stiffness of the embedded beam (Plaxis, 2018)

-Soil-structure interaction of a permanent steel fibre reinforced underwater concrete floor system-

5.4 Pile spacing

When using an embedded beam model a row of piles is modelled, which is realistic for the final situation but not for the suitability tests. During the suitability tests only one pile at a time was tested and not a row of piles. In section 5.3 it was shown that the stiffness of the piles is dependent on the pile distance ($L_{spacing}$). The shear modulus is divided by the pile spacing, so making the pile spacing infinitely large will not lead to a model that can be compared to a single pile. Instead, if the distance is infinitely large the stiffness becomes infinitely small. Instead, the influence zone of one pile should be used for modelling a single pile. The influence zone was determined with D-foundations. Three tension piles were placed in a line in the same ground and excavation conditions as the suitability tests (Figure 35). The distance x was varied until pile 3 and 1 would not influence pile 2. Also a single pile was tested to determine the bearing capacity of a single pile.

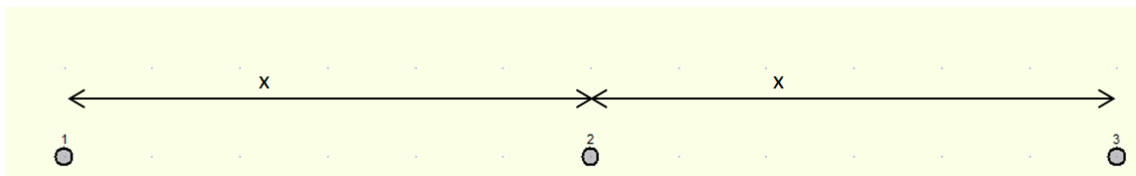


Figure 35 Setup for determining the influence zone of a single pile

The bearing capacity was plotted against the distance x times the diameter of the pile (Figure 36). After a distance of $40D_{pile}$ the single pile and piles in a row have converged. The diameter of grout body is 0.2 m so the influence zone of one micro pile is 8 m.

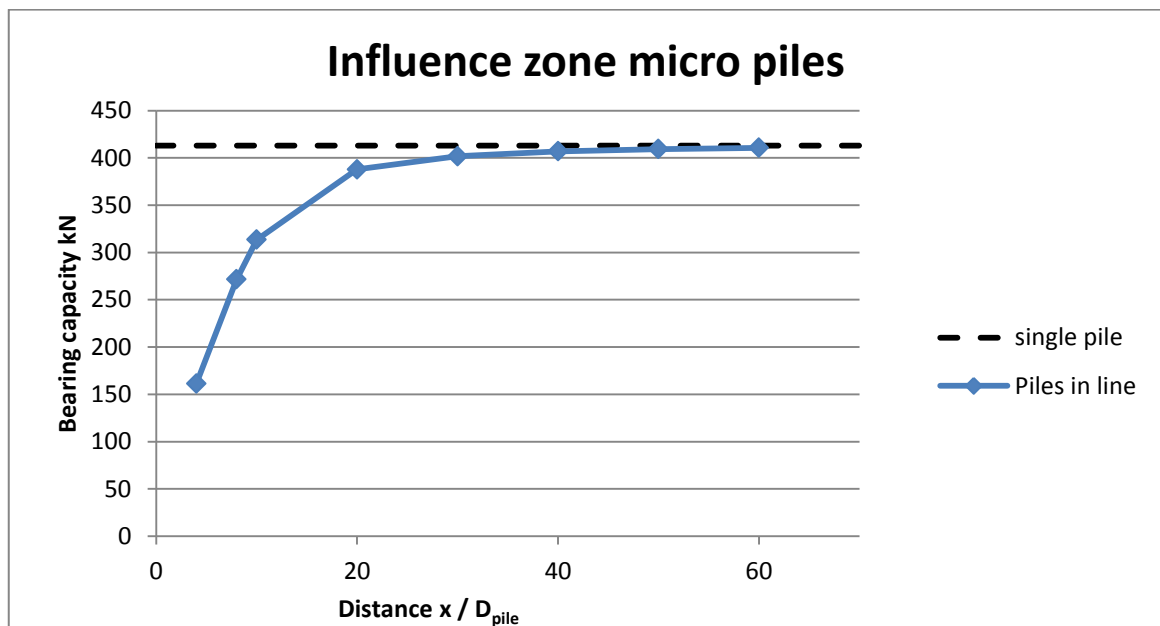


Figure 36 Bearing capacity of a single pile versus piles in line as a function of the distance between the piles.

5.5 Fitting the data in Plaxis

In Plaxis the phases of the suitability test were modelled. The building pit is excavated wet and then the piles are tested from a pontoon (Figure 37).

-Soil-structure interaction of a permanent steel fibre reinforced underwater concrete floor system-

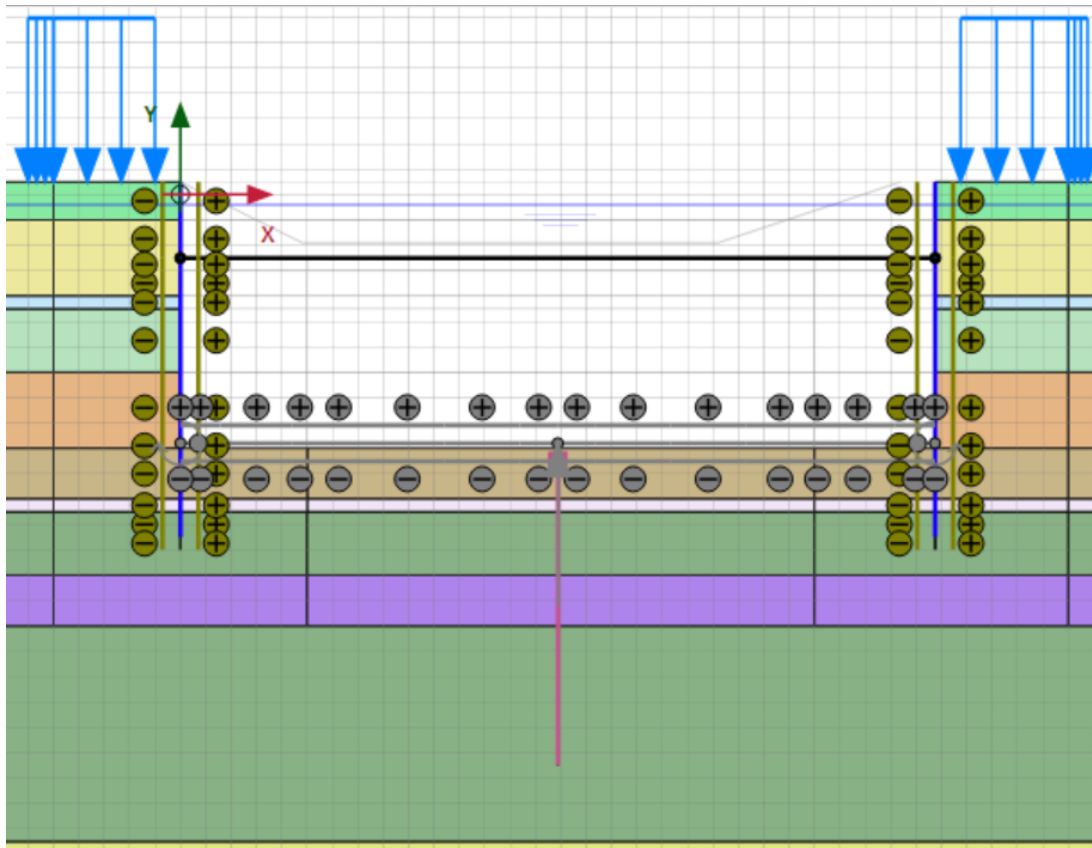


Figure 37 Suitability test in Plaxis

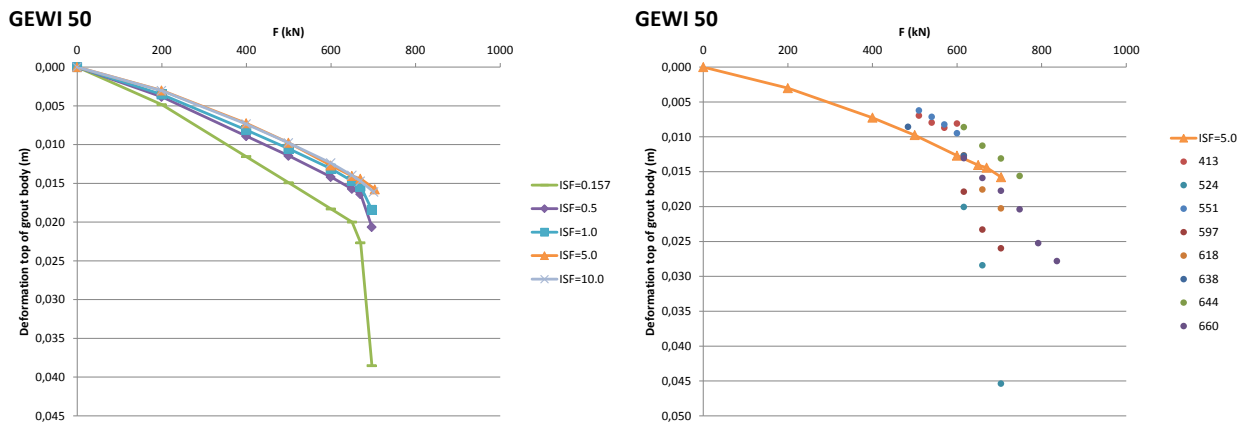


Figure 38 Fitting the Plaxis calculation to the field data GEWI 5. Left: different results for different ISF factors. Right: Best fit with ISF = 5.0.

The field data were fitted to the Plaxis model (Figure 39). Different ISF values were plotted in order to obtain the best fit to the field data. Increasing the ISF value to more than 5.0 did not increase the stiffness of the soil structure interaction, because when the ISF is higher than 5.0 the behaviour of the soil around the pile becomes dominant over the behaviour interaction. Therefore the ISF value of 5.0 was assumed to be the best fit to the field data. However, a perfect fit to the field data could not be obtained. The differences between the field data and the model can be attributed to the installation effect. The same calculation was done for the GEWI 63.5. In this case a good fit to the data was obtained with an ISF of 1.0 (Figure 39).

-Soil-structure interaction of a permanent steel fibre reinforced underwater concrete floor system-

GEWI 63.5

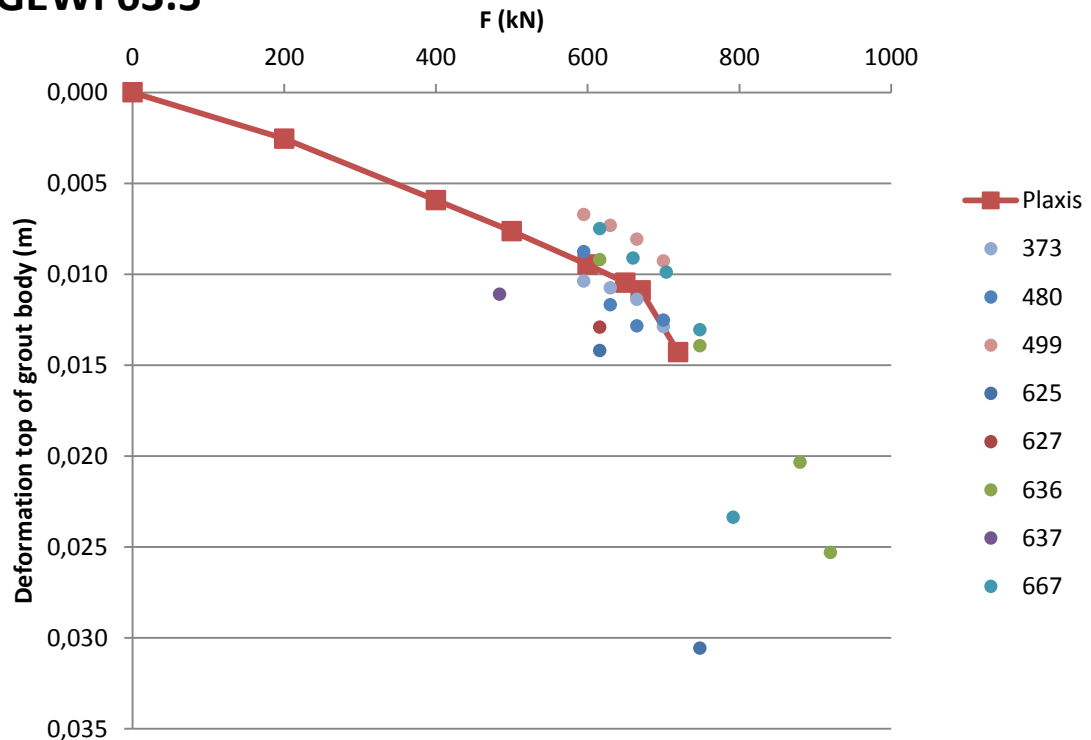


Figure 39 Fitting the Plaxis calculation to the field data GEWI 63.5

5.6 Complete Plaxis model

The Plaxis model was adapted to the new pile plan with embedded beams. The deformation of the UCF was plotted for the different calculation methods that were used (Figure 40). The red line is a fully drained calculation with embedded beams. Due to the heave of the over consolidated Eemclay the whole structure is lifted. The heave in the Eemclay layer will probably take more time to occur which is why an undrained calculation is done as well. The stiffness parameters of the Eemclay are very dominant in the total deformation of the building pit. As expected the whole building pit moves up or down and these stiffness parameters do not influence the shape of the deformation.

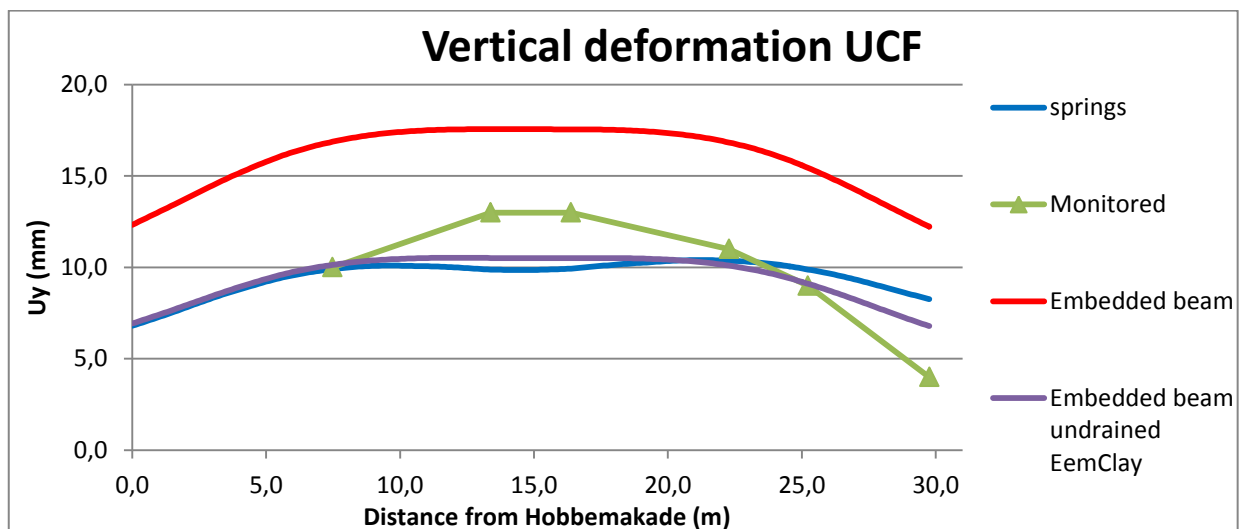


Figure 40 Deformation UCF with different Plaxis calculation methods

-Soil-structure interaction of a permanent steel fibre reinforced underwater concrete floor system-

5.7 Conclusion embedded beam

Modelling the building pit with the embedded beam model does not solve all the uncertainties but it does have some advantages over the spring model:

- The Plaxis model is in force equilibrium.
- More realistic stresses in the subsoil.
- The behaviour of the embedded beam can be fitted with detailed field data.
- Elastic deformations and soil deformations are separated instead of a single spring stiffness.

There are also disadvantages of the embedded beam model:

- Bearing capacity is an input variable so detailed field data are needed to use the embedded beams
- Additional uncertainties in stiffness parameters of the Eemclay.

-Soil-structure interaction of a permanent steel fibre reinforced underwater concrete floor system-

6 Sensitivity analysis

A sensitivity analysis was done with Plaxis to determine the sensitivity of the most important parameters. The sensitivity analysis was divided into two main goals. The first analysis was to show the sensitivity of the current Plaxis model. The second analysis focused on the application of a permanent SFRUCF in general.

6.1 Primary model

A simplified Plaxis model of the Albert Cuyppgarage was used as the primary model (Figure 41). Some soil layers were simplified in order to speed up the calculation process. All the peat and clay layers were combined to weak clay layers. The soil parameters that were used are the same parameters that were used for the Albert Cuyppgarage. To simplify the model, the initial canal is taken out of the design. For the analysis of the behaviour of a permanent SFRUCF the clay and sand layer underneath the UCF were changed in one sand layer. The parameters of this sand layer were varied to study the possibility of a piled raft foundation.

In the previous chapters the Albert Cuyppgarage was only calculated until the dewatering of the building pit. For the sensitivity analysis the final stage was modelled as well. The final stage has additional loads from the weight of the complete structure. These loads are transferred by the middle columns and by the sheet pile walls towards the foundation of the building. At the location of the middle columns the load is F and at the sheet pile walls the load is $1/2F$ (marked in red in Figure 41). The load per column is 5166 kN and the column centre to centre distance is 5.32m. The load F in the model is 971 kN/m.

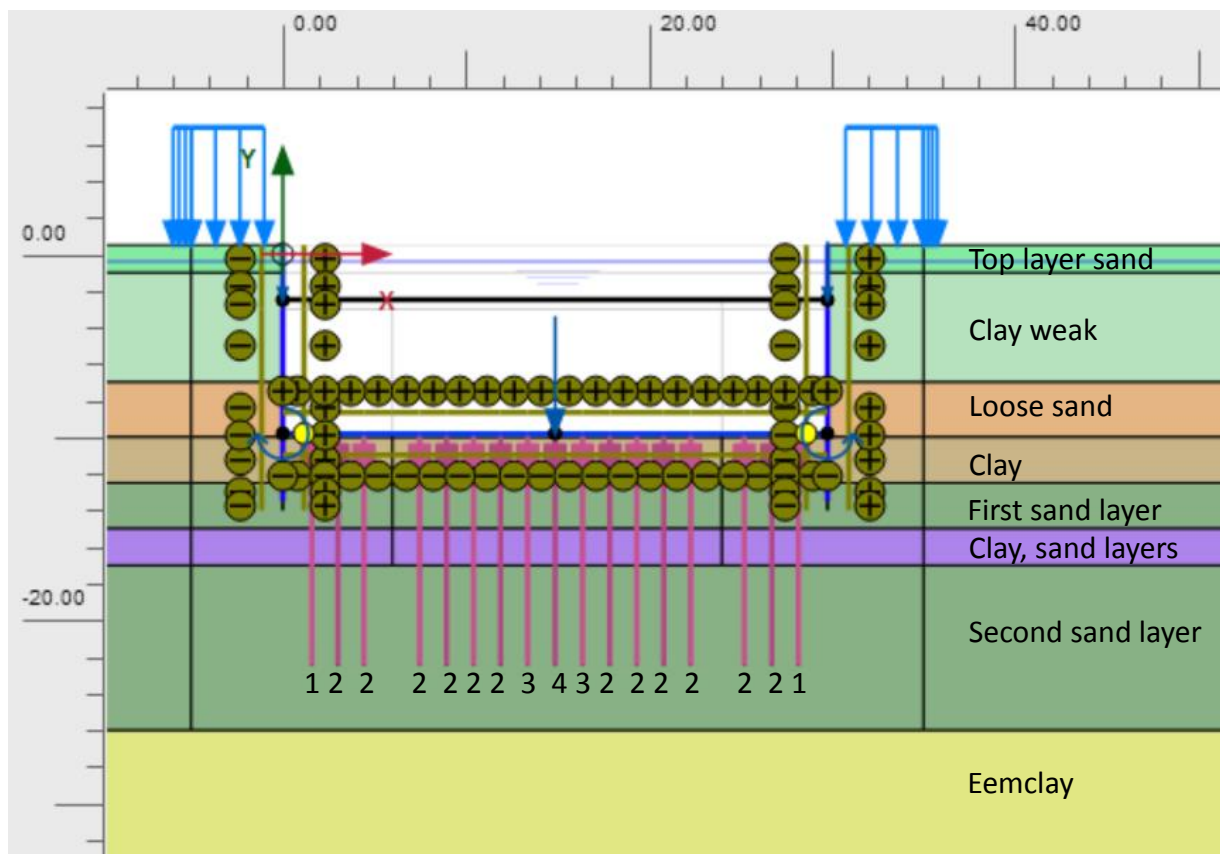


Figure 41 Primary model that was used in the sensitivity analysis.

-Soil-structure interaction of a permanent steel fibre reinforced underwater concrete floor system-

6.2 Output sensitivity analysis

The important output parameters are:

- | | |
|--|----------------|
| • Maximum moment | M_{max} |
| • Minimum moment | M_{min} |
| • Maximum shear force | V_{max} |
| • Maximum deformations | ΔU_y |
| • Effective soil stress directly under the UCF | $\sigma_{yy'}$ |
| • Forces per pile group | |

M_{max} , M_{min}

In chapter 0 it was concluded that the UCF is not likely to fail on bending moment. However, the bending moment will determine the crack width which is an important parameter for water tightness.

V_{max}

The shear force is an important parameter for shear failure and pons.

ΔU_y

The deformations show the behaviour of the structure and this can be used for the comparison with the monitoring results of the Albert Cuypgarage. The plotted output of the deformations will be the difference between maximal and minimal deformation.

$\sigma_{yy'}$

The effective soil stress under the UCF shows whether the load is transferred to the soil and to what extent. It was expected that mainly stiff soils will have high effective stress underneath the UCF during the final phase.

Forces per pile group

The piles are divided into four groups (Figure 41). The average results of the piles within each group will be an output parameter as well in order to compare the pile loads with each other.

The output will be generated for both the construction phase (after the dewatering of the building pit) and during the final phase (includes loads from structure). All the results will be scaled towards the primary model, so all the values of the primary model will be 1. In this way all the output parameters can be compared and it will be clear which parameters influence the design the most.

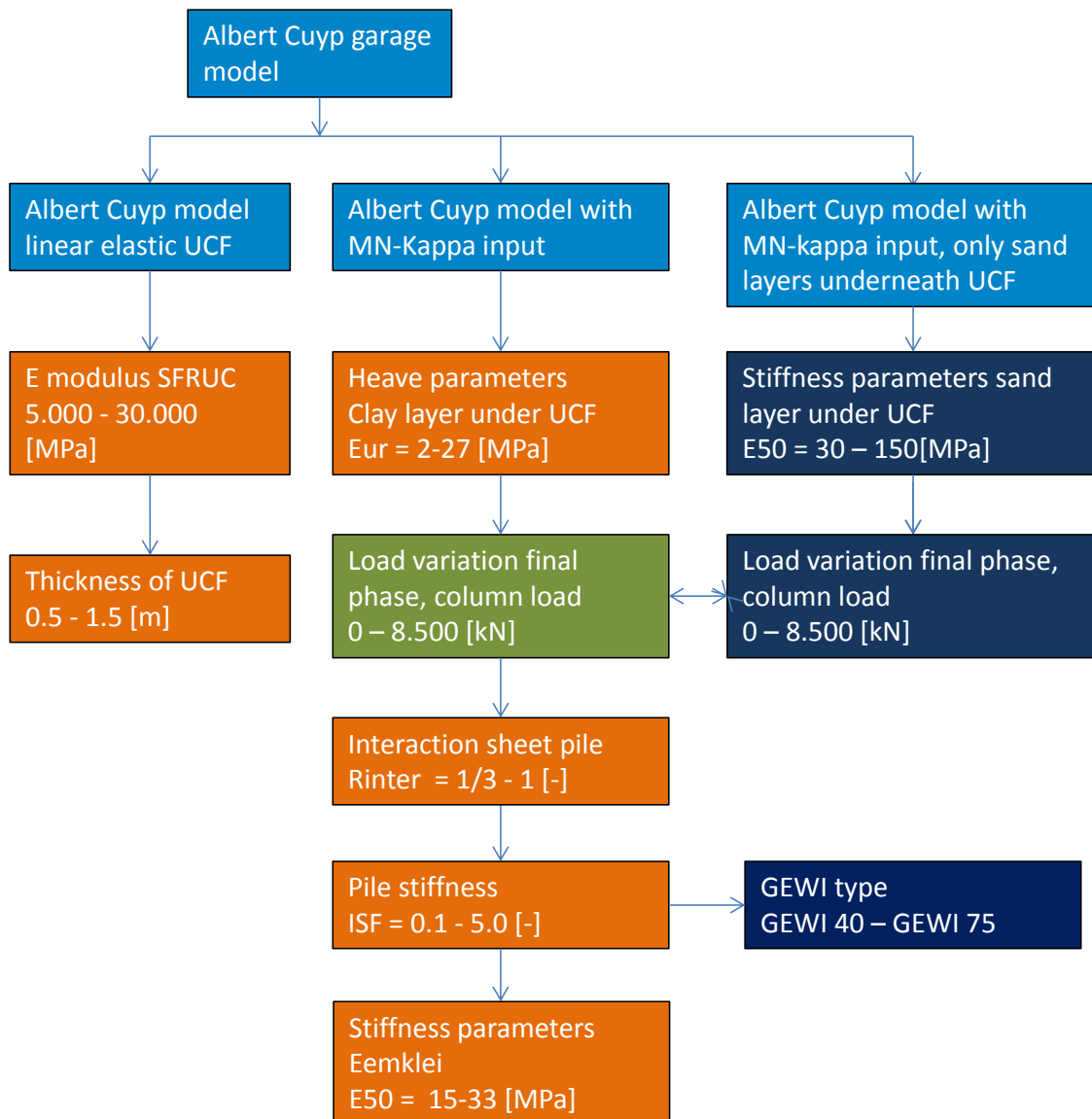
6.3 Varied parameters

The parameters that were varied (Figure 42) were categorized into two main goals. The sensitivity of the Albert Cuyp model and the sensitivity of permanent SFRUCF in general. The variations of the Albert Cuyp model also distinguish the difference between the building phase and the final phase. For these analyses three primary models were used.

- Albert Cuyp model with linear elastic behaviour for the UCF
For varying the E-modulus and the thickness a linear elastic plate is needed. With this linear elastic plate the influence of a fictive E-modulus was shown.
- Albert Cuyp model with MN- κ input for the UCF
This model has the main goal to show the important parameters that might cause the difference between the measured data and the model.
- Albert Cuyp model with MN- κ input and only sand underneath the UCF
The focus of this model is the behaviour of an SFRUCF in general and the goal is to show the influence of the soil parameters underneath the UCF.

Before the results are shown it should be noted that the behaviour of the SFRUCF depends on the loading conditions. For the building phase the SFRUCF is uncracked and behaves linear elastic way. Moving over this linear elastic line means large changes in the in the internal moments and small changes in deformations. In the final phase the concrete is cracked and the behaviour becomes non-linear. Moving over this non-linear line means small changes in the internal moments and large deformations. This behaviour can be seen in all the results.

-Soil-structure interaction of a permanent steel fibre reinforced underwater concrete floor system-



Main goal of different variations:

- Primary model variations
- Sensitivity of the Albert Cuyp garage building phase
- Sensitivity of the Albert Cuyp garage final phase
- Sensitivity of building pits with permanent UCF in general

Figure 42 Varied parameters with the range and main goal of the variation.

6.4 E-modulus of the SFRUCF

In the design of the Albert Cuyp garage it was assumed that the SFRUCF would behave cracked due to the uplift pressure. To model a cracked SFRUCF a fictive stiffness of 10.000 MPa was chosen. In the previous chapters it was concluded that the UCF was not cracked in the building phase and that the E-modulus would be near the 30.000 MPa. This section discusses what is the consequence of modelling the UCF with a fictive E-modulus of 10.000 MPa.

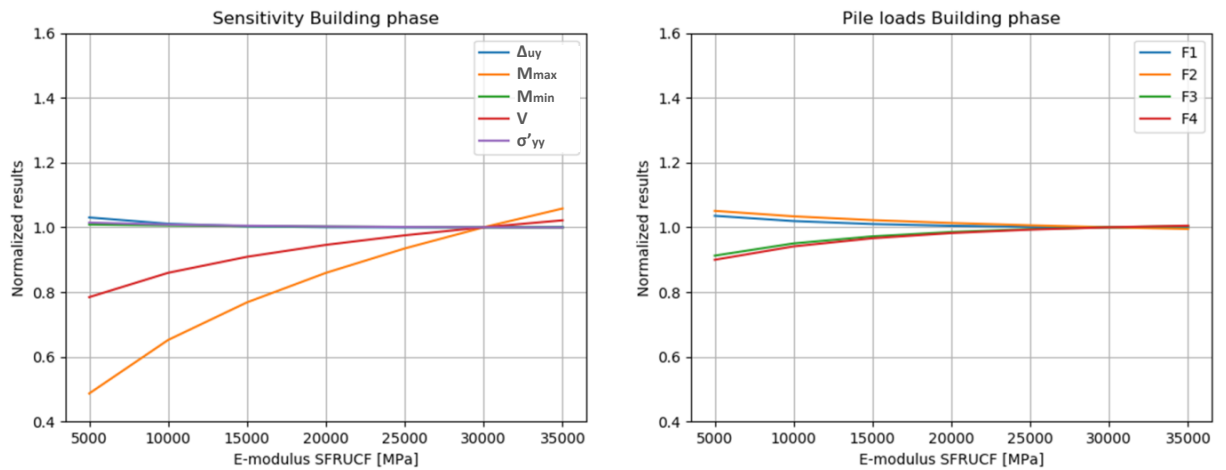


Figure 43 Influence of a varying E-modulus of the UCF in the building phase. The pile forces are averaged over different pile groups, which is shown in Figure 41.

The E-modulus of the UCF is varied between 5.000-30.000 MPa (in 7 steps) to show the difference between the calculated and fictive E-modulus (Figure 43). The influence of varying the E-modulus has hardly any effect on the deformations of the UCF. The stiffness of the UCF was one of the uncertainties in the model, but it does not contribute to the difference between the measured data and the calculated deformations with the Plaxis model.

For this specific case the shear force and the bending moments are respectively 10% and 30% lower when a stiffness of 10.000 MPa is used. The moments and shear forces are underestimated when the fictive E-modulus is used. These results become more interesting when the concrete is actually cracked. This is why another analysis was done where the uplift pressure is increased (Figure 44). This was done for both the model with MN- κ input and for the model with a fictive E-modulus of 10.000 MPa. The output from both calculations was normalized by the original output of the model with the MN- κ input to compare the results.

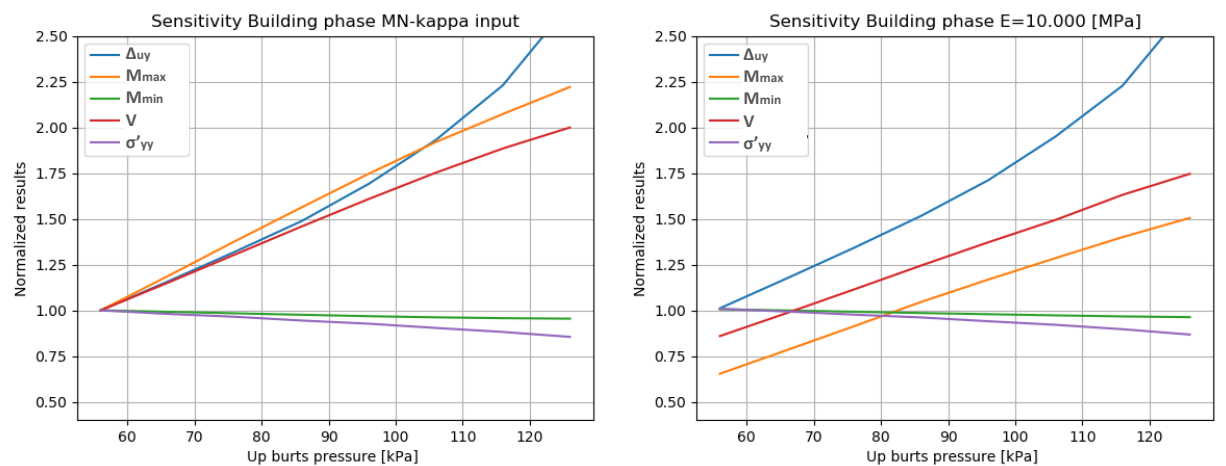


Figure 44 Difference between the internal forces in the UCF for the MN- κ input and fictive E-modulus of 10.000 [MPa].

-Soil-structure interaction of a permanent steel fibre reinforced underwater concrete floor system-

The nonlinearity is not shown yet because under these loading conditions the concrete does not crack that easily. The model is not cracked yet even though the uplift pressure is already unrealistically high. The concrete remains uncracked because of the uniform loading and a relatively small span between the piles. Nevertheless, it can be concluded that the shear force and the moments within the structure are underestimated when a lower fictive E-modulus is used. It is therefore advised to use the original E-modulus of 30.000 [MPa] or, even better, an MN- κ input.

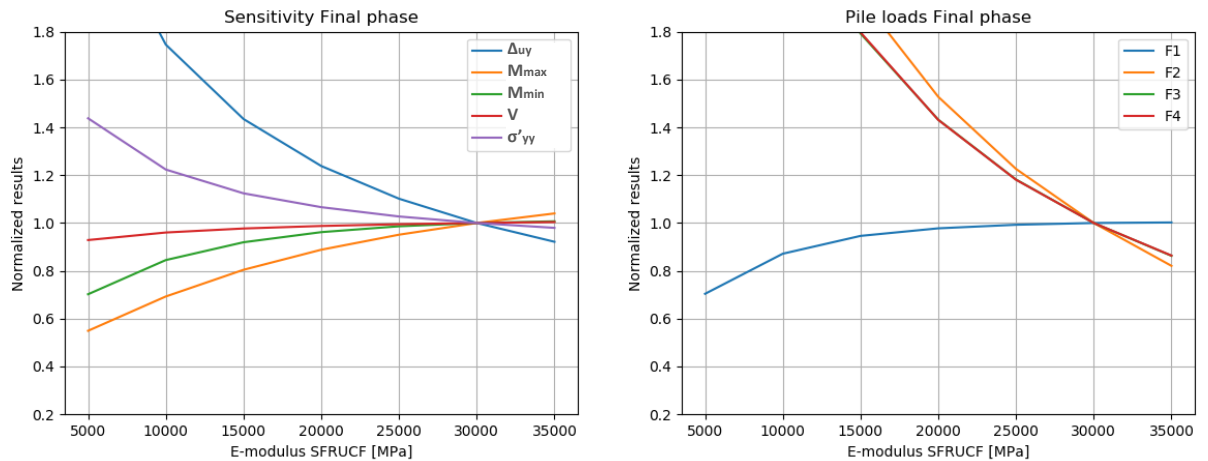


Figure 45 influence of a varying E-modulus of the UCF in the final phase.

For the final phase the behaviour is supposed to be non-linear. But for the variation of the E-modulus the calculations were done in a linear way (Figure 45). For this load situation the effect on the deformation is much larger than for the load in the building phase. The difference in sensitivity is due to the shape of the load. In the building phase the load is uniform over the complete floor. In the final phase a large point load is added that can be distributed over the width of the floor depending on the stiffness of the UCF.

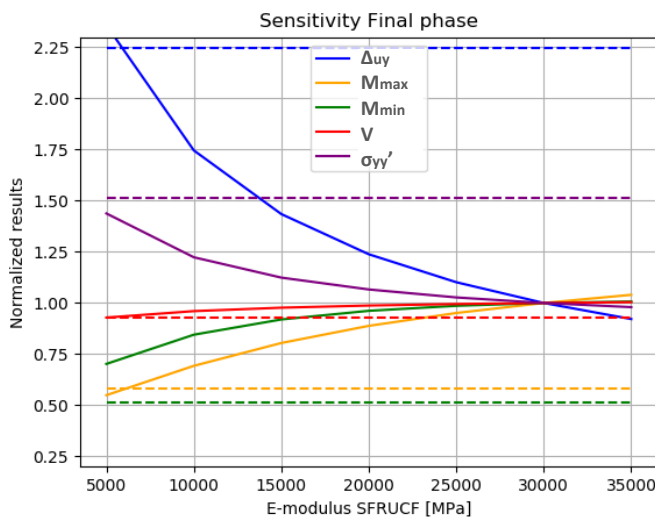


Figure 46 Fictive E-modulus compared with MN- κ input. Dashed lines are the results of the calculation with MN- κ input.

The results of E-modulus variation of the final phase were compared with the model that included the MN- κ input (dashed lines in Figure 46). It can be concluded that it would in theory be possible to use a fictive E-modulus that has approximately the same result as the MN- κ input. In this specific case this fictive E modulus would be around 5.000 [MPa]. However, the fictive E-modulus depends on the loading conditions, so it would not be possible to derive a fictive E-modulus that can be used in any case.

6.5 Thickness of the UCF

The thickness of the UCF is varied between 0.5 and 1.5 m (11 steps) (Figure 47). The linear elastic model is used and this is why only the results in the building phase can be shown. The pile forces decrease with an increasing thickness. This is partly due to the increased weight of the UCF but mainly because the sheet pile walls take more load. The reason why the sheet pile walls take more load in this case is the increased stiffness of the UCF that spreads the load more towards the stiffer sheet pile walls. What can also be observed is the difference in pile forces when the thickness is lowered. Due to the relatively stiff sheet pile walls the pile forces near the sheet pile walls are larger. This was also visible in the variation of the E-modulus but the effect there was smaller.

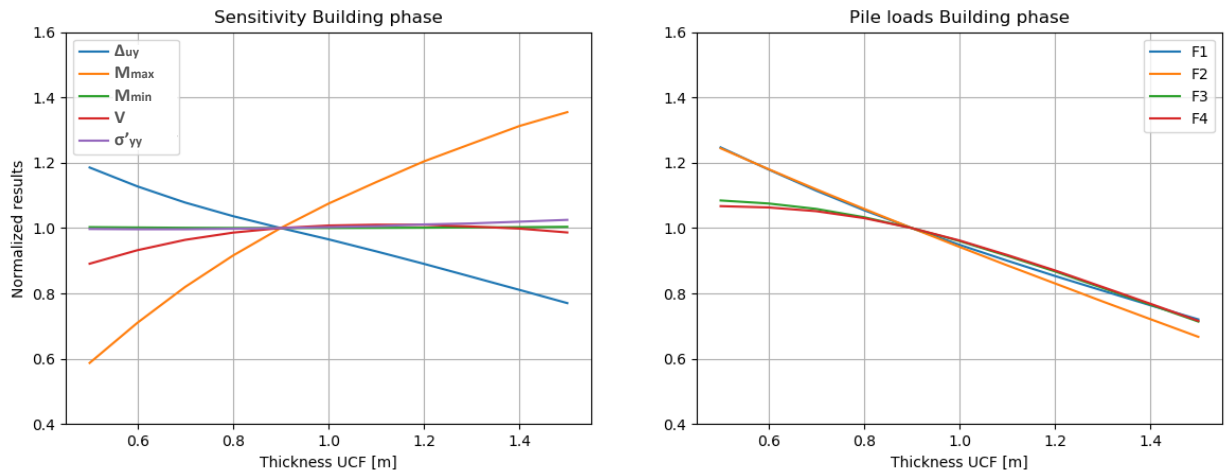


Figure 47 Influence of a varying Thickness of the UCF in the building phase.

By adjusting the thickness the stiffness changes as well. The effect of the thickness is much larger than the effect of the E-modulus, because the thickness dominates the formula to the power of 3. This can be seen in the influence on the deformations. The influence of the thickness on the deformations is much larger than the influence of the E-modulus. For a UCF the exact thickness remains an uncertainty and this is why a lower bound value of the thickness is used in the CUR 77.

6.6 Heave in the clay layer under the UCF

During the analysis of the Albert Cuyp garage it was concluded that heave occurred in the clay layer directly under the UCF. The heave caused an additional load on the UCF during the building phase. The heave parameters were an uncertainty in the model. The stiffness parameters that are responsible for the heave were varied within a range that describes the behaviour of peat and clay ($E_{ur} = 2-27$ [MPa] in 13 steps). The heave is determined by the unloading stiffness E_{ur} . The ratio between the E_{50} , E_{oed} , E_{ur} remained the same during the variation of the E_{ur} because Plaxis does not allow all ratios to be adjusted separately. The ratio is $E_{50} = 1/2 E_{oed} = 4 E_{ur}$.

It can be seen that the variation of the E_{ur} has an influence on the bending moments and on the effective vertical soil stress (Figure 48). It was not expected that a lower E_{ur} value, which means a high heave load, results in a lower bending moment in the UCF. These lower bending moments can be explained with the deformation line (Figure 49). With the increased load the deformations at the sheet pile walls increase more than the deformations in the middle. This reduces the curvature and the bending moments in the UCF. More deformation at the sides means that the sheet pile wall reacted less stiff than the piles with an increased load. It was already concluded that the sheet pile wall will be more stiff in reality. Therefore it is expected that an increased heave load will in reality lead to a higher bending moment even though this cannot be verified with the Plaxis calculation.

The heave causes an additional load on the UCF. The additional load varies between 11% and 30% of the original expected load without heave. This is a significant increase of the load and this heave should definitely be included in the design of a UCF.

-Soil-structure interaction of a permanent steel fibre reinforced underwater concrete floor system-

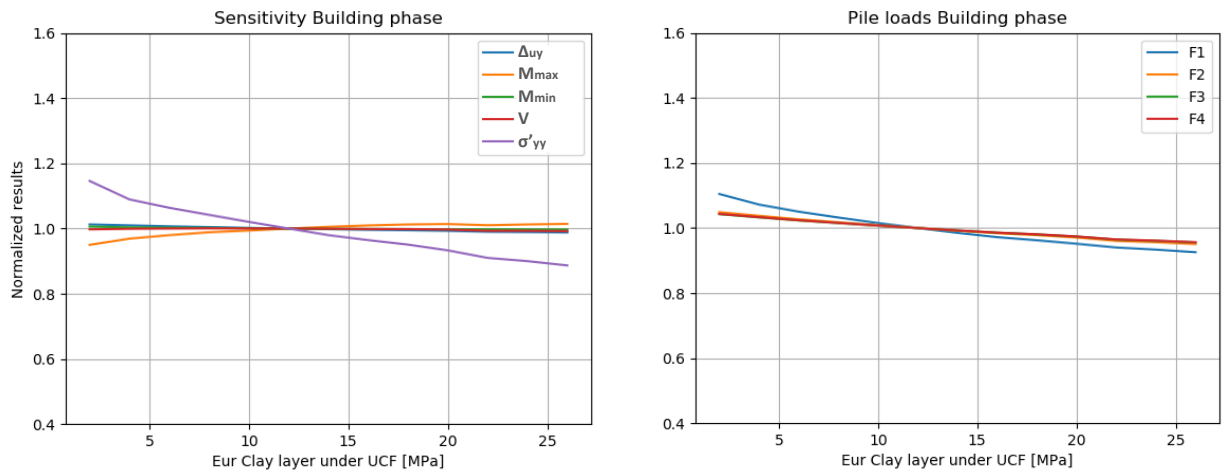


Figure 48 Influence of a varying E_{ur} of the clay layer underneath the UCF in the building phase.

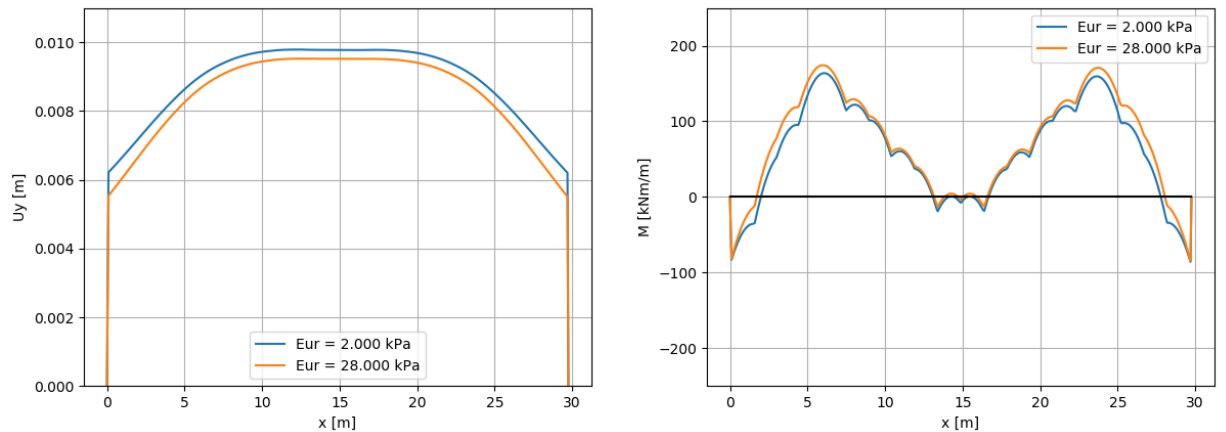


Figure 49 Deformations and bending moments for low and high E_{ur} .

In the final phase the results are opposite to the building phase (Figure 50). Now the clay layer is loaded again. The ratio between the stiffness parameters remained constant. If the stiffness parameters increase the effective soil stress increases as well.

There is also an influence on the bending moments and deformations, which means that the clay layer is part of the load distribution of the column loads. This already shows that for stiff clays the behaviour of the raft is significant.

-Soil-structure interaction of a permanent steel fibre reinforced underwater concrete floor system-

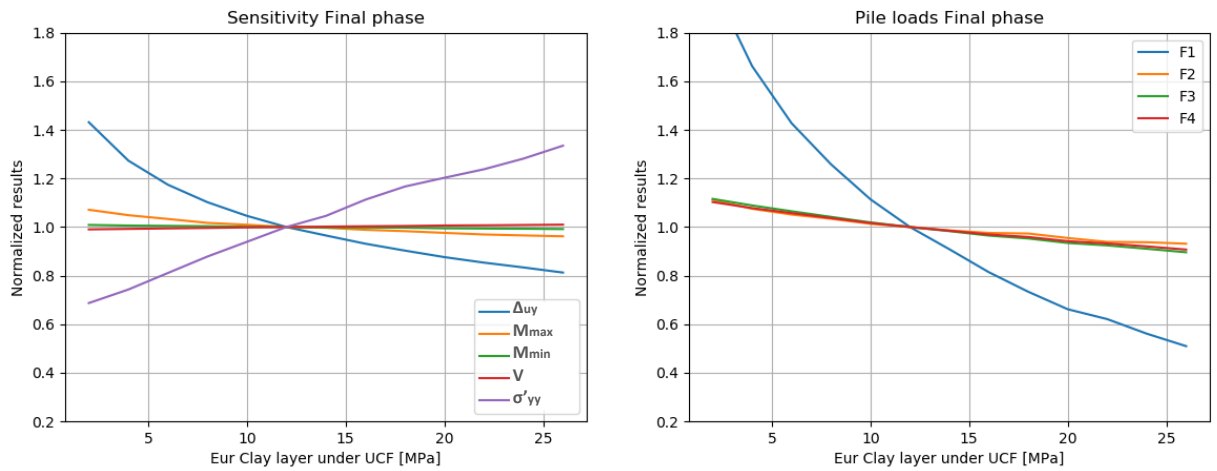


Figure 50 Influence of a varying E_{ur} of the clay layer underneath the UCF in the final phase.

6.7 Stiffness parameters Eemclay

The stiffness parameters of the Eemclay are an uncertainty in the model. Although, the parameters are not completely uncertain. For the North South line the stiffness of the Eemclay was investigated by laboratory testing. The lower and upper bound value for the E_{50} are 20.000 [kPa] and 25.000 [kPa], respectively. With a safety factor of 1.3 this leads to a range of 15.000 [kPa] to 33.000 [kPa]. The main effect of the heave from the Eemclay is the uplift of the complete building pit. The variation of these parameters also has a small influence on the deformations and bending moments in the UCF but not on the pile forces (Figure 51). The difference in deformation and bending moments is in the middle of the UCF (Figure 52). Here the effect of the heave is now exactly the same at the measured results. Also when undrained and drained behaviour of the clay layer are compared the effect on the deformation is the same. No variations in consolidation degree were done, but it was expected that the combination of uncertain stiffness parameters and consolidation degree causes the main difference in deformation between the measured deformation and calculated deformation in the middle part of the building pit. The difference in bending moments in the structure is very small and this justifies the fact that heave from deep layers is mostly neglected.

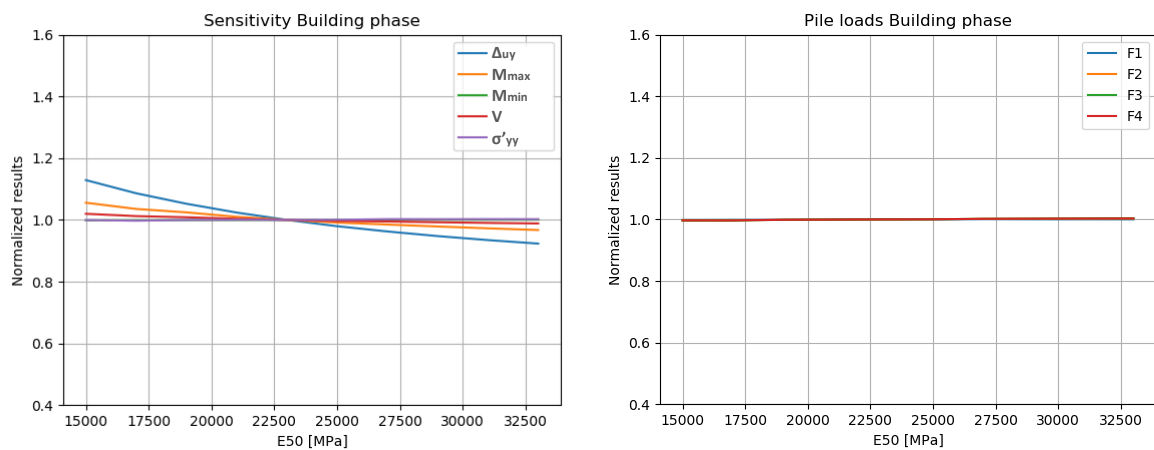


Figure 51 Influence of a varying E_{50} of Eemclay in the final phase.

-Soil-structure interaction of a permanent steel fibre reinforced underwater concrete floor system-

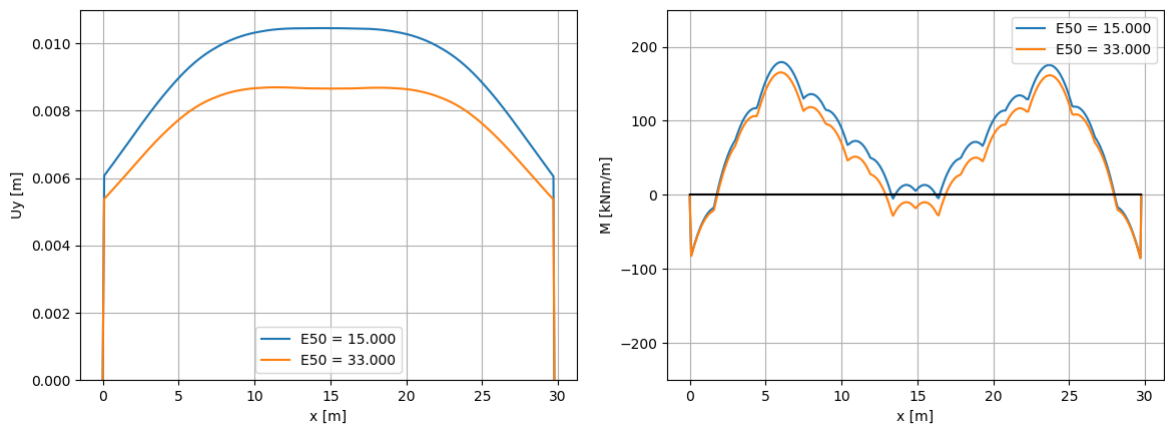


Figure 52 Deformation and bending moments with different E50 for the Eemclay.

6.8 Interface stiffness sheet pile wall

The measured vertical deformations of the sheet piles were smaller than that the Plaxis model showed. To study the effect of this difference, the interface stiffness that determines the stiffness between the soil and the sheet pile walls was varied. R_{inter} is varied from 1/3 towards 1 (Figure 53). If R_{inter} is 1 then the sheet pile response is completely rigid with the soil.

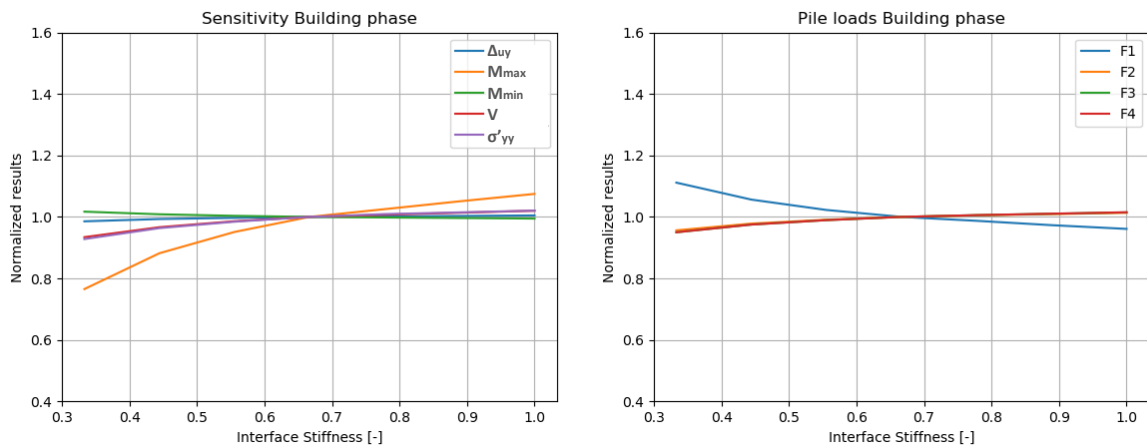


Figure 53 Influence of a varying interface stiffness in the building phase.

When the response of the sheet pile becomes stiffer the bending moments in the structure increase and also the pile force in the first pile increases (Figure 53 and Figure 54). The deformations were mainly influenced near the sheet pile walls (Figure 55). The measured data showed a stiffer response at the locations of the sheet pile walls compared to the calculated deformations. The stiffness response of the sheet pile wall should be modelled stiffer and the biggest uncertainty is the interface stiffness. It was expected that the value should be higher than 2/3 but an exact value cannot be determined.

-Soil-structure interaction of a permanent steel fibre reinforced underwater concrete floor system-

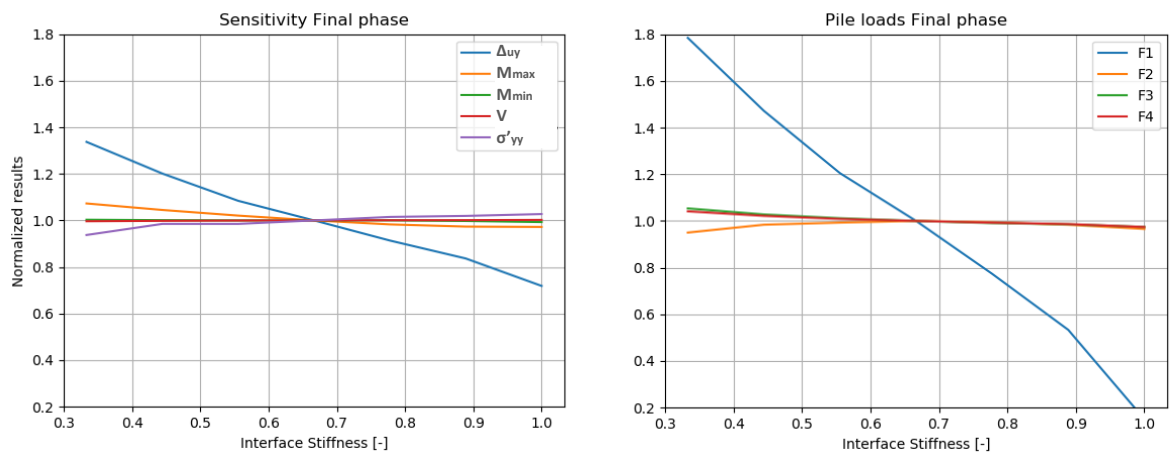


Figure 54 Influence of a varying interface stiffness in the final phase.

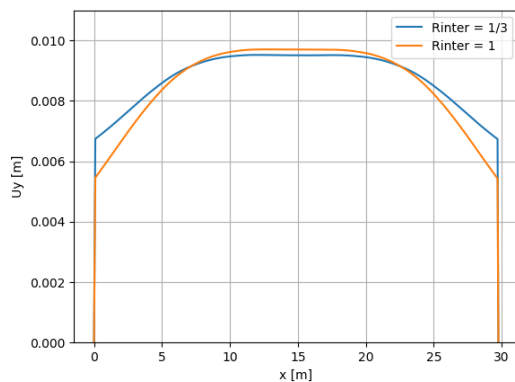


Figure 55 Deformation of UCF for different interface stiffnesses in building and final phase.

6.9 ISF

One of the main uncertainties in the model is the ISF factor, which determines the pile interaction stiffness. In chapter 0 the ISF was derived to fit the pile behaviour of the tested micro piles. A single pile was tested in the field, but in Plaxis this is always a row. The single pile test was used to determine the ISF value. Plaxis automatically determines the ISF value depending on the pile centre to centre distance. This ISF was originally around 0.5 and was changed manually to 1 or 5 depending on the GEWI type.

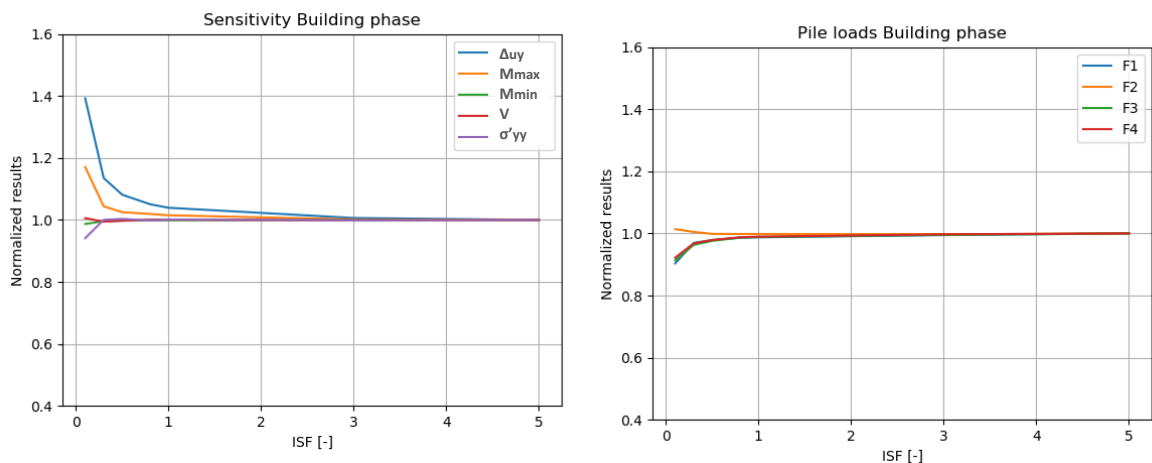


Figure 56 Influence of a varying ISF in the building phase.

With the variation of the ISF (Figure 56) it can be concluded that by increasing the ISF value the result hardly changes. This result was only plotted for the building phase but also for the final phase the influence is very small. Only decreasing the ISF value to almost 0 makes a significant difference in the behaviour of the UCF and the piles. So the ISF is not an uncertainty for this specific case but cannot be used to incorporate the installation effect.

6.10 Type of GEWI anchor

The type of GEWI anchors can determine the behaviour of the UCF. This variation was done to show the influence of the GEWI type for future building pits. This general variation shows why different GEWI anchors can influence the design. The first calculation was done with a building pit with only GEWI 50. The results of the other calculations were divided by the GEWI 50 results to normalize the output. The piles of the original pile plan were varied and the piles that were added later in the building process remain the same GEWI type. The reason not to vary the newly added piles is because these piles were not added for stiffness but for bearing capacity. The piles types are varied from GEWI 40, GEWI 50, GEWI63.5 and GEWI 75. These calculations are shown in the result graphs as dashed lines.

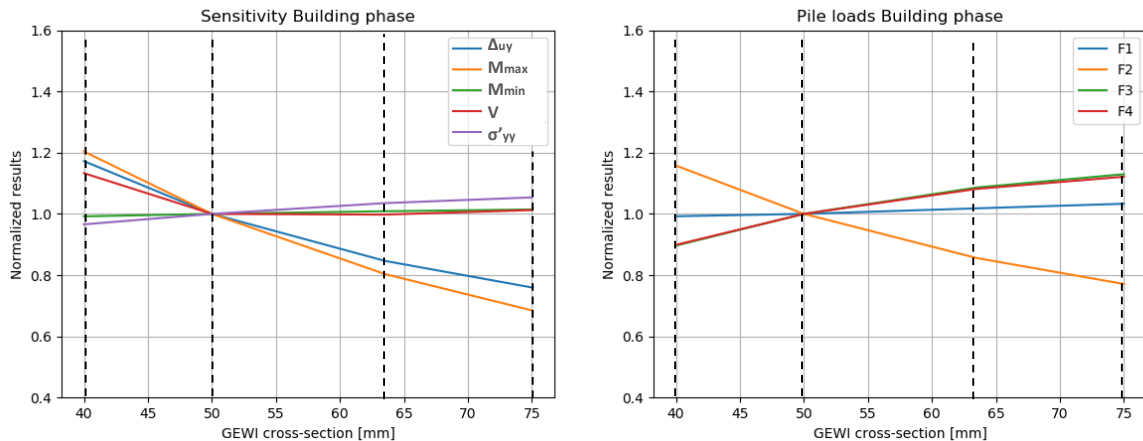


Figure 57 Influence of a varying GEWI type in the building phase.

The variation of the different pile types has a large effect on the deformations and bending moments in the building phase (Figure 57). In the final phase the influence on the bending moments is smaller because the concrete is cracked, which means that the bending moments will not vary that much anymore. Mainly the deformations are influenced by the GEWI piles (Figure 58). It may be concluded that the GEWI type has a lot of influence on the bending moments and deformations and choosing the GEWI type is one of the tools that can be used to control the behaviour of the UCF.

-Soil-structure interaction of a permanent steel fibre reinforced underwater concrete floor system-

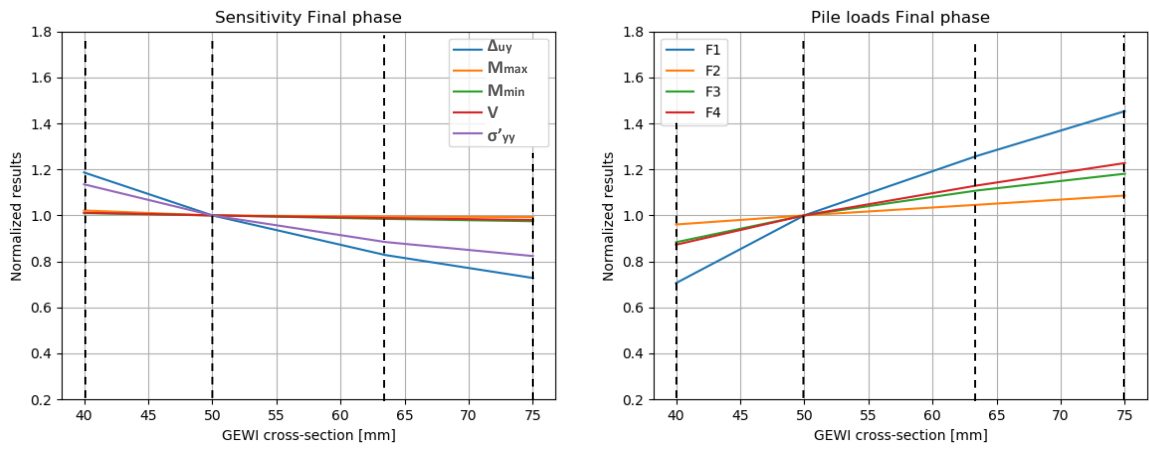


Figure 58 Influence of a varying GEWI type in the building phase

6.11 Load variation

In the former calculations the UCF behaved uncracked in the building phase and cracked in the final phase. But the complete behaviour of such an SFRUCF is interesting, to see for which loads a permanent SFRUCF can be applied. The load starts at zero and is increased until failure occurred.

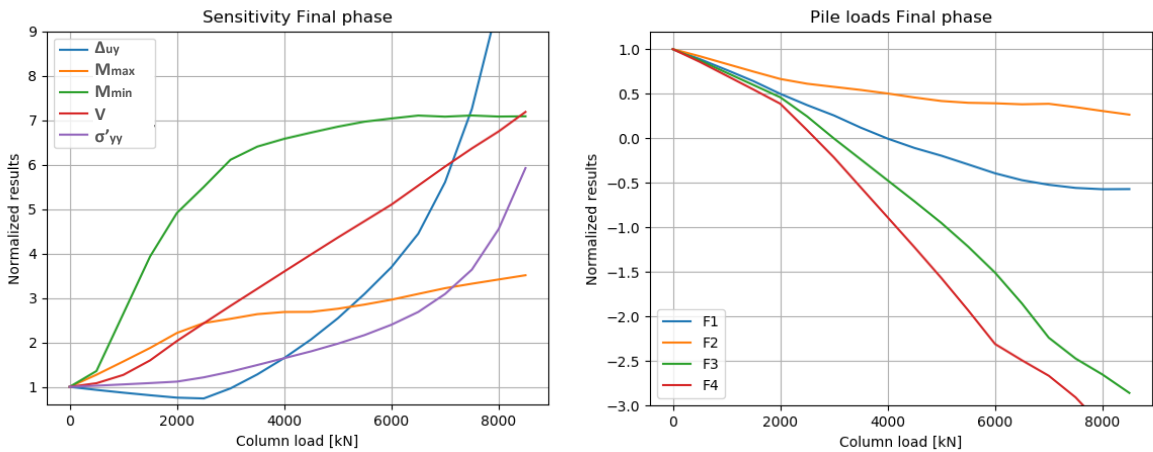


Figure 59 Influence of a varying load in the final phase.

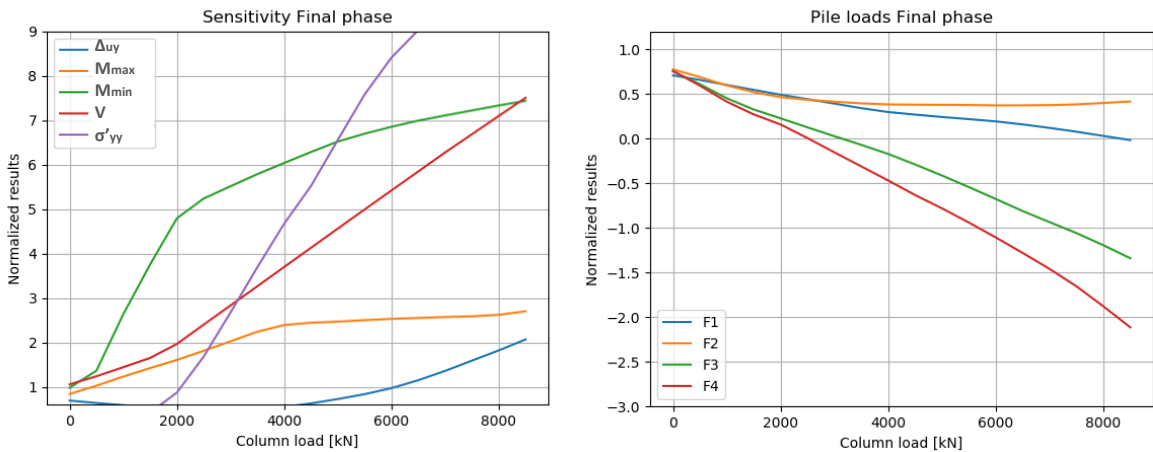


Figure 60 influence of a varying load in the final phase with only sand layers underneath the UCF.

-Soil-structure interaction of a permanent steel fibre reinforced underwater concrete floor system-

It can be seen that the behaviour of the UCF is linear at first and around 2000 kN the first cracks start to appear (Figure 59). The bending moments stop increasing and the deformations start to increase. The shear force, however, remains linear even when the concrete is cracked. It is likely that the shear force related failure mechanism will dominate the design of a permanent SFRUCF.

Until now the soil underneath the UCF was a clay layer. But the permanent SFRUCF was expected to be more suitable with a stiff sand layer. With this stiff sand layer a piled raft foundation would be possible. This effect was already seen for stiff clay layers and the effect is expected to be larger for a sand layer. In this new model the second sand layer starts at the bottom of the UCF. The results of these calculations were divided by the original model with clay to be able to see the differences (Figure 60). The main difference is the increase in effective vertical stress directly underneath the UCF. Also the deformations are reduced by a factor of 4.5. The presence of this stiff raft reduces the forces and the deformations. These deformations determine the crack width and the water tightness of the structure. Taking into account the raft as well can increase the suitability of a permanent SFRUCF and reduce the crack width. Again, there is almost no influence on the shear force within the structure.

6.12 Stiffness parameters sand

In the previous calculation the stiffness was taken from the second sand layer. Now the E_{50} stiffness was varied in the range of 35.000 to 150.000 [MPa]. It can be seen that deformations are highly influenced by the stiffness of the raft (Figure 61). Knowing the stiffness of the raft exactly can improve the design significantly. It is advised to do proper soil investigation when a permanent SFRUCF is designed with the capacity of the raft.

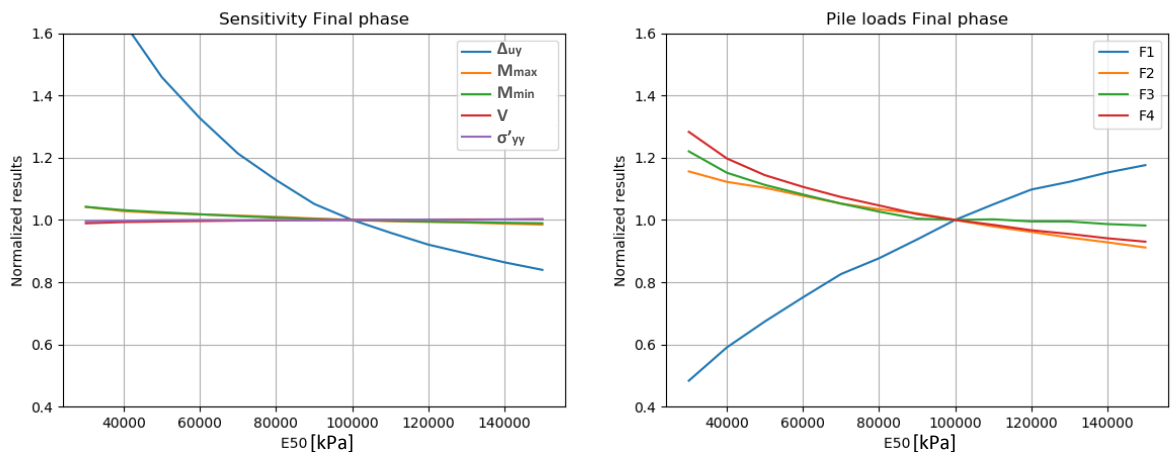


Figure 61 Influence of a varying soil stiffness in the final phase with only sand layers underneath the UCF.

-Soil-structure interaction of a permanent steel fibre reinforced underwater concrete floor system-

7 Discussion

This thesis focused on the applicability of a steel fibre reinforced underwater concrete floor and which design parameters influence the behaviour of such a system with a temporary function or a permanent function. This study consist of two parts. Firstly a model was created that could model the soil structure interaction of such a floor system and include the highly non-linear behaviour of SFRC. The FEM software that was used is Plaxis 2D, which is known for modelling soils and soil structure interaction. The plate model in Plaxis with an MN- κ input was able to describe the behaviour an SFRUCF. The model was validated with the measured field data of the Albert Cuyp garage in Amsterdam to verify if the model could be used for further research. The second part of the thesis shows which parameters influence calculation results, the design and the suitability of a permanent SFRUCF.

7.1 Modelling method

Currently, a linear elastic beam model is used to describe the behaviour of a UCF system, according to CUR77. In the case of a temporary UCF the current model is sufficient, because the behaviour of the floor is only considered in the building phase. However, when the UCF is used permanently, the behaviour in the final phase needs to be considered as well. Since the soil structure interaction plays a major role in the final phase, it is important to use a model that takes this interaction into account. The aim of this thesis was to construct a model for a permanent underwater concrete floor system, taking into account the soil structure interaction.

The model constructed in this study was validated using the Albert Cuyp garage as a case study. It was shown that the model is capable of describing the behaviour of an SFRUCF in a way that is comparable to measured data. For complex situations such as pile raft foundations and for research purposes this model is an improvement compared to the current model.

Additionally, a fictive E-modulus of 10.000 MPa is often used to reflect a cracked behaviour of the concrete in the building phase. This study shows that using the fictive E-modulus can lead to an underestimation of the shear forces and bending moments. The bending moments will redistribute due to the cracking of the concrete but the shear force will increase linearly and has a brittle behaviour. It was therefore advised to do the calculation using the uncracked stiffness of the UCF or, even better, with an MN- κ input for the building phase. For the final phase a fictive E-modulus could be used but it is not possible to determine a universal value because it is dependent on the load.

The biggest uncertainty in the model are the piles. The piles were modelled with springs or embedded beam rows. Springs are easier to model and using CUR236 a spring stiffness can be calculated. For the behaviour of the UCF both the springs and the embedded beam row gave comparable results, also when taking into account the heave from the clay layers directly under the UCF. However, when a piled raft foundation is designed the soil structure interaction is more realistic for the embedded beam row than for the springs. The main disadvantage of the embedded beam row is that it is wished in place, so it does not take into account the installation effect. Adjusting the ISF value manually does not fully compensate for this installation effect. Modelling these piles would be more suitable in Plaxis 3D but the order of magnitude of the 2D calculations was correct when it was compared to field data.

7.2 Validation of the Albert Cuyp garage case

Due to the uplift pressure heave occurred in the clay and peat layer underneath the UCF. Due to this heave the actual load can be 13% to 30% higher than the uplift pressure alone. When the model and the field data are compared it can be concluded that the heave of the deep Eemclay results in more deformation at the middle part of the UCF than was predicted by the model. The heave of this deep layer did not have much influence on the internal forces of the UCF and therefore the heave is mostly neglected. Also, the stiffness of the sheet pile walls was higher in reality than predicted by the model. In the ULS calculations a variation of the pile stiffness and wall stiffness is required. The different stiffness response remained within the range of the variation coefficients and justified the reason for the need of these variation coefficients.

7.3 Sensitivity analysis

The parameters that can be controlled by the engineer to influence the design of the SFRUCF are the thickness and the GEWI type. The choice in thickness and GEWI type have large influences on the

-Soil-structure interaction of a permanent steel fibre reinforced underwater concrete floor system-

deformations and bending moment in the floor. For the complete picture also the pile distances and wall type (sheet pile wall or diaphragm wall) should have been varied.

For the final phase the parameters that have a large influence but cannot be chosen are the soil type and stiffness of the raft. If a stiff soil layer is located under the SFRUCF the raft takes a large part of the load. Due to this stiff raft a large reduction in deformations can be seen. The reduction in the deformations means a decreased crack width which is favourable for the water tightness of the UCF. It should be noted that the calculations did not use safety factors because the behaviour was fitted to field data. When a piled raft foundation is used the stiffness upper and lower bound of structural elements and soils volumes should be used. This decreases the load that can be taken by the raft.

The main difference in demands and design between a permanent SFRUCF and a temporary unreinforced UCF is the water tightness. For a temporary floor no water tightness guidelines are required. If this floor will be used permanently the water tightness guidelines should be implemented. In the old CUR 77 there was also an SLS check for the UCF. This SLS should return because of the permanent function of the UCF. The crack width, water tightness and displacements should be implemented in the guideline.

8 Conclusion

This study addresses the following research questions.

1. What is a good modelling method to describe the soil structure interaction of an SFRUCF?

The current modelling techniques described in CUR77 can still be used when the soil structure interaction is less important. This is the case for a clay layer that is not sensitive to heave. When the building pit is calculated as a piled raft foundation the soil structure interaction can be modelled in Plaxis 2D with the plate model with MN- κ input. With the model constructed in this study it could also be concluded that due to the uplift of the clay and peat layer heave can occur. This heave causes an additional load on the UCF which can be up to 30% higher than would be expected based on calculation without heave.

2. A fictive E-modulus of 10.000 MPa is often used as an assumption for the cracked stiffness. What is the effect of this assumption?

In the building phase a fictive E-modulus can lead to an underestimation of the shear forces and bending moments. The bending moment can be redistributed when the concrete cracks but the shear force will increase linearly. Mainly regarding the shear force it is advised to work with an uncracked E-modulus or a MN- κ input in the building phase. For the final phase a fictive E-modulus can be used but a standard value cannot be derived in this study.

3. Which parameters have the most influence on the design of an SFRUCF system?

For the building phase the floor thickness has the most influence, followed by the GEWI type. For the final phase also the stiffness of the raft determines the design of a permanent SFRUCF. The variation study also showed that the heave from the deep Eemclay influences the deformations of the UCF but hardly has any effect on the internal forces in the UCF. This justifies the fact that this heave is usually not taken into account in the design.

4. How does the static load distribution work in such a floor system? And can it be seen as a piled raft foundation?

Depending on the stiffness of the soil underneath the SFRUCF the raft can be taken into account. This can largely reduce the deformations (up to 4.5x less deformation) and the pile forces (up to 1.5x smaller pile forces). When the deformations are reduced also the crack width and leakage are reduced. Even with a stiff clay layer this reduction in deformations and pile forces can be observed.

5. What are the best conditions to apply a permanent SFRUCF instead of the traditional or integrated principal?

The best conditions for a permanent SFRUC are the situations where the final load is not too large or, when the column loads are large, the raft should consist of a stiff soil to reduce the deformations and crack width. Whether a permanent SFRUCF can be applied depends on the SLS requirements. The water tightness demand will probably be leading in the design. The water tightness is influenced by the bending moments and deformations of the SFRUCF.

6. What should change in the current guidelines to implement a permanent SFRUCF?

An SLS check should be included for water tightness, crack width and deformations.

Main question: What determines the suitability of a permanent steel fibre reinforced underwater concrete floor and how can the soil structure interaction of this non-linear steel fibre reinforced underwater concrete be modelled?

The suitability of an SFRUCF is determined by the loads in the final phase and the presents of a stiff raft. The interaction between the raft and the UCF can be modelled in Plaxis 2D with the plate element that has the behaviour of SFRC. For cases that do not include a stiff raft simpler models can be used, for example the Plaxis model with springs or even a beam model with SFRC input.

-Soil-structure interaction of a permanent steel fibre reinforced underwater concrete floor system-

9 Recommendations for further research

- The modelling of the micro piles is probably more accurate in Plaxis 3D. Whereas Plaxis 2D uses an embedded beam row, Plaxis 3D uses a volume element or an embedded beam enabling the user to study the micro pile behaviour in more detail. When the difference between 2D and 3D modelling is determined, a statement can be made on the effectiveness of the 2D model used in this study.
- In this research not all parameters were varied. For the full behaviour of a building pit also the pile locations and pile distances should be varied. This will give insight into the essential pile locations and the influence of the piled raft foundation with different pile distances. Also the type of soil retaining structure is an interesting parameter to vary, since the difference between sheet pile walls and the much stiffer diaphragm walls is expected to have a large influence on the deformations and bending moments of the UCF.
- This thesis started off with the idea to check the dynamic response of a permanent SFRUCF. Possible applications for a permanent SFRUCF are traffic tunnels or underpasses. In these applications the dynamic loading will play an important role in the design. Until now the behaviour of SFRC for dynamic loading is still uncertain. Research that takes into account the dynamic loading and the behaviour of the SFRC could increase the knowledge on the suitability of a permanent SFRUCF.
- As stated in the literature study, the fatigue behaviour of SFRC is still uncertain. This fatigue behaviour is important when a sign change in the bending moment is expected to occur regularly due to the load in the final phase. The fatigue behaviour of the SFRC should be investigated to ensure the life span of such a structure.
- The current guidelines regarding the modelling of a permanent SFRUCF should be adapted. The most important components that should be added to the guidelines are the SLS requirements. These requirements should describe the deformations, crack width and leakage of the SFRUCF. The current CUR77 describes the behaviour of a UCF that is unreinforced. The behaviour of SFRC is only described in CUR111, which focusses on storage room floors. The behaviour of the SFRUC should be incorporated in CUR77. CUR77 also describes a relatively simple beam model to calculate the internal forces. This beam model does not take into account the interaction with the soil. If a beam model would be derived that can take into account these soil reactions as well, the design of a permanent SFRUCF would be much easier.
- A piled raft foundation is calculated in this thesis. The influence of the raft is significant in these calculations but in reality the lower and upper bound of all stiffnesses should be used: the pile stiffness, soil retaining wall stiffness and soil stiffness. The most unfavourable combination of stiffnesses should be used to model the piled raft foundation. In the best practice CUR report about piled raft foundations some advice is given to decrease the range of the soil stiffness when both the raft and piles are in the same soil layer and when the loads in the piles and soil retaining walls are measured. But further research into the actual behaviour of such a system could decrease the range even further. To decrease the stiffness range of the soil, proper soil investigations should be done including lab tests. For future projects with a UCF it is advised to measure the strain in the UCF to back calculate the bending moments. Also the pile forces should be measured. With these measurements the real behaviour of the UCF and the influence of the raft can be modelled in more detail. This might reduce the stiffness range that needs to be taken into account.

10 References

- A.G. Kooiman, C. v. (2000). Modelling the post-cracking behaviour of steel fibre reinforced concrete for structural design purposes. Delft.
- ABT. (2016). 13722G UO Geïntegreerde keldervloer.
- Arkesteijn, r. (2012). Dimensionering van onderwaterbetonvloeren. Delft.
- Bos, A. v. (2011). Rekenen aan staalvezelbeton. Cement, p. 6.
- CEB-fib model code 2010. (2013). FIB model code for concrete structures . Lausanne: Ernst and sohn.
- Cederhout, R. (2012). Crack width in reinforced steel fibre concrete. Delft.
- CRUX. (2015). RA14153c2 Resultaten UO damwandberekening. Amsterdam.
- CRUX. (2015). RA14153e1 Totaal gedrag bouwkuip – incl. paalfundering. Amsterdam.
- CRUX. (2015). RA14153f2 UO Funderingsadvies. Amsterdam.
- CUR. (2007). CUR111.
- CUR. (2007). CUR111 Staalvezelbeton bedrijfsvloeren op palen - dimensionering en uitvoering. SBR CUR NET.
- CUR. (2014). CUR aanbeveling 77:2014 Rekenregels voor ongewapende onderwaterbetonvloeren. Rotterdam: SBR CUR net.
- CUR 236. (2011). Ankerpalen.
- H.G.Poulos. (2001). Piled raft foundations: design and applications. Geotechnique 51, No. 2, 95-113, 19.
- Hillerborg, A. (1980). Analysis of fracture by means of the fictitious crack model, particularly for fibre reinforced concrete. The International Journal Of Cement Composites, Volume 2, Number 4, 8.
- ir. Ruud Arkesteijn, i. M. (2013). Staalvezelversterkt Onderwaterbeton. Cement, 3.
- J.C. Walraven, S. F. (2013). Gewapend Beton. Delft: TU Delft.
- J.Sluis. (2012). Validation of the embedded beam pile row in Plaxis 2D. Delft.
- Lars Gödde, P. M. (2014). Numerical simulation of the structural behaviour of SFRC slabs with or without. Material and structures, 13.
- Maatkamp, T. (2016). The capabilities of the Plaxis Shotcrete material model for designing laterally loaded reinforced concrete structures in the subsurface. Delft.
- Max Bögl. (2016). Monitoring measurements.
- Molendijk, J. (2017). The influence of the group effect on the micro pile behaviour. Delft.
- Plaxis. (2018). Plaxis 2D Material models manual 2018. Delft.
- Plaxis. (2018). Plaxis 2D reference manual 2018. Delft.

-Soil-structure interaction of a permanent steel fibre reinforced underwater concrete floor system-

R. Schütz, D. P. (2011). Advanced constitutive modelling of shotcrete: Model formulation and calibration. Vienna: Elsevier.

SBRCURnet. (2016). SBRCURnet Definitieve Onderwaterbetonvloeren Haalbaarheidsstudie.

SBRCURnet. (2017). CUR236 Ankerpalen. Delft.

SBRCURnet. (2017). Piled Raft Foundations . Delft.

Volker Staal en Funderingen. (2015). Parkeergarage Boerenwetering GEWI proefpalen.

Volker Staal en Funderingen. (2016). Deelwerkplan GEWI palen TBV Parkeergarage boerenwetering.

Appendix A
Python script for determining the MN-kappa diagram

```
1 0.000000000000000000e+00
2 4.110000000000000000e+02
3 4.978367399080985365e+02
4 5.334296472244989218e+02
5 5.510453441373562100e+02
6 5.621188685358740713e+02
7 5.699275613674469696e+02
8 5.758245528590944105e+02
9 5.804862976364025826e+02
10 5.842943555178788984e+02
11 5.874827830066769820e+02
12 5.902043338127888319e+02
13 5.925635779810697841e+02
14 6.038210759768016942e+02
15
```

```
1 0.00000000000000000000e+00
2 2.182397451214655411e-04
3 2.455625662675801728e-03
4 4.362161789037189569e-03
5 6.204920946591229065e-03
6 8.014060349845232578e-03
7 9.801541600614050234e-03
8 1.157356718232950554e-02
9 1.333384580517493062e-02
10 1.508480448337806354e-02
11 1.682813433342229825e-02
12 1.856506957356719029e-02
13 2.029654367259823081e-02
14 4.882869762960402593e-02
15
```

```
1 import matplotlib.pyplot as plt
2 import numpy as np
3 from scipy.optimize import fsolve
4
5 a='SLS'          #SLS or ULS
6
7 ##Parameters
8 b=1.0           #m
9 h=0.9           #m
10 E=31000000.0   #kN/m
11 fc=25000.0     #kN/m2
12 ft=2600.0      #kN/m2
13 ftp=1147.0     #kN/m2
14 N=400          #kN
15 i=10           #Number of points
16 ycc=1.2        #safety factor concrete compression
17 yft=1.25       #Safety factor concrete in tension
18
19
20 ##Parameters ULS or SLS
21 if a == 'ULS':
22     fc = fc/ycc
23     ft = ft/yft
24     ftp = ftp/yft
25     ec=1.75
26 else:
27     ec=2.1
28 print(a, 'Calculation')
29
30 ##Initial
31 sign=N/(b*h)
32 n=i+4
33 epsb=np.zeros(n)
34 epso=np.zeros(n)
35 M=np.zeros(n)
36 Kappa=np.zeros(n)
37 xu=np.zeros(n)
38
39 ##Cracking moment
40 epsb[1]=(-(ft+2*sign)/E)
41 epso[1]=(ft/E)
42 M[1]=(b*h**2*(ft+sign))/6
43 Kappa[1]=(abs(epsb[1])+abs(epso[1]))/h
44
45 ##yielding concrete
```

```

46 def T1(xu):
47     y1=(xu/(fc-sign))*(ft+sign)*0.5*(ft+sign)*b
48     return y1
49 def T2(xu):
50     y2=0.5*b*(ft-ftp)*(0.1*xu/(ec))
51     return y2
52 def T3(xu):
53     y3=(h-xu-xu*(ft+sign)/(fc-sign))*b*(ftp+sign)
54     return y3
55 def N1(xu):
56     y4=0.5*b*xu*(fc-sign)
57     return y4
58
59 def f(xu):
60     y5=-N1(xu)+T1(xu)+T2(xu)+T3(xu)
61     return y5
62 xu[n-2]=fsolve(f,0.5)
63 epsb[n-2]=(-ec/1000)
64 epso[n-2]=-(epsb[n-2]/xu[n-2])*(h-xu[n-2])
65 M[n-2]=(2/3)*N1(xu[n-2])*xu[n-2]+(2/3)*T1(xu[n-2])*xu[n-2]
        *(ft+sign)/(fc-sign)+T2(xu[n-2])*(xu[n-2]*ft/fc+1/3*(.1*xu
        [n-2]/(ec)))+T3(xu[n-2])*(1/2*(h-xu[n-2]-xu[n-2]*(ft+sign)
        /(fc-sign))+xu[n-2]*(ft+sign)/(fc-sign))
66 Kappa[n-2]=(abs(epsb[n-2])+abs(epso[n-2]))/h
67
68 ##Failure
69 def N1(xu):
70     y4=0.75*b*xu*(fc-sign)
71     return y4
72 def f(xu):
73     y5=-N1(xu)+T1(xu)+T2(xu)+T3(xu)
74     return y5
75
76 xu[n-1]=fsolve(f,0.5)
77 epsb[n-1]=(-0.0035)
78 epso[n-1]=-(epsb[n-1]/xu[n-1])*(h-xu[n-1])
79 M[n-1]=(11/18)*N1(xu[n-1])*xu[n-1]+(2/3)*T1(xu[n-1])*xu[n-1]
        *(ft+sign)/(fc-sign)+T2(xu[n-1])*(xu[n-1]*ft/fc+1/3*(.1*
        xu[n-1]/(ec)))+T3(xu[n-1])*(1/2*(h-xu[n-1]-xu[n-1]*(ft+
        sign)/(fc-sign))+xu[n-1]*(ft+sign)/(fc-sign))
80 Kappa[n-1]=(abs(epsb[n-1])+abs(epso[n-1]))/h
81
82 ##Other points
83 def T1(xu):
84     y1=(.5*xu*(ft+sign)/(fc-sign))*(ft+sign)*b

```

```
85     return y1
86 def T2(xu):
87     y2 = .5*b*(ft-ftp)*(0.1*xu/(ec))
88     return y2
89 def T3(xu):
90     y3 =(h-xu-xu*(ft+sign)/(fc-sign))*b*(ftp+sign)
91     return y3
92
93 for m in range(2,n-2):
94     epso[m]=((epso[n-2]-epso[1])/(n-3))*(m-1)+epso[1]
95     def N1(xu):
96         y4=(1/2)*b*xu*(fc*epso[m]*xu/((ec/1000)*(h-xu))-
sign)
97         return y4
98     def f(xu):
99         y5 = -N1(xu) + T1(xu) + T2(xu) + T3(xu)
100        return y5
101    xu[m] = fsolve(f, 0.5)
102    epsb[m]=epso[m]*xu[m]/(h-xu[m])
103    Kappa[m] = (abs(epsb[m])+abs(epso[m]))/ h
104    M[m]=(2/3)*N1(xu[m])*xu[m]+(2/3)*T1(xu[m])*xu[m]*(ft+
sign)/(fc-sign)+T2(xu[m])*(xu[m]*ft/fc+1/3*(.1*xu[m]/(ec)
)))+T3(xu[m])*(1/2*(h-xu[m]-xu[m]*(ft+sign)/(fc-sign))+xu[
m]*(ft+sign)/(fc-sign))
105
106 plt.plot(Kappa,M)
107 plt.show()
108 np.savetxt('M', (M))
109 np.savetxt('Kappa', (Kappa))
110
```

Appendix B Monitoring data pressure head under the UCF

The water pressure directly under the UCF was measured during the construction phase. Pressure relief pipes were installed through the UCF. The head in these pipes and in the gravel layer under the UCF could have a maximum value of -2.75 meters NAP. In five of these pipes the pressure was also measured and in the middle of the building pit the pressure head was measured in the gravel layer under the UCF.

The results in the different measurement points are similar to each other (). The pressure head is lower than the expected maximum value which means that the pressure is mainly influenced by the water level in the building pit. So the UCF is more permeable than the clay and peat layer underneath the UCF.

Multiple phases can be seen in the graphs. In the first dewatering stage the building pit is dewatered until -3 meters NAP and a strut layer is installed. After the installation of the struts the water level is lowered towards -4 meters NAP and the dewatering had to stop because the deformations of the sheet pile walls became too big. Around 9 January a drop in the pressure head can be spotted. Additional precautions were taken to prevent the sheet piles from deforming too much in order to continue dewatering. However the sheet pile walls continued to deform too much and the water had to be pumped in the building pit again. Additional struts were installed at both ends of the building pit.

In the last phase the building pit is completely dewatered. After the dewatering the water head stabilizes at approximately -5.0 meters NAP. At -5 meters NAP the inflow from the clay and peat layers and the outflow through the UCF is in equilibrium. Before an equilibrium is reached a dip can be seen in the water head. This is because the UCF was lifted due to the pressure difference. The water could not flow through the clay layer towards the gravel layer that quickly so an under pressure is visible.



figure B 1 Pressure relief pipe 9380 (Max Bögl, 2016)

- Appendix B -
 - Monitoring data pressure head under the UCF -

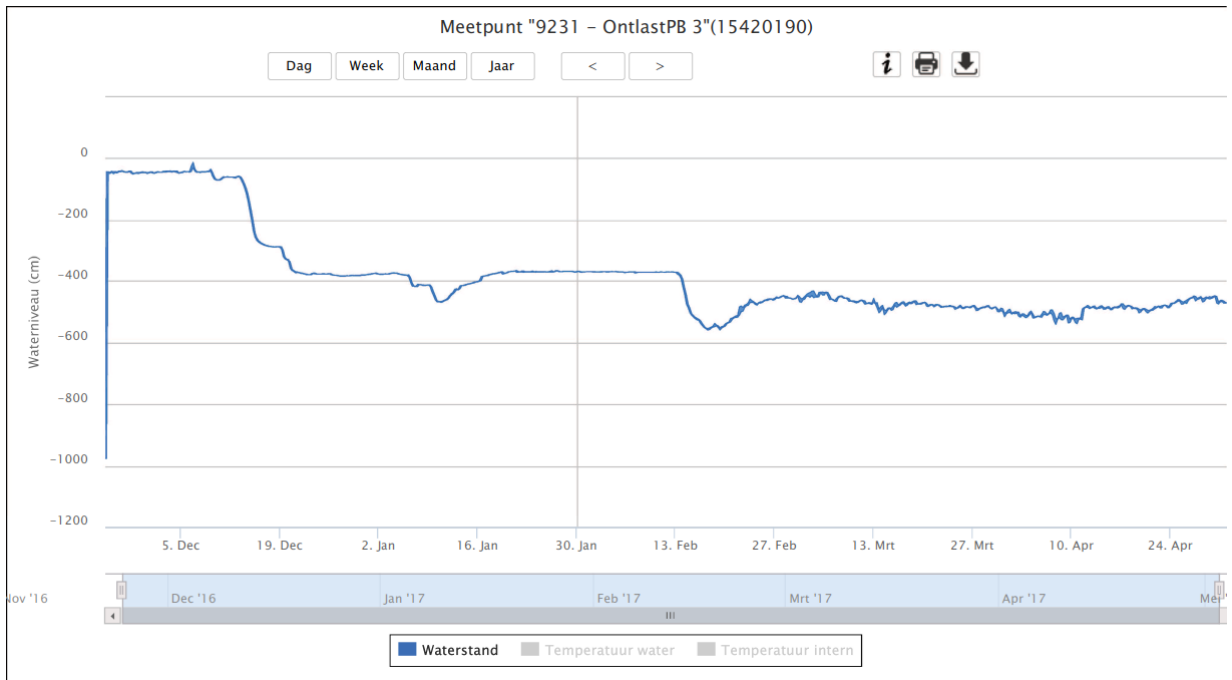


figure B 2 Pressure relief pipe 9231 (Max Bögl, 2016)



figure B 3 Pressure relief pipe 9396 (Max Bögl, 2016)

- Appendix B -
 - Monitoring data pressure head under the UCF -



figure B 4 Pressure relief pipe 9256 (Max Bögl, 2016)



figure B 5 Pressure relief pipe 9256 (Max Bögl, 2016)

- Appendix B -
 - Monitoring data pressure head under the UCF -

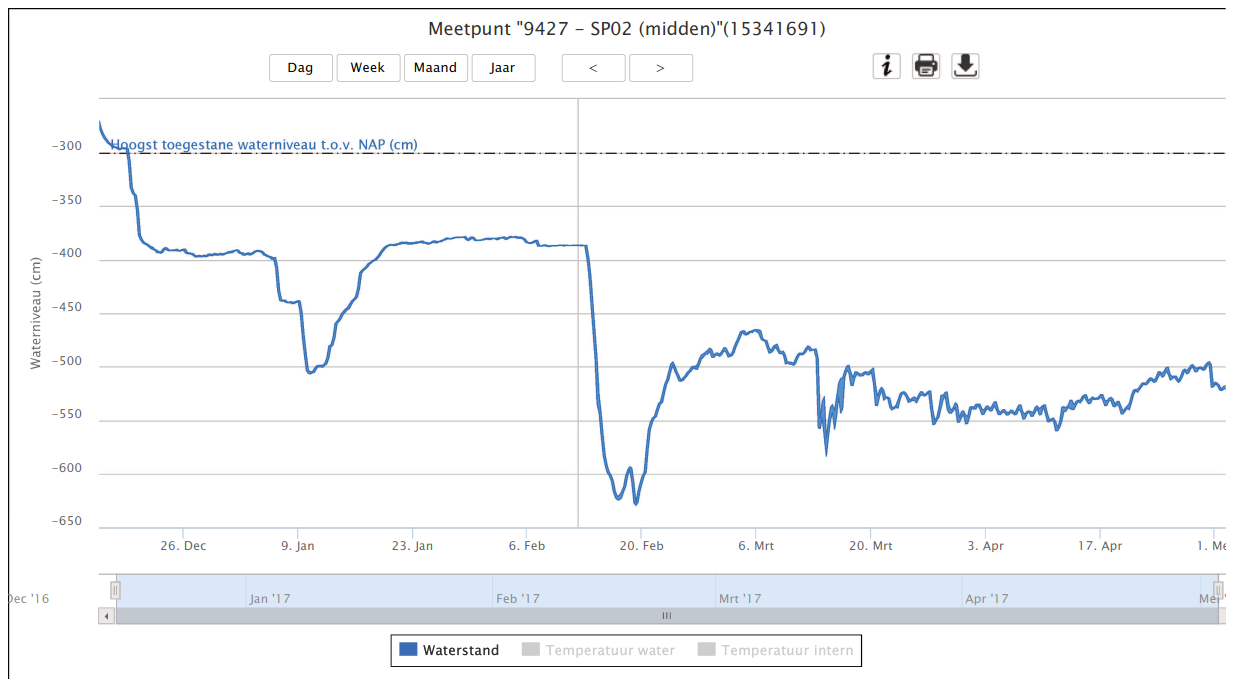


figure B 6 Pressure point under UCF 9427 (Max Bögl, 2016)

Appendix C
Monitoring data of the SFRUCF Albert Cuyppgarage

BUZING GEWOI

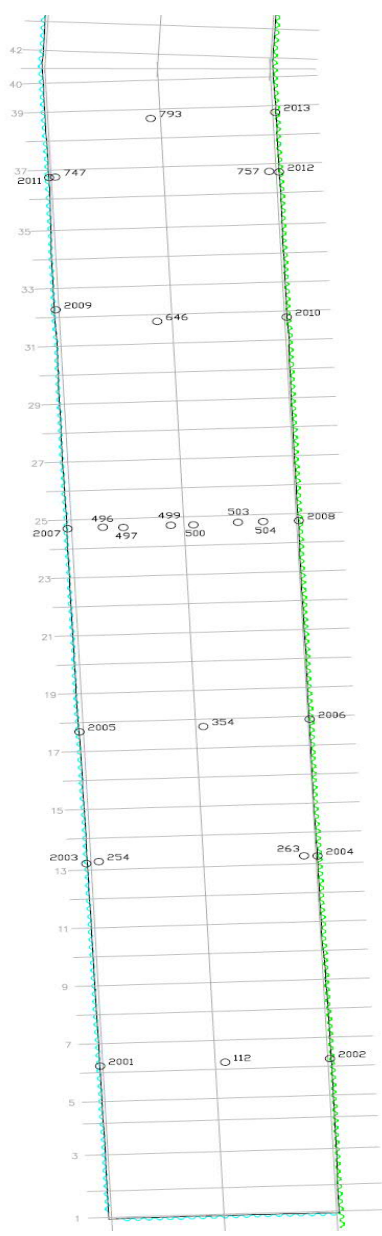
Gewi anker nr.	0-meting		meting 1		meting 2		meting 3		meting 4		meting 5		meting 6		meting 7		meting 8		verschil m8 - m0
	15.12.2016	15.12.2016	05.01.2017	10.01.2017	14.02.2017	15.02.2017	16.02.2017	17.02.2017	18.02.2017	19.02.2017	20.02.2017	17.02.2017	18.02.2017	19.02.2017	20.02.2017	17.02.2017	18.02.2017	19.02.2017	
793	500	501	501	501	501	501	501	501	501	501	501	501	501	501	501	501	501	501	3
797	476	476	0	477	477	477	477	477	477	477	477	477	477	477	477	477	477	477	3
747	497	497	0	497	497	497	497	497	497	497	497	497	497	497	497	497	497	497	3
486	487	487	0	488	488	488	488	488	488	488	488	488	488	488	488	488	488	488	3
497	482	482	1	481	481	481	481	481	481	481	481	481	481	481	481	481	481	481	5
499	481	481	1	481	481	481	481	481	481	481	481	481	481	481	481	481	481	481	3
501	514	514	0	515	515	515	515	515	515	515	515	515	515	515	515	515	515	515	3
503	514	514	0	515	515	515	515	515	515	515	515	515	515	515	515	515	515	515	3
504	514	514	0	515	515	515	515	515	515	515	515	515	515	515	515	515	515	515	3
505	491	491	0	491	491	491	491	491	491	491	491	491	491	491	491	491	491	491	3
354	479	479	0	479	479	479	479	479	479	479	479	479	479	479	479	479	479	479	2
263	500	500	1	500	500	500	500	500	500	500	500	500	500	500	500	500	500	500	2
112	490	490	0	490	490	490	490	490	490	490	490	490	490	490	490	490	490	490	2

BUZING DAMVANDPLANK

Gewi anker nr.	0-meting		meting 1		meting 2		meting 3		meting 4		meting 5		meting 6		meting 7		meting 8		verschil m8 - m0
	15.12.2016	15.12.2016	05.01.2017	10.01.2017	14.02.2017	15.02.2017	16.02.2017	17.02.2017	18.02.2017	19.02.2017	20.02.2017	17.02.2017	18.02.2017	19.02.2017	20.02.2017	17.02.2017	18.02.2017	19.02.2017	
793	500	501	501	501	501	501	501	501	501	501	501	501	501	501	501	501	501	501	3
797	476	476	0	477	477	477	477	477	477	477	477	477	477	477	477	477	477	477	3
747	497	497	0	497	497	497	497	497	497	497	497	497	497	497	497	497	497	497	3
486	487	487	0	488	488	488	488	488	488	488	488	488	488	488	488	488	488	488	3
497	482	482	1	481	481	481	481	481	481	481	481	481	481	481	481	481	481	481	5
499	481	481	1	481	481	481	481	481	481	481	481	481	481	481	481	481	481	481	3
501	514	514	0	515	515	515	515	515	515	515	515	515	515	515	515	515	515	515	3
503	514	514	0	515	515	515	515	515	515	515	515	515	515	515	515	515	515	515	3
504	514	514	0	515	515	515	515	515	515	515	515	515	515	515	515	515	515	515	3
505	491	491	0	491	491	491	491	491	491	491	491	491	491	491	491	491	491	491	3
354	479	479	0	479	479	479	479	479	479	479	479	479	479	479	479	479	479	479	2
263	500	500	1	500	500	500	500	500	500	500	500	500	500	500	500	500	500	500	2
112	490	490	0	490	490	490	490	490	490	490	490	490	490	490	490	490	490	490	2

BUZING OVR

Gewi anker nr.	Na meting 1		Na meting 2		Na meting 3		Na meting 4		Na meting 5		Na meting 6		Na meting 7		Na meting 8	
	15.12.2016	20.12.2016	05.01.2017	10.01.2017	15.02.2017	20.12.2016	05.01.2017	10.01.2017	15.02.2017	20.12.2016	05.01.2017	10.01.2017	15.02.2017	20.12.2016	05.01.2017	10.01.2017
793	2	2	2	2	2	3	3	3	3	3	3	3	3	3	3	3
797	1	1	1	1	1	0	0	0	0	0	0	0	0	0	0	0
747	2	2	2	2	2	4	4	4	4	4	4	4	4	4	4	4
486	0	0	0	0	0	-1	-1	-1	-1	-1	-1	-1	-1	-1	-1	-1
497	0	0	0	0	0	3	3	3	3	3	3	3	3	3	3	3
499	0	0	0	0	0	5	5	5	5	5	5	5	5	5	5	5
501	1	1	1	1	1	3	3	3	3	3	3	3	3	3	3	3
503	1	1	1	1	1	4	4	4	4	4	4	4	4	4	4	4
504	1	1	1	1	1	3	3	3	3	3	3	3	3	3	3	3
354	3	3	3	3	3	2	2	2	2	2	2	2	2	2	2	2
263	2	2	2	2	2	1	1	1	1	1	1	1	1	1	1	1
112	1	1	1	1	1	3	3	3	3	3	3	3	3	3	3	3



Appendix D

Plaxis Input stages Albert Cuyppgarage

A Plaxis calculation of the Albert Cuyppgarage was compared with a calculation in SCIA and D-sheet piling and also with the monitoring data. The Plaxis calculation consisted out of multiple phases. This appendix describes the different phases of the calculation.

The phases:

1. Initial phase
2. Initial canal
3. Installation of the sheetpille walls
4. Excavate until -3 meters NAP
5. Installation of a pre-stressed strut
6. Excavate until -10.5 meters
7. Install gewi-anchors
8. Pore Underwater concrete
9. Dewatering of the building pit
10. Load from user phase (only in variation study)

1. Initial phase

The initial phase should model the initial stresses in the soil. In the initial phase a canal is at the location of the building pit. The initial stresses in the soil depend on the calculations settings. There are three different settings that can be used for the initial stresses: Field stresses, Gravity loading and K0 procedure. The setting Field stresses is mainly used when a rotation of the principle stress is needed, which is mainly used for rock formations that have undergone a rotation of the principal stress. Gravity loading determines the initial stresses based on the volumetric weight of the soil. K0 procedure defines the initial stresses taking into account the loading history of the soil. The K0 procedure is not recommended when dealing with non-horizontal surfaces.

Field stresses: Not suitable because principle stresses are not rotated.

Gravity loading: Suitable but failure of canal slope occurred in the initial phase.

K0 procedure: Not suitable because the surface is non horizontal.

Because the Gravity loading was not stable in the initial phase the K0 procedure was used. The first stage is a horizontal surface without a canal. The second stage is the excavation of the canal. After the second stage all displacements and strains were reset to 0 again.

2. Initial canal

The second stage was the excavation of the existing canal. After this stage the displacements and strains were reset to 0 again. So actually this second stage was the initial stage of the calculation.

3. Installation of the sheetpille walls

The sheet pille walls are installed. During this stage horizontal deformations occurred in Plaxis. But in reality the installation of the sheet pille walls was done in stable ground. After the installation of the sheet pile walls the displacements and strains were reset again.

4. Excavate until -3 meters NAP

The first excavation stage until -3 meters NAP was for the first strut layer.

5. Installation of a pre-stressed strut

A strut was installed with a pre-stressing force of 250 kN at -2.5 meters NAP.

6. Excavation until -10.5 meters NAP

The second excavation stage was also the final excavation stage.

7. Install gewi anchors

The installation of the gewi anchors had to be done in a separate phase.

- Appendix D -
- Plaxis Input stages Albert Cuyppgarage-

8. Pore gravel and underwater concrete

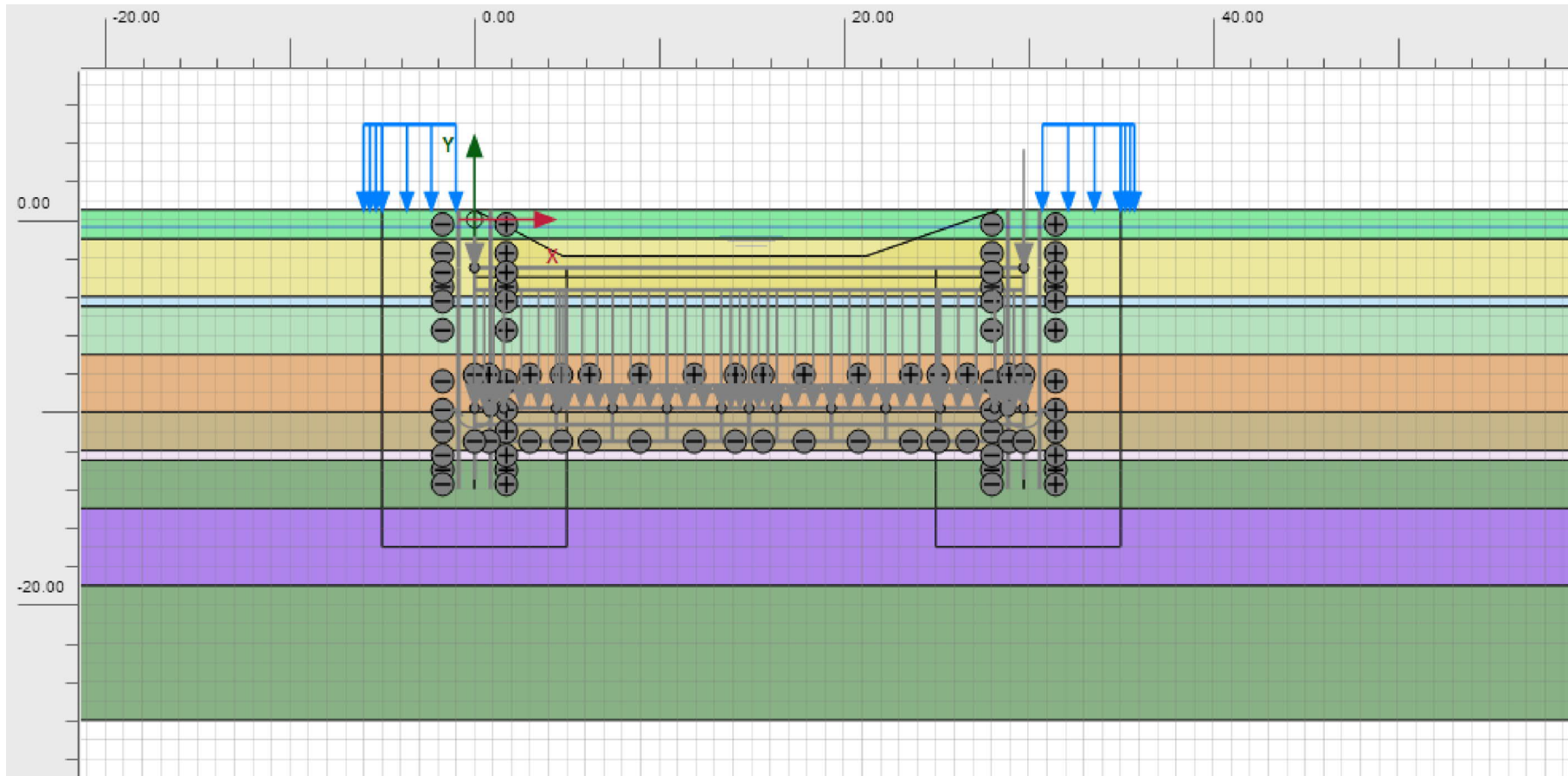
In reality the UCF was poured without stresses in the concrete (not taking into account shrinkage). But when the concrete plate has a self-weight, stresses will already occur due to the self-weight of the concrete. Because of this the self-weight of the concrete is put to 0 and the self-weight is added in the form of a line load on the plate during the dewatering phase.

9. Dewatering of the building pit

In this phase the building pit was dewatered. Also the line load for the self-weight of the concrete floor was added in this stage.

10. Load from user phase (only in variation study)

In the user phase three point loads were added. Two point loads on the sheet pile walls and 1 point load in the middle of the UCF. This represents a tunnel or a parking garage like the Albert Cuyppgarage. The pointload in the middle was twice as big as the point loads on the sheet pill walls.



Project description

Phase 1 Initial phase

Date

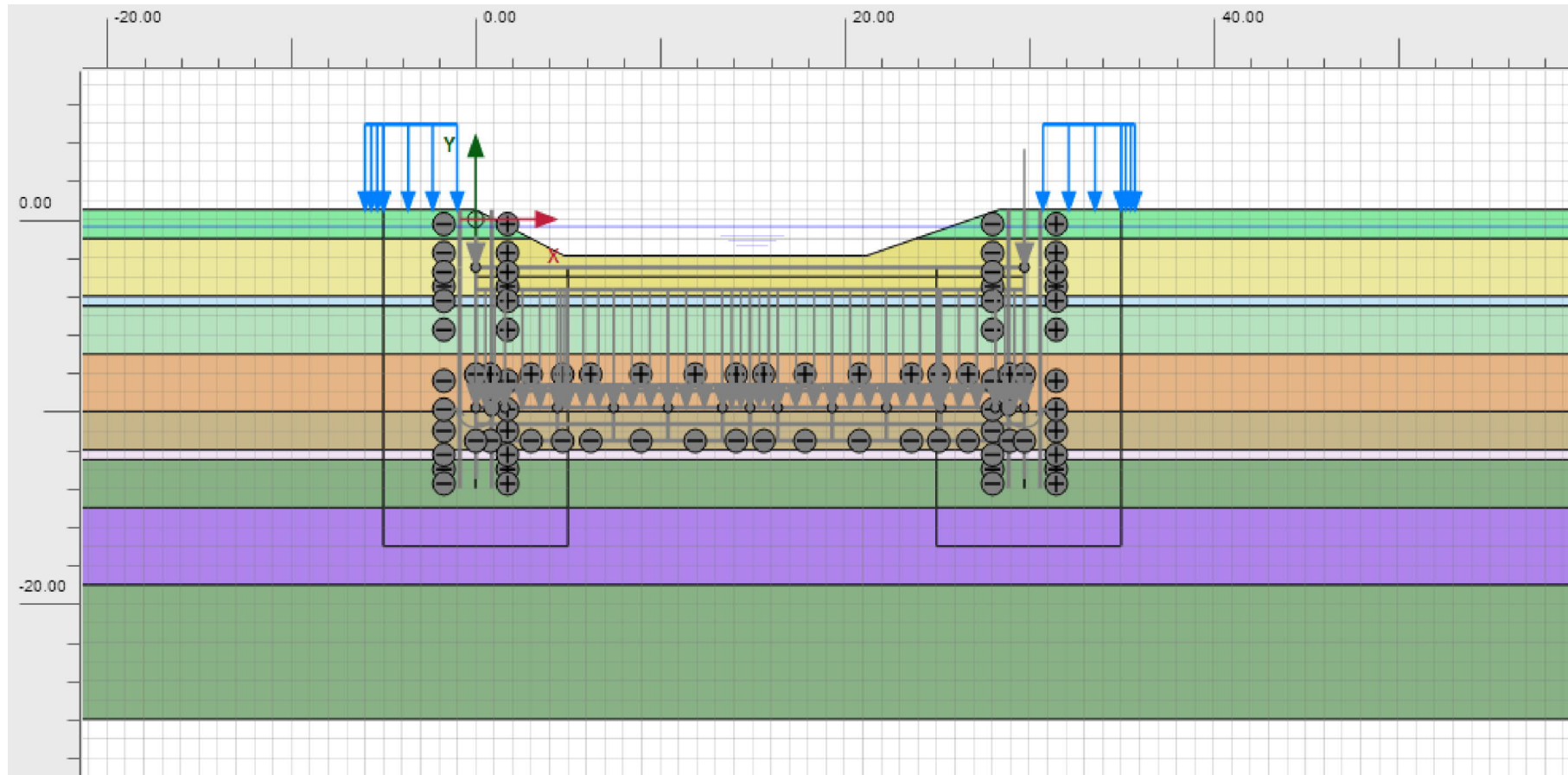
21-11-2018

Project filename

Albert cuypgarage.p2dx

User name

ABT bv



Project description

Phase 2 Initial canal

Date

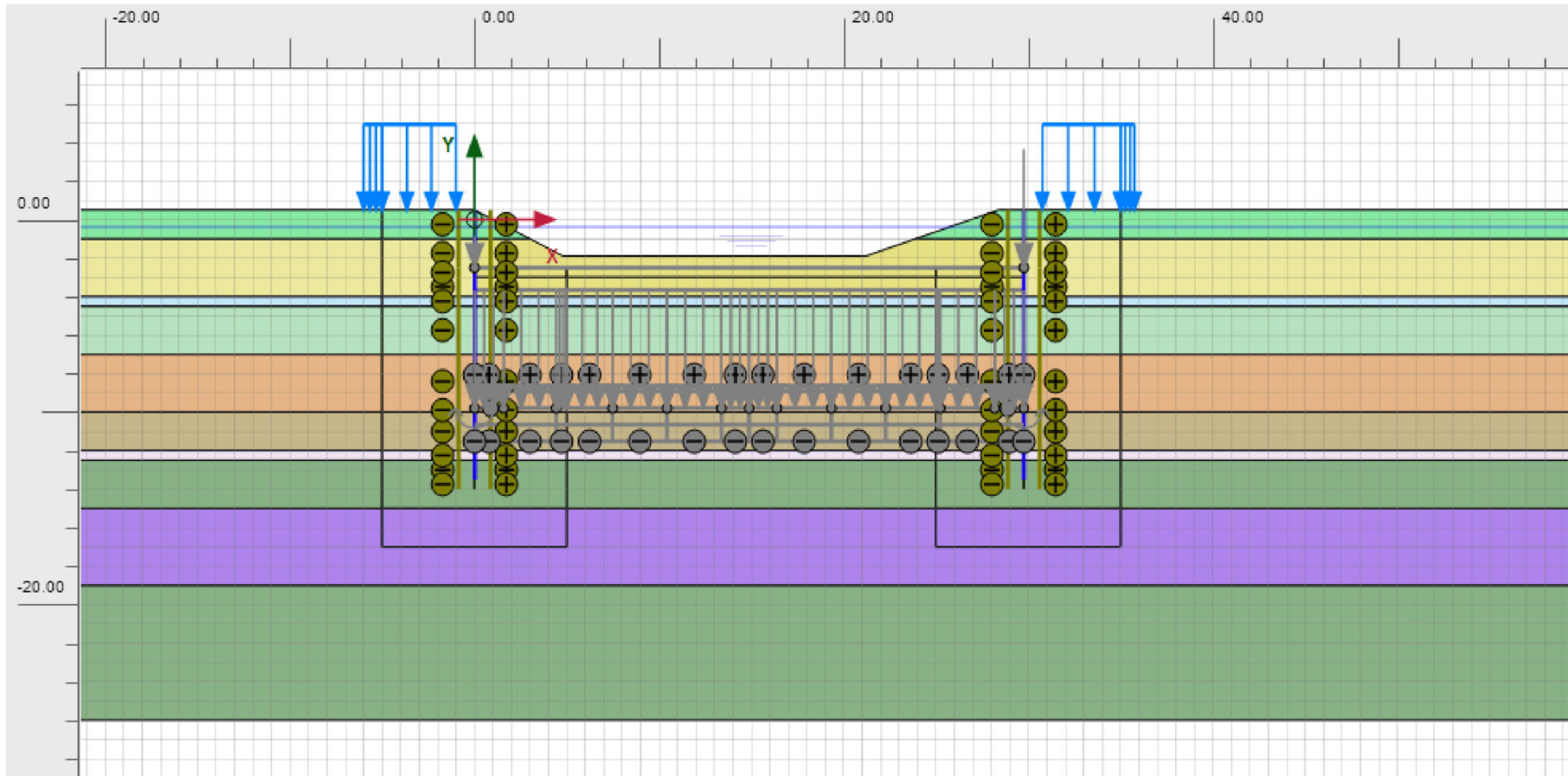
21-11-2018

Project filename

Albert cuypgarage.p2dx

User name

ABT bv



Project description

Phase 3 Installation of the sheetpile walls

Date

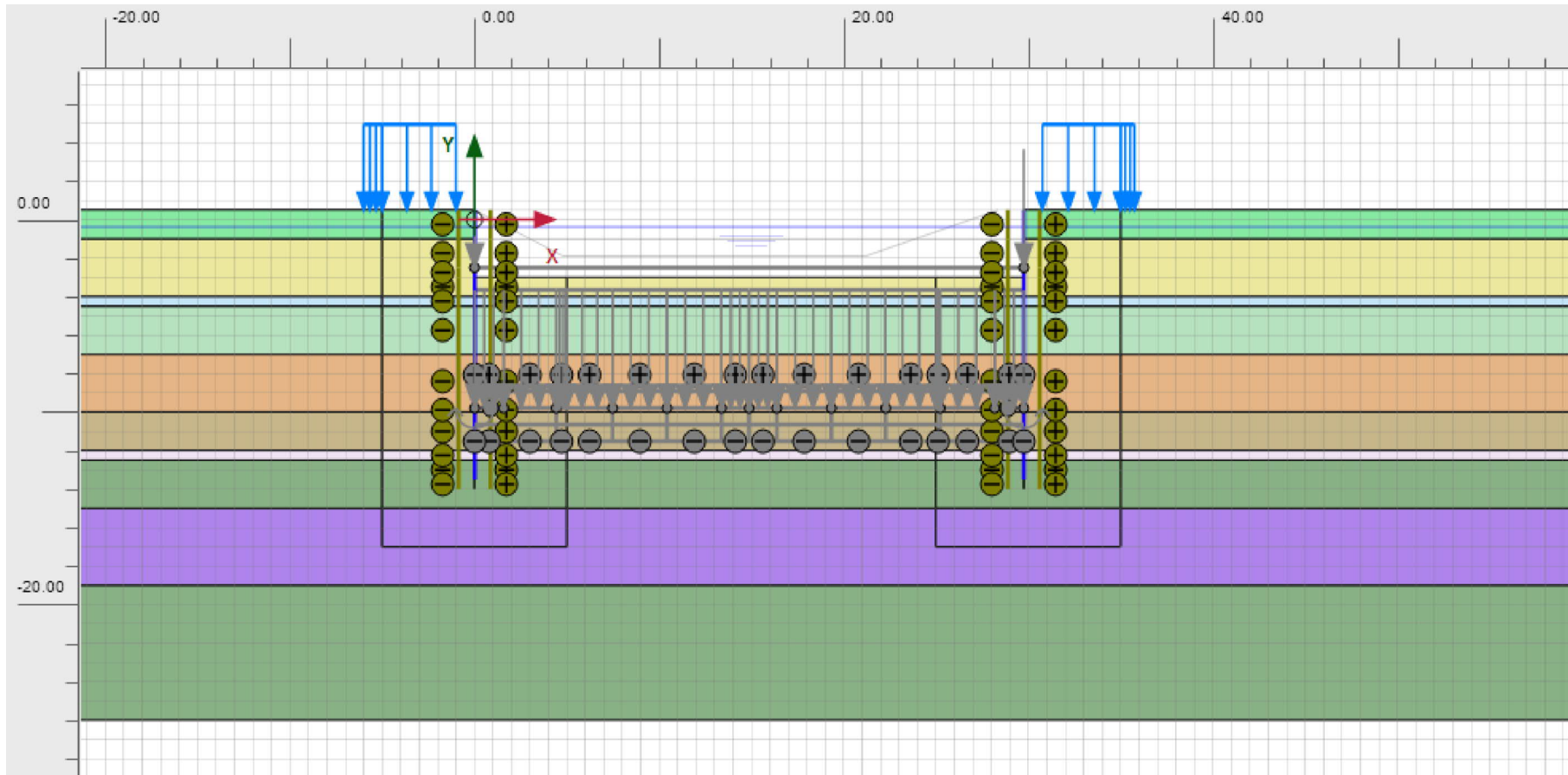
21-11-2018

Project filename

Albert cuypgarage.p2dx

User name

ABT bv



Project description

Phase 4 Excavate until -3 meters NAP

Date

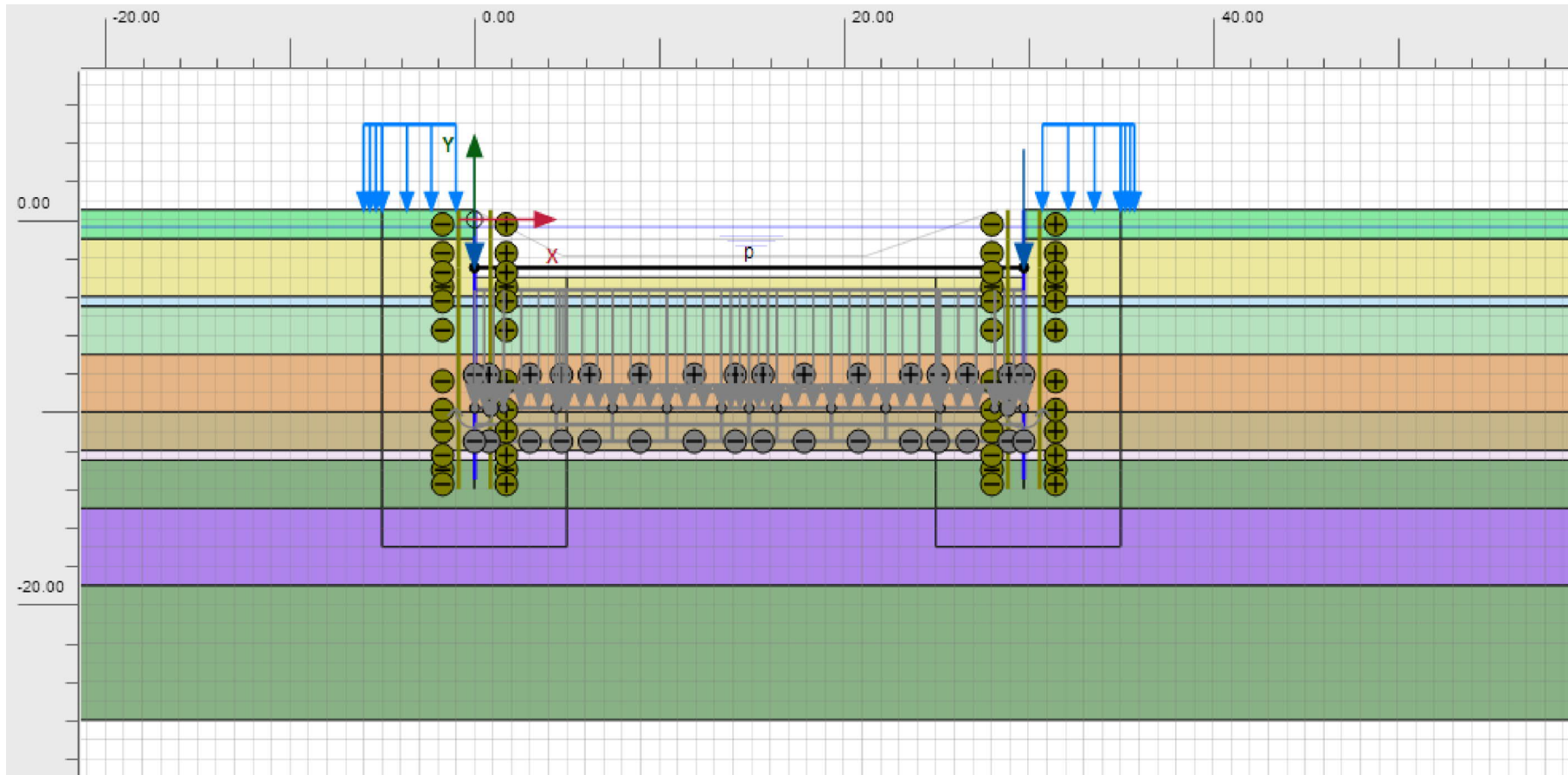
21-11-2018

Project filename

Albert cuypgarage.p2dx

User name

ABT bv



Project description

Phase 5 Installation of a pre-stressed strut

Date

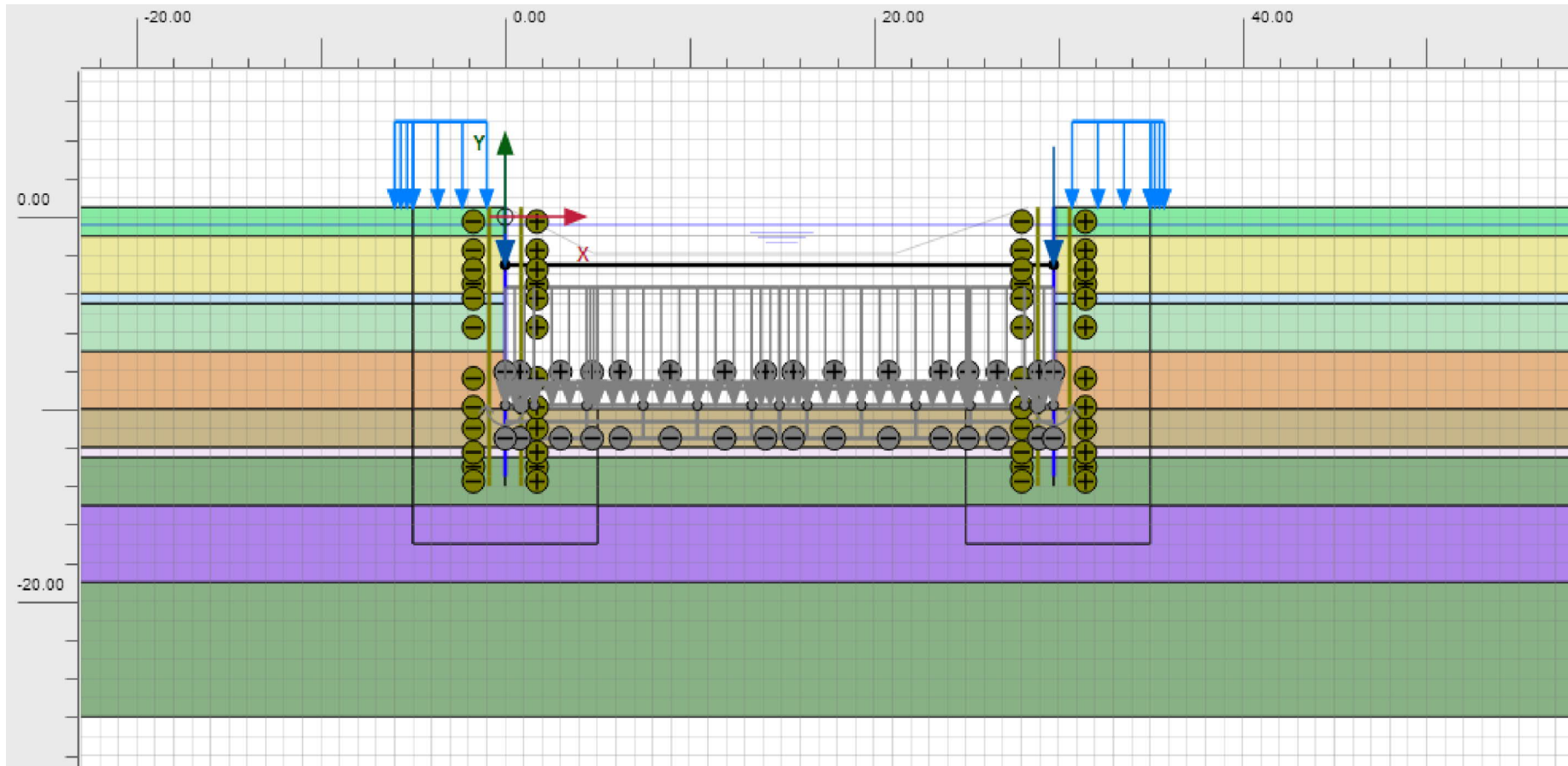
21-11-2018

Project filename

Albert cuypgarage.p2dx

User name

ABT bv



Project description

Phase 6 Excavate until -10.5 meters

Date

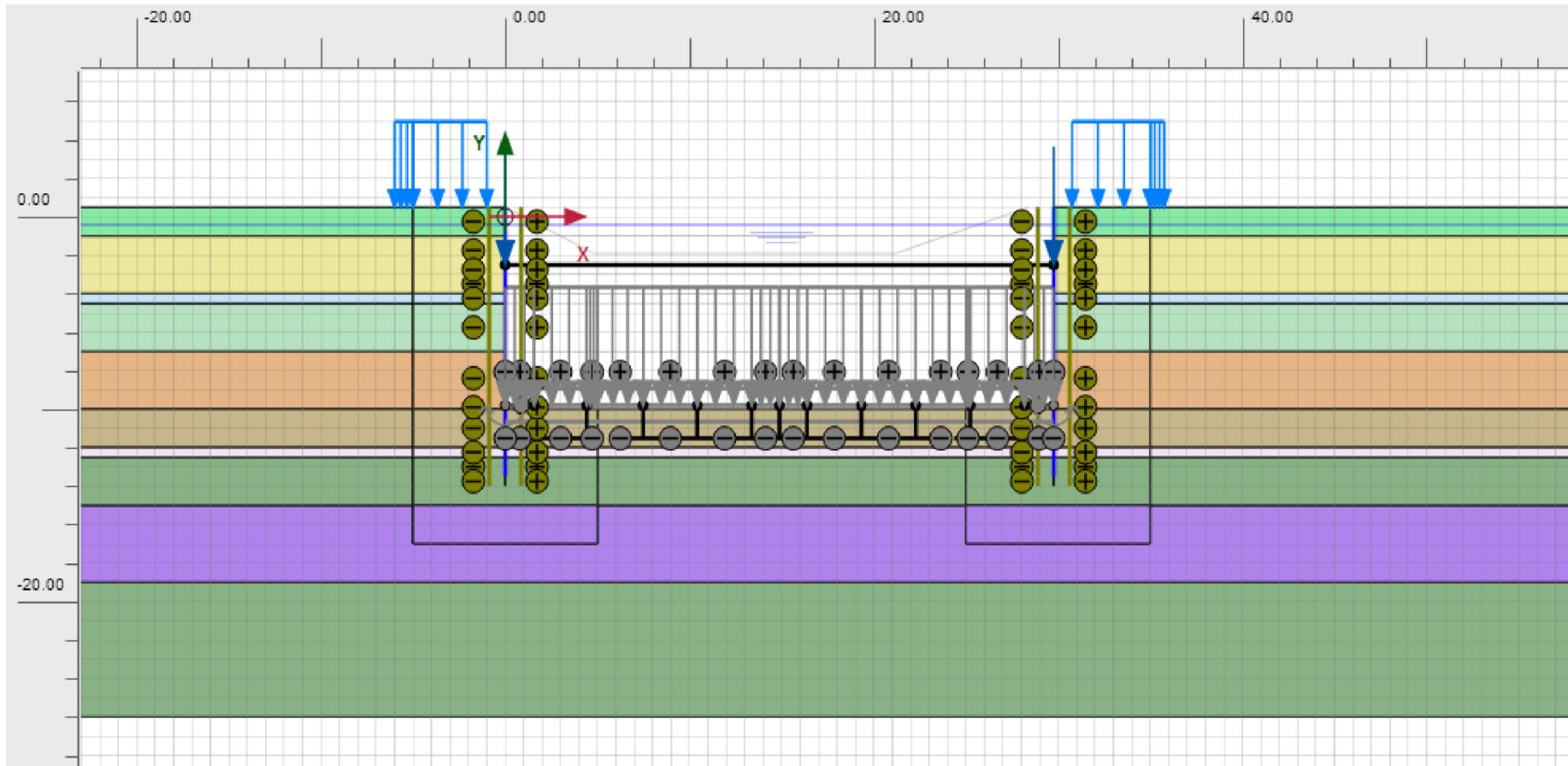
21-11-2018

Project filename

Albert cuypgarage.p2dx

User name

ABT bv



Project description

Phase 7 Install gewi-anchors

Date

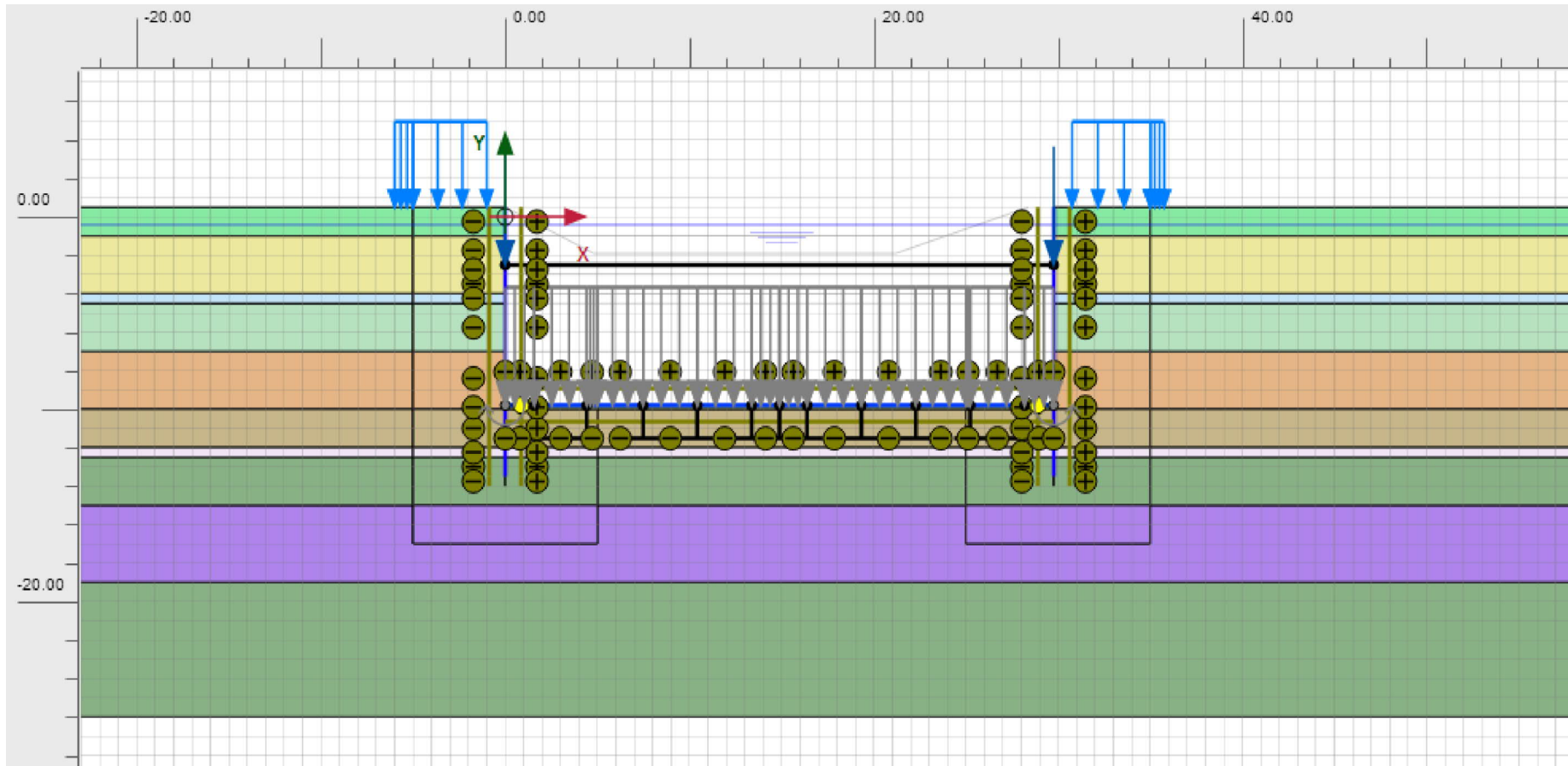
21-11-2018

Project filename

Albert cuypgarage.p2dx

User name

ABT bv



Project description

Phase 8 Pore Underwater concrete

Date

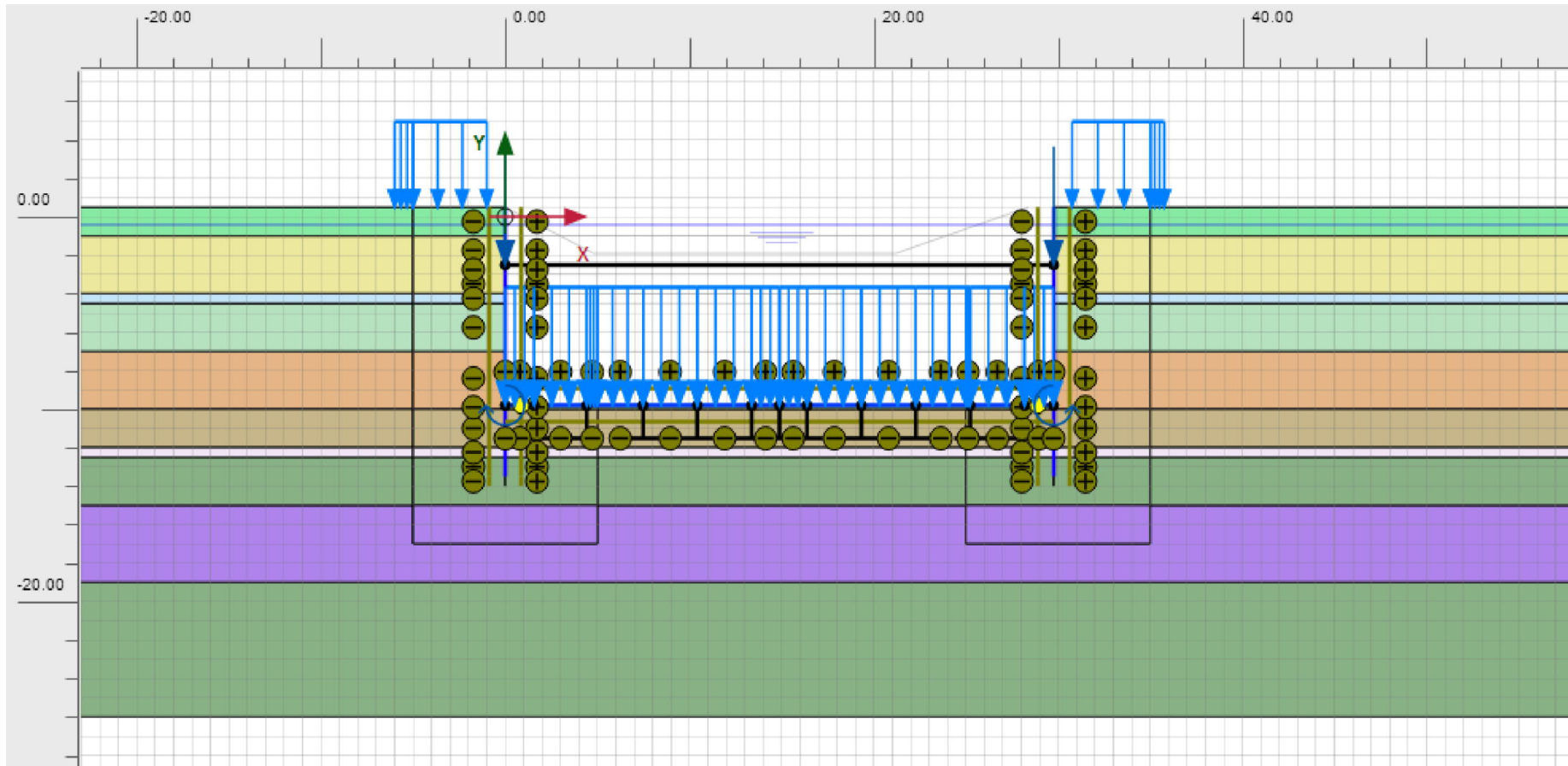
21-11-2018

Project filename

Albert cuypgarage.p2dx

User name

ABT bv



Project description

Phase 9 Dewatering of the building pit

Date

21-11-2018

Project filename

Albert cuypgarage.p2dx

User name

ABT bv